GES - Gravity Explorer Satellite

Providing data on temporal changes in Earth's gravity field for scientific use at low cost

Céline Dohmen	4008103	Stephanie Lubbers	4016718
Ariadad Fattahyani	4086554	Erik Orsel	1356976
Fabian Grondman	4103068	Evelyne Roorda	4044398
Daan Houf	4009509	Sander Vancraen	4057856
Bushra Kiyani	1148826		

Final Report

Design Synthesis Excercise

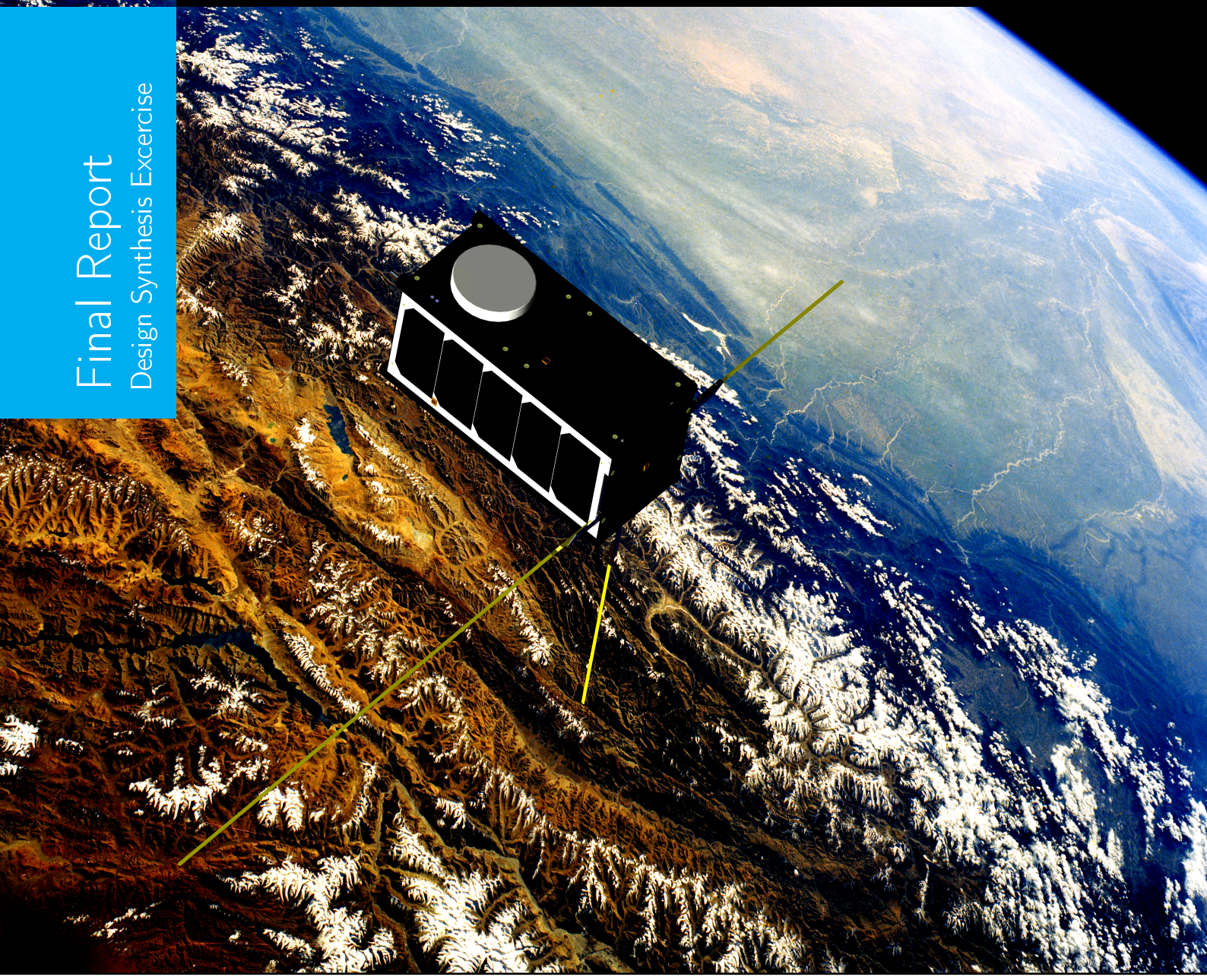

TU Delft Delft University of Technology

Aerospace Engineering

January 28, 2014

Preface

This technical report is the fourth progressive manuscript of the Design Synthesis Exercise team "Gravity Explorer Satellite". We would like to express our gratitude to Dr. Ir. W. van der Wal, assistant professor at the Aerospace Engineering faculty of the Delft University of Technology and tutor during the project, and our two coaches, Ir. S. Engelen and Ir. Z. Xu, for their valuable support during the realization of this report.
Furthermore, we would like to thank Dr. Ir. P.N.A.M. Visser, Ir. J. de Teixeira da Encarnacao, M. Klein BSc, Dr. M. Weigelt, Dr.-Ing. C. Siemes, Ir. P.P. Sundaramoorthy, Dr.ir. E.N. Doornbos, Ir. J.A.A. van den IJssel and Ir. M.F van Bolhuis for their willingness and enthusiasm in responding to enquiries.

Contents

List of Figures

List of Tables

List Of Abbreviations

AD&C Attitude Determination and Control
AGI Analytical Graphics Inc.

C/A Coarse/Acquisition
CAD Computer Aided Design
CATIA Computer Aided Three-dimensional Interactive Application
CBR Constant Bit Rate
CBS Cost Breakdown Structure
CD&H Command, Data and Handling
CHAMP CHAllenging Minisatellite Payload
CIGS Copper Indium Gallium Selenide
CNR Carrier-to-noise ratio
COCOM Coordinating Committee for Multilateral Export Controls
COTS Commercial-Off-The-Shelf
CPU Central Processing Unit
cubSTAR cubSatellite Space Three-axis Accelerometer for Research mission

DLR Deutsche Luft- und Raumfahrt
DOD Depth Of Discharge
DSE Design Synthesis Exercise

EIRP Equivalent Isotropically Radiated Power
EMI Electro Magnetic Interference
EOL End Of Life
EPS Electrical Power System
ESA European Space Agency

FFD Functional Flow Diagram
FMH Free Molecular Heating

GaAs Galium Arsenide
GES Gravity Explorer Satellite
GLONASS GLObal NAvigation Satellite System
GNSS Global Navigation Satellite System
GOCE Gravity field and steady-state Ocean Circulation Explorer
GPS Global Positioning System
GRACE Gravity Recovery And Climate Experiment
GRAS GNSS Receiver for Atmospheric Sounding

IADC Inter-Agency Debris Coordination Committee
IR Infrared Radiation
ISIS Innovative Solutions In Space

LEO Low Earth Orbit
LNA Low-Noise Amplifier
LV Launch Vehicle

MATLAB Matrix Laboratory
MEMS Micro Electro Mechanical System
MPPT Maximum Power Point Tracking

NASA National Aeronautics and Space Administration
NTR Non-Technical Requirement

P-POD Poly-Picosatellite Orbital Deployer
PCB PolyChlorinated Biphenyl
PCV Phase Center Variation
PDOP Positional Dilution of Precision
POD Precise Orbit Determination
PPP Precise Point Positioning

RAAN Right Ascension of the Ascending Node
RCM Requirements Compliance Matrix
R&D Research and Development

SBF Septentrio Binary Format
SMAD Space Mission Analysis and Design
SNR Signal-to-noise ratio
SPL Single Pico-satellite Launcher
SSO Sun-Synchronous Orbit
STK Systems Tool Kit
SWOT Strenghts, Weaknesses, Oppertunities and Threats

T-POD Tokyo Picosatellite Orbital Deployer
TID Total Ionizing Dose
TR Technical Requirements
TT&C Telemetry, Tracking and Command
TU Technical University

U Unit
UHF Ultra High Frequency

VBR Variable Bit Rate
VHF Very High Frequency

X-POD Experimental Push Out Deployer

List of Symbols

A Area
A_{sa} Area of solar array
B Earth's magnetic field
C_D Drag coefficient
C_r Solar radiation pressure coefficient
D Monthly acquired data
F_{EIR} View factor of Earth's IR
F_{albedo} View factor of Earth's albedo
I_y Mass moment of inertia about the y-axis
I_z Mass moment of inertia about the z-axis
I_{EIR} IR flux of Earth
I_d Inherent degradation
I_{solar} Solar flux
J_2 Second zonal gravity harmonic of Earth
J_n Dimensionless geopotential coefficients
L Lenght
L Geocentric latitude
L_d Lifetime degradation
P_0 Solar flux
P_{BOL} Power beginning of life
P_{av} Power average
P_{batt} Power battery
P_d Power daylight
P_e Power in eclipse
P_n Legendre polynomials
$Q_{EarthIR}$ Earth's IR heat
Q_{albedo} albedo heat
$Q_{external}$ External heat
$Q_{internal}$ Internal heat
$Q_{radiated}$ Radiated heat
Q_{solar} Solar heat
R_E Radius of Earth
T Radiator temperature
T_d Time of daylit period
T_e Time of eclipse
V Velocity
X_d Path efficiency sunlit period/day time
X_e Path efficicency eclipse
Ω Right ascension of the ascending node
Φ Gradient of the gravitational potential function
α Absorptivity
α_L Material specific thermal expansion factor
δL Expansion
δT Temperature variation
μ Gravitational constant of Earth
ω Argument of perigee
ρ_{albedo} Percentage of sunlight reflected by Earth
σ Stefan-Boltzmann constant
ε Emissivity
a Semi major axis
e Eccentricity
h Height
i Inclination
m Mass
n Mean motion of the satellite
r Radius

Abstract

Earth is experiencing an increase in average temperature due to the increasing amount of greenhouse gases. The ice in Greenland and Antarctica is melting at a high pace, causing changes in Earth's gravity field. Scientifically speaking, it is very important to monitor these changes in order to keep track of the environmental changes as well as to be able to take action against global warming. Currently there are satellite systems monitoring the gravity changes, however these systems are known to be very expensive. The challenge for the project at hand is to design a satellite system that monitors the change in Earth's gravity field at a low cost.

The main purpose of this report is to present the reader with the detailed design of the GES mission. This is done by giving an elaboration on the payload design, showing the error mitigation methods as well as the choices in GNSS receiver and receiver antenna. Furthermore, all different subsystems are designed and presented. The characteristics of all systems, as well as the system integration, are listed to provide an overview. Also the geometry and characteristics of the orbit are defined, such as the orbit type, decay & End Of Life (EOL) and the eclipse time.

Several conclusions can be drawn, starting with the orbit. For the orbit type it was decided to operate in a dawn-dusk sun-synchronous orbit. This orbit is most favourable for it has an almost constant lighting and thermal condition. The inclination is 97.7 degrees, making it a retrograde orbit. The height at which the largest ground track was found is 580 km, at this height the whole Earth is covered within a month. To get to the orbit it is decided to use a piggyback launch, as that is low cost.

For the GNSS receiver the AsteRx-m OEM was selected after a trade-off, based on its low mass, small dimension and low power consumption. Also the receiver complies with the requirement given on the maximum error in centre of mass position due to measurement noise. The GNSS receiver antenna that will be used for GES is the ACCG5Ant-2AT1, it is the most prefered one due to its respectively small length and width, and its low mass.

The attitude determination and control system was selected to be the iADCS-100. For the communication architecture the in-house groundstation located at the TU Delft campus was chosen, the satellite will pass over this groundstation seven to eight times a day. For the operation of the data flow within the satellite the Innovative Solutions In Space (ISIS) On Board Computer was selected, as it is the only viable one for the mission. For the thermal control subsystem passive control was found to suffice, therefore only coatings will be applied to control GES's temperatures, amongst which white and black paint. For the power supply only body-mounted cells proved necessary, five are placed on the panel facing the sun and on the panel facing Earth, of which two are redundant. Furthermore, two cells are placed on the side facing away from the sun in case of safe-mode. All the subsystems are concluded to fit in a 2 unit CubeSat, the bus that will be used for GES.

Using all COTS components, the total cost of the mission is about 300.000 *euros*.

1 Introduction

Since the beginning of its existence, Earth has always been subject to natural dynamic processes that can drastically affect life on Earth. For a few decades, the Global Warming phenomenon and the melting of the ice in the polar regions have become a major concern for life on Earth. For these and many more reasons, understanding the behaviour of these phenomena is of vital significance. In order to have a sense of how these phenomena function, measuring the change in the mass and gravity field of Earth is essential. Although really important, understanding these phenomena is not the only advantage of measuring the gravity field of Earth; high accuracy Geoid determination, which can be done by measuring the gravity field, will improve the orbit determination of satellites and provide a global unified reference system. Furthermore, the knowledge of Earth's gravity field can be used to improve recognizing the geodynamic processes occurring in the mantle. Since the year 2000, several satellite missions have been designed to contribute to the knowledge of Earth's gravity field.

The main purpose of this report is to present the design of a new satellite system that shall provide data on temporal changes in Earth's gravity field for scientific use at low cost; several scientific disciplines will profit from accurate gravitational data: Geodesy, Oceanography, and Geophysics. During its mission, the satellite will orbit Earth in a Low Earth Orbit (LEO) with a GNSS device mounted on the satellite for measuring purposes. While in orbit, the satellite will experience some deviations from its actual trajectory due to the uneven shape and mass distribution on Earth. This means that the locations on Earth's surface with a higher mass will cause the satellite to deviate more from its trajectory; measuring this deviation using the GNSS device and collecting data over certain intervals and for a certain period of time will provide scientists with data for visualizing the mass redistribution over Earth.

There are certain restrictions applied to this mission. First of all, the satellite has to be designed and launched with a budget as low as possible; this limits the use of high accuracy expensive devices on the satellite such as very accurate GNSS devices or AD&C systems. Secondly, there are certain limitations with respect to the orbit of the satellite and the accuracy of the obtained data. While a high-tech GNSS device might be enough to measure the deviation of the orbit, there are certain factors that cannot be taken into account to a very accurate extent such as the deviations due to the atmospheric drag and Earth's natural phenomena. The goal is to reduce the effect of these unwanted perturbations on the data as much as possible. Finally, there are certain limitations with respect to the sustainable development of the satellite, which includes rules about materials used and reducing space debris.

This report covers the detailed design of the Gravity Explorer Satellite (GES). The market analysis in chapter 2 gives an overview of the market the satellite will compete in and elaborates on the need for a low-cost gravity exploration mission such as GES. Next, the restrictions and guidelines for the design are presented in chapter 3. To give an overview of the functions GES will perform, chapter 4 introduces the operations and logistics. Based on the requirements and the operations the orbit is selected. Chapter 5 describes the orbit design process and results. The next step is the detailed design. The detailed design of the payload and other subsystems are presented in respectively chapter 6 and 7. The electronic units and system characteristics that form GES are summarized in chapter 8 together with the configuration and production plan. Based on the system characteristics the final mass and financial budget are calculated in chapter 9. Also the technical risks associated with the final design are derived in chapter 10. Chapter 11 goes from these risks to the reliability, availability, maintainability and safety. Next, the approach with respect to sustainability is discussed in chapter 12. Chapter 13 shows the compliance of

GES with the requirements with a performance and sensitivity analysis. Chapter 14 shows the verification of the models used in the design and the process to validate GES in the end. Finally, chapter 15 introduces the project design and development logic that follow from the work that has been performed up untill now. The report is concluded with the conclusions and recommendations in chapter 16.

2 Market Analysis

The market analysis in this section offers more insight into why there is a need for a low cost mission that measures Earth's gravity field. First, the space economy is divided in segments to give an idea of where the stakeholders are. Secondly, a basis is formed to support the idea that new space missions must be more independent and less cost intensive to anticipate for reducing government funding. This will be followed by the overview of the competitors. Opportunities are verified in a business model. After the business model, the first cost analysis is presented. A Strenghts, Weaknesses, Oppertunities and Threats (SWOT) analysis will show the most important threats and weaknesses. The benefits, disadvantages and application of CubeSat technology will be analyzed. Finally, the vision of the market segmentation focused on the satellite is discussed.

2.1 Market segmentation

The space economy is divided in four sectors according to [18]:

1. Research and Development (R&D), laboratories and universities: are public or private and often funded by government institutions. These organizations often work on basic space technology or space related science.
2. Manufacturers: design, build and assemble final products or components. Since 2000, many small actors have emerged.
3. Operators: offer services from space such as Global Positioning System (GPS), telecommunication and data provision.
4. Information service providers: distribute data which includes retail activities. Information providers work closely with ground equipment developers.

2.2 Developments in the space sector

The space economy is changing due to the increase of commercial initiatives that result from government supported research. Space is seen by many governments as a key sector for exploration, science and security [19]. One of the great examples of a technology invented in a government project that matured to the commercial world is GPS [20].

There are two main reasons why most space programs are government funded. First of all their motives are related to the aforementioned exploration, science and security. These are sectors that have an intrinsic value or give value to primary human needs. Secondly, governments are more able to carry the risks involved. Commercial businesses require a potential return on investment in the order of 200 tot 300%. Next to that the development time frame creates a large obstacle for commercial initiatives to innovate. Large space mission can be overtaken by new technical innovations and economic changes [21].

The recent period of USA's austerity measures in October 2013, which temporarily shutdown space activities at National Aeronautics and Space Administration (NASA) [22] and the reports that the European Space Agency (ESA) financially depends on joining member states [23], shows that the space

sector is getting less reliable in terms of economic stability. A future decrease of government funding for space activities is therefore to be expected.

However, an expected decrease in government funding does not mean that the demand for space activities is lowering. For instance, the growing smartphone industry means a growing demand for GNSS services. Other examples are climate and environmental changes on Earth that still needs monitoring. A challenge thus arises to design low cost Earth observation missions that are low risk and have a short development time span.

The above findings provide an incentive to come up with low cost space mission solutions that could be designed and deployed by institutions and private companies with low budgets. One way of doing this, is by lowering the involved risks and shortening the time frame in which the mission must be designed, manufactured and launched.

2.3 Competitors

The mission statement of the Gravity Explorer Satellite is as follows:

"Providing data on temporal changes in Earth's gravity field for scientific use at low cost"

Table 2.1 gives a few satellite missions that have been used for similar objectives. The mission cost includes the satellite(s), launch and operations.

Table 2.1: Competitors mission cost and time-frame

Satellite	Mission cost [Euro]	Mission time frame
CHAllenging Minisatellite Payload (CHAMP) [24]	unknown	July 2000 - September 2010 [24]
Gravity field and steady-state Ocean Circulation Explorer (GOCE) [25]	350m	March 2009 - November 2013
Gravity Recovery And Climate Experiment (GRACE) - 1 [26]	93m	March 2002 - September 2015 (expected) [27]
GRACE - 2 [28]	327m	2016 - 2020

The GOCE, GRACE - 1 and GRACE - 2 mission prices are in the order of hundred million euro. It is known that smaller satellite missions, like those using CubeSat technology, are less cost intensive. This creates an opportunity to design a gravity explorer satellite mission using technology that relatively cheap to design.

2.4 Business Model

The business model below gives a first approximated idea of how a gravity exploration mission could be designed from a business perspective [29]. It is meant as an overview to check the connection between stakeholders, funding and organization infrastructure, shown in figure 2.1.

Proposition
The main value proposition is the accessibility of the produced gravity data. Next to that, cost reduction will lower the needed funding, thereby also lowering the bar for universities or institutions to join the mission. Risk reduction in the mission makes convincing stakeholders to join the mission easier. The value of the gravity data in itself is commercially not attractive.

Customer segment and customer relationship
The data is provided to scientists who monitor and study climate change. Most of the scientists are connected to R&D centers. Therefore, universities and institutions are seen as the most important customers. These organizations are likely to be government funded.

Key activities and channels
The key activities for daily operations is measuring and distributing time variable gravity field data. The business part of distributing data to costumers is described in the channels section where the most

important costumer interface phases are mentioned. The delivery of data and analyses support are the key phases for the technical design.

Key resources and key partners
Key resources are needed the design, deploy and maintain the mission. Knowledge and facilities come from key partners such as the Technical University (TU) Delft, service providers and manufacturers who help to customize the acquired satellite components. Funding could be covered by companies, universities, other institutions and investors.

Cost Structure
From the Midterm design, an estimation of the total cost of the mission is made. This is presented in section 2.5

Funding Structure
The mission is quasi non-commercial, meaning that a profit is not required but a compensation for the invested money would be pleasant. Selling the data could be an option. Crowd funding via a website, asking for support in climate research, could be an addition as. Though, more research is needed to find out the potential of crowd funding. General funding via government funded institutions creates more certainty with respect to the availability and time frame of acquisition.

<table>
<tr>
<td rowspan="2">Key Partners:
TU Delft
Other R&D institutions/Universities
Manufacturers
Service providers</td>
<td>Key Activities:
Collect and provide data on time variable gravity field</td>
<td rowspan="2">Value Proposition:
Accessibility of data
Cost reduction
Risk reduction</td>
<td>Costumer Relationship:
Still open, depends on the preference in data accessibility</td>
<td rowspan="2">Costumer Segments:
Scientists and institutions who monitor or/and study climate change</td>
</tr>
<tr>
<td>Key Resources:
Knowledge
Facilities
Funding</td>
<td>Channels:
Awareness
Evaluation
Purchase
Delivery
Support</td>
</tr>
<tr>
<td colspan="2">Cost structure:
A financial budget is set up as part of the resource allocation</td>
<td colspan="3">Funding structure:
Data selling
Crowd funding
University/Institution/Government funding
Sponsorship/Investor</td>
</tr>
</table>

Figure 2.1: Business model

2.5 Cost analysis

The aim is to keep the cost as low as possible. The first cost estimate for CubeSat can be seen in table 2.2, which has been used as a starting point for the detailed design. Most prices can be found on CubeSat web-shops such as Cubesatshop.com and Clydespace.com [13] [30]. They offer almost all parts required to put a working satellite together. A very rough estimate of the cost for the chosen concept is made.

Table 2.2: First cost estimation of concept

	Price (euros)	% of total costs
GPS receiver and antenna	10,000	1.4
Mems acclerometer	10,000	1.4
AD&C	52,000	7.3
Communications	8,500	1.2
Power	3,300	0.5
C&DH	4,500	0.6
Solar panels	5,000	0.7
Structure	3,000	0.4
Launch	434,350	83.4
Deployer	22,500	3.2
Total costs	553,150	

The exact cost for the payload software is not known. The price of Micro Electro Mechanical System (MEMS) accelerometer is estimated with a margin for the software costs [31]. The AD&C system price comes from Berlin space Technologies [4]. Participants in launch of CubeSats include Russia, USA, ESA, Japan, Space X and India. For the deployment of CubeSats four types of deployers are available. The Poly-Picosatellite Orbital Deployer (P-POD) holds three single CubeSats stacked on top of each other. The Tokyo Picosatellite Orbital Deployer (T-POD) holds one single CubeSat. The Experimental Push Out Deployer (X-POD) holds one satellite but can be tailored for satellites of different dimensions. The Single Pico-satellite Launcher (SPL) hold one single CubeSat [32]. As can be seen the launch cost is 83.4% of total cost. This is an area where improvements have to be made. NASA is considering free launch for educational missions [33]. Similar initiatives might occur in the European Union in the near future. The total cost of the mission are about half a million. For the final design, the financial budget is presented in 9.2.

2.6 SWOT analysis

The largest opportunity of the gravity explorer mission is created by the compact and proven design of CubeSats. This reduces the cost and increases the reliability. What should be considered is that the satellite is designed at low cost and will be measuring the gravity field with only GNSS. This combination becomes unique, hence it will create more uncertainty in reaching the required accuracy. Simulations can take most of the uncertainties away. Another point of attention is that the lower budget and use of COTS components restrict the mission from innovation. This with respect to the GRACE 2 mission which has an estimated budget of 327 million *euros*. A lower budget also means that there is no luxury of selecting a dedicated launcher. The designed satellite shall thus share its launcher with several other satellites. An overview of this analysis is presented in table 2.3.

Table 2.3: SWOT analysis

	strength (internal)	weakness (internal)
opportunity (external)	Use of COTS components lowers development time. Provision of data when no mission is active.	New approach in measuring is innovative, but not proven.
threats (external)	Launch windows and orbits are limited.	Probability of low accuracy compared to competitors.

2.7 Mission types and applications

By having the Gravity Explorer Satellite measuring the gravity of the Earth, other Earth exploring opportunities will arise. With the current system of the satellite it also becomes possible to determine the atmospheric density. A different out-of-the-box idea is to launch multiple satellites.

2.7.1 Atmospheric density

By implementing an accelerometer to the system it becomes possible to measure the density [34]. An accelerometer is very expensive, so this would not be an option to still keep it as a low cost mission. A new method is found that estimates the total neutral atmospheric density from Precise Orbit Determination (POD) of LEO satellites [35]. The drag force acting on the satellite is determined through centimeter-level reduced-dynamic precise orbit determination using onboard GPS tracking data, where the total atmospheric density is derived. The results demonstrate that this method is applicable to data from a variety of missions and can provide useful total neutral density measurements for a atmospheric study up to altitudes as high as 715 km, with precision and resolution between those derived from traditional special orbit perturbation analysis and those obtained from onboard accelerometers [35]. This method is particulary useful for a satellite with a high-quality GPS receiver.

2.7.2 Multi-satellites

With the current systems it is possible to obtain the atmospheric density in LEO. To get a better overview of the density, one needs to measure at different local solar times, and measurements from different inclinations [36]. This can be solved by launching multiple CubeSats. This constellation of satellite will be flying at different altitudes and inclinations. Also the satellites will orbit in different local time sectors then others, somewhat what has been done in the Swarm mission [37]. This will lead to multipoint measurements, which will result in a better and more precise insight in the measurements. This could change the way the temporal gravity changes and the atmospheric density are measured nowadays, since the CubeSats can be used for several purposes. Having a swarm of satellites the production cost can be reduced. As can be seen from the learning curve in figure 2.2, if 100 satellites are produced the cost per unit will be halved because aerospace system usually have a learning curve of 85-90% [1].

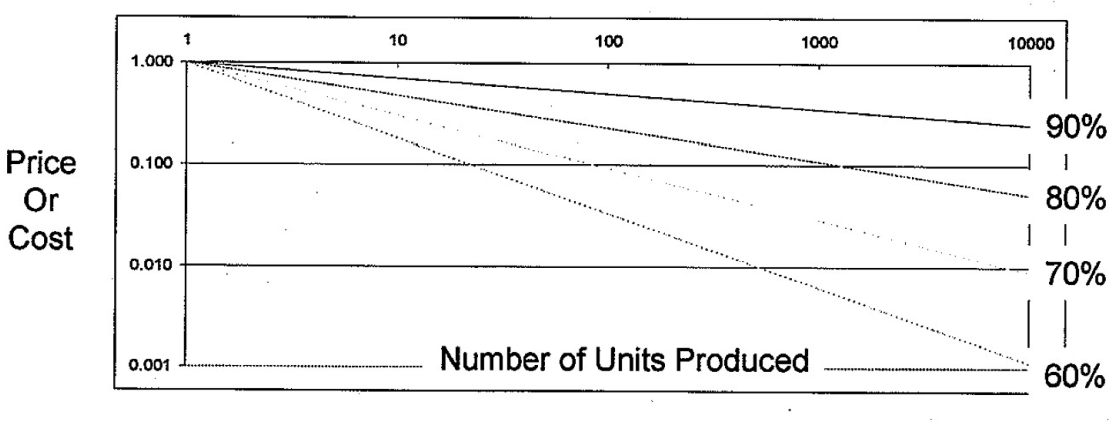

Figure 2.2: Learning curve [1]

2.7.3 Applications

The aerospace community can benefits from having precise and up-to-date measurements of the atmospheric density. Understanding the atmospheric effects on spacecraft in low Earth orbit will lead to improved calculations for orbit determination and collision avoidance. Improving calculations that are used when observing an orbit may lead to advancements in the fields of mathematics and physics on Earth [38].

2.8 Technology

Competitors during the mission of the gravity explorer satellite are very few. NASA is working on a second generation gravity recovery satellite (GRACE-II) expected to launch between 2016-2020 with a budget of approximately 327 million euros. The satellite will use microwave- or laser-based ranging system for accurate positional measurements and a resolution of 100 km. CubeSats are very popular among universities for research and many examples can be found where CubeSats have been used for remote sensing, earth imaging, radar measurements, ionosphere radiation etc. From market research it can be concluded that satellite mission for gravity measurements with GNSS have not been launched yet. So the idea for this project will be a first of its kind on paper. Given the speed with which CubeSat missions are being launched, it will be a matter of time before similar concepts might become reality. However, at the moment there is little competition and given the valuable application of data the mission provides, it might be of great interest as an alternative design.

2.8.1 CubeSats

CubeSats are defined as type of miniaturized satellite with a weight less than 1.33 kg per U. CubeSats can be 1U, 2U, 3U or 6U in size. The maximum weight can be 12-14 kg for 6U satellite.

2.8.1.1 Advantages

The ease by which CubeSats can be designed with existing Commercial Off The Shelf Components gives them the advantage that only the payload needs to be designed in detail. This is introducing endless possibilities for small satellite design and testing which were too expensive before. The market is bound to grow as the low costs make it possible for less developed countries to use satellites for testing even though a space program might not be present.

The low cost and mass allows for mass production of satellites. With a small size comes the advantage of reducing the propulsion and power costs. The integration of COTS components means that the satellite can be produced in a smaller amount of time and will be available faster. Several satellites can be developed, each with their own specific purpose instead of designing one large scale mission with all experiments on one system. This way new technologies and innovative applications can be tested as the mission can be designed for that purpose only. With this flexibility the variety of aims of satellite missions is bound to increase. This can already be noticed from the CubeSat missions already launched. Not only are this type of satellites suitable for a variety of missions but they are also developed by a variety of countries. CubeSats make it possible for developing countries to layout a roadmap for research programs in space. Good incentive for these countries is to further develop communication infrastructure which is highly needed in this age of information technology [39].

The launcher design is not required and this will reduce the costs even further. This mission is planned to have a piggy-back launch, section 7.8 elaborates on the launcher selection. Using a CubeSat deployer the launcher interface does not need to be tested as the deployers are certified. The Gravity Explorer Satellite is designed to be a follow-up to the existing gravity mapping mission mentioned before. It gives the advantage of continuation of measurements of temporal changes in gravity and is a better alternative than having no mission at all. In the long run additional improvements can be implemented to improve accuracy but still keeping the costs at a minimum.

The low cost of the projects enables students to participate and gain valuable engineering experience. Also the students do not need to be paid which saves costs. TU Delft has recently demonstrated their keen interest in this field by the launch of Delfi-n3xt, the third satellite in a series of nanosatellites developed by the Faculty of Aerospace Engineering. There is no need for extra infrastructure during the development stage and existing facilities can be used.

2.8.1.2 Disadvantages

Despite the benefits of CubeSat missions, they might face some limitations. Although cost are lowered due to piggy-back launches, a suitable launcher is needed and launch dates are limited. Most missions are in LEO and the rocket choice should comply with that requirement. The other disadvantage is that CubeSat technology is in its infant stages and miniaturization of COTS components may pose some

reliability challenges. Further testing and verification of components in space is still required. The Gravity Explorer Satellite has the purpose of providing a platform for continuing measurements once the previous missions retire however, with the risk of a lower accuracy.

2.8.2 Market development

Since the launch of the first batch of CubeSats in June 2003 on a Eurockot Launch Vehicle (LV) rocket from Plessetsk (Russia) a market has emerged for small satellite launch. At least 20 launches have been attempted, each with a batch of satellites onboard. The low cost of CubeSats is an enormous driving factor in the expanding market. Cost estimation is crucial to predict the further expansion of the market. With more advances in technology and cooperation between countries CubeSat costs can further be reduced. One example of such a cooperation is the QB50 [40] project planned to launch in April 2015. This is a joint project between China and the EU with the aim to launch 50 CubeSats in one launch. The participating countries include mainly EU nations but also non-EU countries such as Brazil, Ethiopia, India, Iran, Israel, Portugal, Singapore, south Korea, Turkey and Vietnam [40].

2.9 Vision

In the last decade, the space sector is changing from a government agency controlled sector to a sector with more commercial activities. The demand for space activities will not decline with government budget cuts. Climate research and monitoring is still necessary and CubeSat and GNSS technology offer the opportunity to reduce mission costs. CubeSat missions in general will lead to development of new ways to reduce launch costs and hence give the market a competitive edge. It is important to improve accuracy of data so that the scientific community could benefit from it. The vision for this mission is to be at the forefront of application of GNSS technology on a small mission and to demonstrate the need to shift funding from costly long term projects to more viable and alternative low cost missions.

3 Requirements

In the previous reports an elaboration on the requirements has been made. This chapter serves as a recap and an overview on these requirements. The requirements are divided into a Technical Requirements (TR) and Non-Technical Requirement (NTR) group. The technical requirements are those that give an abstract demand that can be applied directly to the satellite system, whereas the non-technical requirements are more general. Different layers of requirements are identified, starting with the top-level requirements which can be split up in sub-requirements.

3.1 Technical requirements

Top-level technical requirements

- TR-1 The mission should yield observations of yearly mass transport at a spatial scale of 1000 km or less.
- TR-2 The measurement principle to be used is the tracking of navigation satellites (e.g. GPS, GLObal NAvigation Satellite System (GLONASS)).
- TR-3 The error in centre of mass positioning due to inaccurate pointing of the satellite should be smaller than 1 cm.
- TR-4 The error in centre of mass positioning due to GNSS measurement noise should be smaller than 1 cm.
- TR-5 The temporal changes of the Earth must be moniterd by covering the entire Earth within a time frame of one month.

Technical sub-requirements

- TR-1.1 The groundtrack must be such that the spatial scale is 1000 km or less.
- TR-1.2 The orbit altitude must be such that the spatial scale is 1000 km or less.
- TR-3.1 The satellite mechanisms must be modeled such that the error in centre of mass positioning is smaller than 1 cm.

3.2 Non-technical requirements

Top-level non-technical requirements

- NTR-1 The minimum operational lifetime should be 3 years.
- NTR-2 The cost of the satellite mission should be as small as possible given the requirements.
- NTR-3 The design should be eco-friendly and all parts of the satellite must burn up entirely during re-entry to avoid creating space debris.

Non-technical sub-requirments

- NTR-2.1 The operating costs must be kept as low as possible, i.a. by using an autonomous satellite and a cheap ground station.
- NTR-2.2 The orbit must be selected in such a way to keep the costs as low as possible, i.a. by selecting a cheap launch system.
- NTR-2.3 The mass of the satellite should be as low as possible given the requirements.
- NTR-2.4 Wherever possible, commercial off-the-shelf components should be used.
- NTR-3.1 The satellite must re-enter within 25 years after EOL.
- NTR-3.2 Where possible the most sustainable materials should be selected for the satellite.

4 Mission Overview

Based on the requirements and mission objectives the functions of the system can be identified. Before starting the detailed design it is important to visualize these functions, so they can act as a guideline throughout the design process. In this chapter a functional flow diagram and functional breakdown structure are presented to illustrate the mission objectives. Also the operations and logistics of the satellite system are introduced in section 4.3 to provide a mission overview.

4.1 Functional flow

The logical order of functions the satellite system will perform can be represented by a Functional Flow Diagram (FFD). The first diagram shows the functional flow of the satellite mission (see figure 4.1) and the second diagram shows the payload operations specifically (see figure 4.2).

The satellite system FFD gives a simplistic order of steps for a generic satellite system, but the payload FFD is distinctly for this mission. The satellite receives three sources of measurement data and sends it to the Command, Data and Handling (CD&H) unit. Data from the payload consists of GNSS data to determine the position of the satellite. Other factors that need to be taken into account are house-keeping data and position & attitude control data, because they can determine influences on the position measurements. Therefore the data from all three sources are transmitted to the ground station. Scientists can then process this data and filter out the noise and other erros to make the data ready for distribution, as discussed in section 4.3.

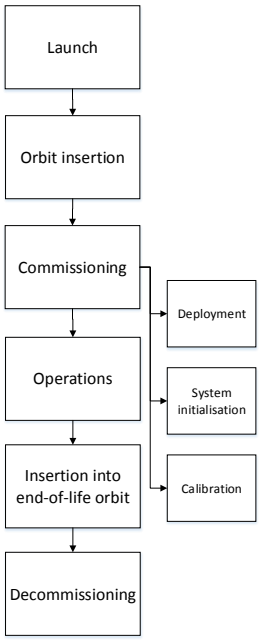

Figure 4.1: Functional flow diagram satellite mission

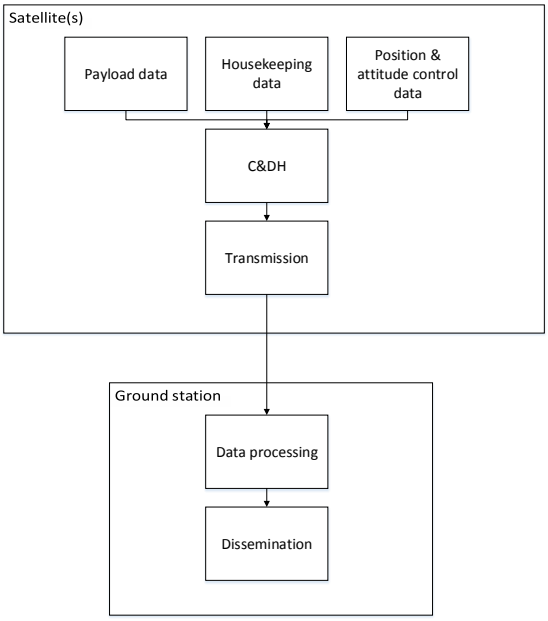

Figure 4.2: Functional flow diagram payload

4.2 Functional breakdown

The functional breakdown structure, as shown in figure 4.3, is a hierarchical representation of the functions that the mission performs. The diagram is split into five stages representing the five satellite mission phases; this is done because the functionalities of the system will differ in each phase. The diagram starts with the launch to get the system into space and is followed by the orbit insertion to get the system in the right position. Next, the commissioning phase is initiated consisting of the system initialization and calibration to prepare for the operational use of the system. After deployment, the system/component check must be performed to make sure the system is working properly before starting the measurements. Once the start-up is completed, the system is ready to start operating. The operations the system will perform consist of measuring and transmitting data. The combination of the different measurements will give accurate data on the temporal changes in gravity. This data is transmitted to the ground station for data processing and distribution. Once the operations are completed and the mission is accomplished, the system goes into its end-of-life phase. Keeping sustainability in mind, the system will be decommissioned.

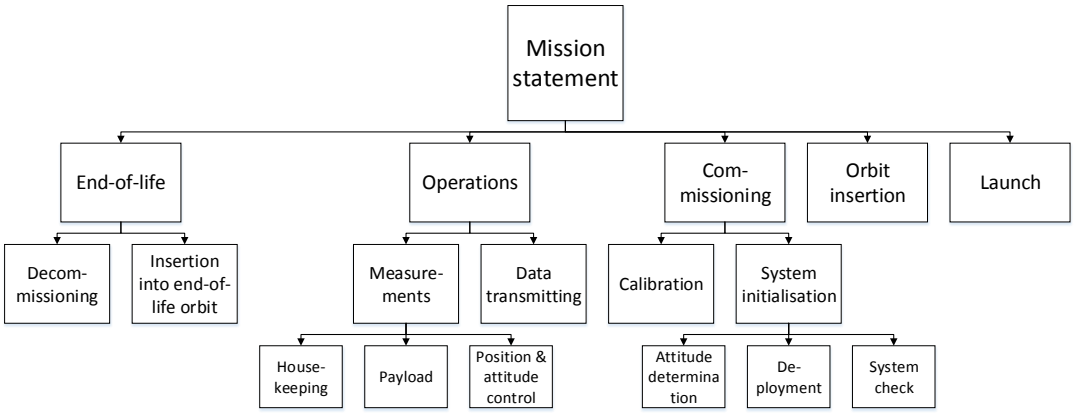

Figure 4.3: Functional breakdown structure

4.3 Operations & logistics

The operations and logistics describe the functions of the system during its operational lifetime and the logistics from the design phase untill the end-of-life of the satellite.

Operations
To measure the temporal changes in gravity a number of measurements are made. The position of the satellite will be determined to derive the deviation from its orbit by Earth's gravity field. The GNSS measurements will provide an accurate position of the satellite(s). The accumulation of all position data shows the changes in the gravity field over time. A dual-frequency GNSS receiver will be used to cancel out errors to achieve sufficient accurate data after data processing. The operations of the satellite therefore entail measuring and transmitting the GNSS data.

The satellite operations are supported from the ground. The ground segment is responsible for controlling the satellite and ensuring the signals are received. One ground station is employed according to the ground track of the satellite, such that there is sufficient contact between the satellite and the ground. The CD&H system and the ground segment are interlinked. According to the amount of data that can be stored on the satellite the time interval at which data needs to be transmitted is determined. Based on this time interval one ground station has been chosen to keep contact with the satellite. After the data has been received at this ground station the data will be merged and processed to go from raw data to refined data.

Data processing is necessary to make sense of the measurement data. Firstly, the known errors are removed. Next to that a filter will be applied to estimate unknown errors and remove this estimation from the final values. The precise filtering of the measurement data is beyond the scope of this project and is left to the scientist.

The refined data will be disseminated to all parties interested as mentioned in chapter 2.

Logistics

The first phase of the project is the design phase. During ten weeks of the Design Synthesis Exercise (DSE) nine students work on the design of the satellite system of which the results are published in this report.

The second phase is the manufacturing, integration and production phase. Because the focus of this project is to design a low cost satellite most of the components are off-the-shelf. This saves manufacturing, testing and production costs. This process is described in more detail in section 8.3.

Next step is the actual launch of the satellite. As indicated in the previous report the launch costs are the main cost driver of the system, thus a piggyback launch is chosen to save costs. Therefore the launch planning is dependant on the availability of a space (of the right size) on a launcher to the right orbit. Chapter 15 will elaborate on the launch process and support.

When the satellite has been launched and enters its orbit the operation phase takes off as described in the previous paragraph.

After its operational lifetime of at least 3 years, set by requirement NTR-1, the satellite enters its end-of-life phase. Keeping sustainability in mind the satellite has to burn up in the atmosphere within 25 years. An orbit will be selected to meet these requirements. During the end-of-life phase the satellite will still be tracked and controlled by the ground station. After the satellite has been decommissioned the mission continues until all the datasets have been processed, because compiling and analysing the data may take more time than the lifetime of the satellite. This will be explained in more detail in chapter 15.

5 Astrodynamic Characteristics

The geometry and characteristics of the orbit of a satellite has an important effect on all the subsystems of the satellite, therefore these characteristics have to be carefully defined. This section presents the main astrodynamic characteristics of the satellite and gives a brief description on each of them.

5.1 Orbit decay and end-of-life

In this section the orbit decay and the end-of-life is be discussed. The satellite will decay during its life time due to different perturbations and undesired effects. This decay will influences the satellite's position and orbital elements.

5.1.1 Perturbations and undesired effects

The perturbations and undesired effects that occur in space all have some kind of influence on the satellite. Third body perturbations are perturbations caused by the gravitational forces of the moon and the sun. Solar radiation pressure are types of perturbations which are more dominant at higher altitudes where the atmosphere is negligible. Since the satellite is near-Earth these types of perturbations will not have a very large influence on the satellite. The dominant perturbation and undesired effect working on the satellite are the atmospheric drag and the non-spherical Earth, respectively.

Atmospheric drag
The atmospheric drag in LEO is the main source of perturbation for the satellite. The drag force acts in the opposite direction of the velocity vector of the satellite and causes a certain amount of energy loss in the orbit. The interaction with the atmospheric drag can be calculated by equation 5.1 [41]:

$$F_D = -\frac{1}{2}\rho\frac{C_D A}{m}V^2 \tag{5.1}$$

where ρ is the atmospheric drag and the value of C_D is 2.2. The satellite's cross-section is A, its mass is m, and velocity V.

Non-spherical Earth
The non-spherical Earth causes a dominant undesired effect on the satellite. The Earth has a bulge at the equator and is flattening at the poles, so there is a non-symmetrical mass distribution. This undesired effect can be calculated with the geopotential function Φ, see equation 5.2, [41]:

$$\Phi = \frac{\mu}{r}\left(1 - \sum_{n=2}^{\infty} J_n \left(\frac{R_E}{r}\right)^n P_n(sinL)\right) \tag{5.2}$$

where μ is the Earth's gravitational constant of 398600.5 km^3s^2, R_E is the radius of the Earth, P_n are Legendre polynomials, L is the geocentric latitude, and J_n are dimensionless geopotential coefficients of which J_2 is 0.00108263. The gravitational potential causes periodic variations in all the orbit elements, but the two main effects are changes in right ascension of the ascending node and argument of perigee

because of the Earth's oblateness, represented by the J_2 term in the geopotential expansion. The rates of change, in deg/day, of Ω and ω due to J_2 are formulas 5.3 and 5.4, respectively, [41]:

$$\dot{\Omega}_{J_2} = -1.5nJ_2\frac{{R_E}^2}{a}(\cos i)(1-e^2)^{-2} \tag{5.3}$$

$$\dot{\omega}_{J_2} = 0.75nJ_2\frac{{R_E}^2}{a}(4-5sin^2 i)(1-e^2)^{-2} \tag{5.4}$$

where n is mean motion in deg/day, a is semimajor axis in km, e is eccentricity, and i is inclination.

5.1.2 Lifetime

For the design it is decided that no propulsion system on board of the satellite will be implemented. The satellite will consists of less complex systems, which will save cost on the design, and makes the system more reliable. There are two requirements that should be fulfilled, namely requirement NTR-1 and NTR-3.

To determine the orbit decay and lifetime of the satellite the program Systems Tool Kit (STK) has been used. An iterative process of different orbit altitude is done. Keeping in mind that the operational phase of this mission can be extended longer than 3 years if all the components still work; therefore, altitudes with a lifetime close to 3 years are eliminated. Furthermore, the satellite should cover enough of the Earth during its mission, see next section about the ground track, therefore, an altitude of 580 km has been chosen for this mission. Inputs for the calculation are satellite characteristics and space environmental parameters. The total frontal area of the satellite is 10,975 mm^2. Assuming that during operational lifetime the satellite will not always fly in prefect conditions, an extra margin is added to this value. This is done to give a better estimation of frontal area during operational phase. Hence, the input of the drag area is 0.012 m^2. The mass of the satellite is equal to 1.61 kg, see chapter 9.1 for more information. The solar radiation pressure coefficient C_r is 1, which indicates that the satellite perfectly absorbs solar radiation. For the atmospheric density the model of NRLMSISE2000 is chosen, which is the most recent atmospheric density model. The solar file file used is called Solfx_Schatten.dat, which predicts values of solar flux and geomagnetic activity. This simulation has a starting date of 1 Januari 2015, and the results are presented in figure 5.1.

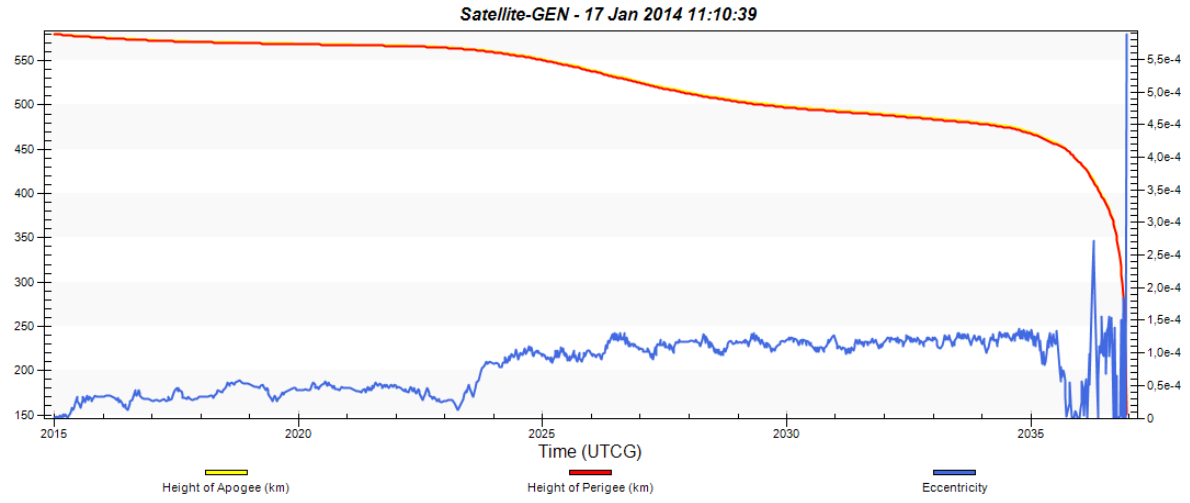

Figure 5.1: The orbit decay over the satellite's lifetime

The top curve represents the orbit decay. For this on the left vertical axis the orbit altitude is given in km. The bottom curve shows the eccentricity, the right vertical axis gives the corresponding values. On the horizontal axis the time in years is given. The change in eccentricity is very small, which stays more or less the same during its operational phase. For an altitude of 580 km the corresponding lifetime of the

satellite is 22 years, and the orbit decay over the 3 years operational phase is 8.83 km. The requirements NTR-1 and NTR-3 are satisfied. It has to be noted that after its operational lifetime, which can be more than 3 years, the satellite will not function and has no controlled stability anymore. The satellite will turn, which results into a larger frontal area, and will decay faster. Hence, the end-of-life is smaller than the calculated lifetime, unless the satellite will keep functioning until it burns up in the atmosphere.

5.2 Sun-synchronous orbit

A special combination between the altitude and inclination of a satellite creates a type of orbit that is called the Sun-Synchronous Orbit (SSO). The combination of altitude and inclination in this type of orbit is such that the satellite passes over any given Earth latitude at the same mean solar time having a constant illumination angle every time. Using a sun-synchronous orbit provides the satellite with some unique characteristics. First of all, the satellite will have a constant position of line of nodes with respect to the sun, which means that the eclipse time will remain constant during the orbit and since the eclipse time affects the design of the thermal subsystem, knowing that the satellite will always have the same amount of shadow time, it will be easier to design the thermal control subsystem. If a special type of the sun-synchronous orbit, namely the dawn-dusk orbit is chosen, the satellite will always be facing the sun and it will never experience eclipse (this is the ideal case for this type of orbit, which is impossible to achieve. see section 5.3. This can be useful since the solar panels can constantly generate power and reduce or even eliminate the battery requirements (however, batteries will be considered for the satellite even in the case of dawn-dusk orbit). The second reason to choose a sun-synchronous orbit is that it is a popular orbit and a lot of satellites are launched into this orbit, so it makes it easier to find a launching vehicle for the satellite. The Spaceflight website schedule shows that all their launches are either in an inclination of below 65° , or in case of a higher inclination, they are launched into SSO [42], this will save a lot of cost as well as time for the launch of the satellite. Based on these reasons, for the design of the satellite, a sun-synchronous orbit will be chosen as the orbit type of the satellite.

Selecting an inclination for a SSO is not optional and has to be calculated and it differes as the altitude changes. Based on the calculations, the most suitable altitude for the satellite will be about 580 km. For an altitude of 580 km, the inclination of the SSO can be calculated to be about 97.7° [43].

Disadvantages of sun-synchronous orbit

Although a sun-synchronous orbit has many advantages that make it a suitable orbit option, it might have some disadvantages that require examining before choosing the orbit and basically determining whether the satellite will be able to overcome these disadvantages if a sun-synchronous orbit is chosen. One of the major concerns of choosing a SSO comes from the special dawn-dusk SSO; when the satellite is put into this special orbit, one side of the satellite will be facing the sun, therefore heating up and the other side will be away from the sun and therefore, will face the cold temperature. If the satellite's attitude is kept constant towards the sun, it will cause a lot of temperature difference between the two sides of the satellite. This can be avoided by rotating the satellite on a certain plane while putting the antenna on a position vertical to that plane so the satellite can rotate and distribute heat on different surfaces, while having the antenna at the same place so it can always receive the signals.

Another disadvantage of the SSO comes from calculating and eliminating some special type of errors. A satellite in SSO will always pass a certain place at an exact same time every time; this means that the satellite will always be measuring the same error caused by the tides. Since the Sun is one of the main causes of the tides, a satellite in a sun synchronous orbit will always measure the Sun's tidal effects as a constant sea surface elevation, which is a false signal [44]. On a non-SSO the satellite can obtain high and low tide errors since it passes by the location at different times and therefore, can eliminate to a high degree by averaging these high and low tide errors. In case of a SSO, eliminating the error will not be easy using only the data from the satellite. This will be done using help from very accurate tide models obtained from other satellites and in some cases, the data from this satellite can be used to improve the data on those models.

5.3 Eclipse time

Any satellite orbiting the Earth will experience some of its orbit time in the shadow of the Earth. During this time, which is known as eclipse, the satellite will not be illuminated by the sun and therefore the solar panels will not be functional and the battery has to be used as the power source; therefore, in order to be able to to correctly size the batteries for the satellite and also designing the thermal subsystem, it is important to know what fraction of the satellite orbit is spent in eclipse. In the special (and perfect) case of a dawn-dusk SSO, which is also the most promising orbit type to be chosen for the satellite, the satellite will always be illuminated by the sun and it will never experience eclipse; however, this perfect case almost never happens in launching real orbits due to the non-spherical Earth effect and the non-zero eccentricity. A perfect example of this can be found in ESA's GOCE satellite. GOCE was supposed to be operational in a circular dawn-dusk SSO, however this satellite still experienced some eclipse seasons. Based on ESA's website [45], GOCE experienced short eclipses of around 11 minutes per orbit during the months June and July and longer eclipses of about 28 minutes in the months October and February. It is obvious that the satellite will inevitably experience these eclipses even when put in a dawn-dusk SSO.

The existence of the eclipse periods bring the need for reconsideration in battery sizing. during the eclipse periods, the batteries will be responsible for providing power to the satellite, therefore it is important to have an estimate of how much these eclipse periods will be. In order to do so, the STK software will be used as guidance since it is very hard to calculate the imperfections of the orbit by hand. In the STK software, the special SSO orbit is chosen with an altitude of 580 km. Once the altitude is inserted, the other parameters will be calculated by the software. The only parameter that can vary is the Right Ascension of the Ascending Node (RAAN). In order to have the closest possible scenario to the dawn-dusk SSO, the RAAN is chosen to be 15°. (the STK software does not automatically provide the special dawn-dusk SSO, therefore the RAAN can only be estimated.) Using these values the maximum eclipse time will be calculated by the software. Finally, based on the calculations of the software, it can be seen that for an interval of a year, the maximum eclipse time will be about **26** minutes.

5.4 Coverage density

throughout the year 2004, the orbit of the GRACE satellite started to slowly fall into a short repeat track. This continued to deteriorate until September, 2004 when the satellite was experiencing a very short repeat track of 61 revolutions per 4 days; this caused the gravity field resolution of the satellite to drop to one fourth of its expected value [46]. This experience shows that as the satellite decays in its orbit, different ground tracks will be achieved by the satellite and it has be made sure that the satellite, especially with an operational lifetime of only 3 years, covers enough ground track every month as its orbit altitude decreases.

In section 5.1, it was discussed that the altitude of 580 km will be the most appropriate altitude for the satellite based on the decay and life time. It was also mentioned that the satellite will decay about 8.83 km within the first 3 years of its operational life, therefore in order to make sure that the satellite will be able to cover enough ground track and will not face the same problem the GRACE did, the ground track coverage ability of the satellite has to be investigated. In order to do so, it will assumed that the ground track coverage of the satellite can change significantly every 2 km. Using a Matrix Laboratory (MATLAB) code, plots for the coverage density of the orbit for the altitudes of 580, 578, 576, 574, 572, and 570 km for a period of one month will be produced, shown in figures 5.2, 5.3, 5.4, 5.5 and 5.6. Additional figures regarding the coverage density will be given in appendix B. The plots are produced by J. Encarnacao (TU Delft, 2014).

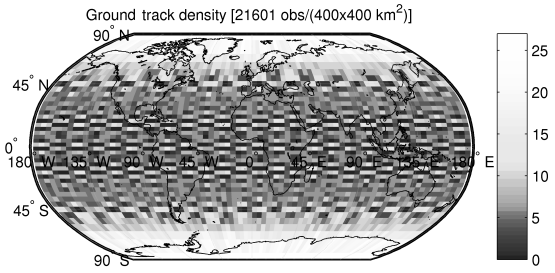

Figure 5.2: Coverage density of satellite's orbit at 580 km

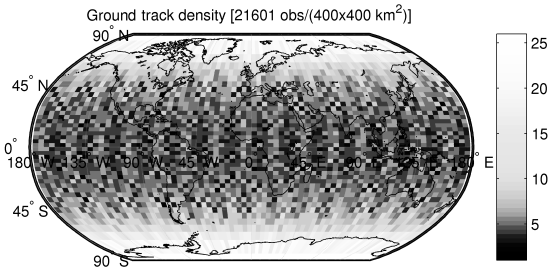

Figure 5.3: Coverage density of satellite's orbit at 578 km

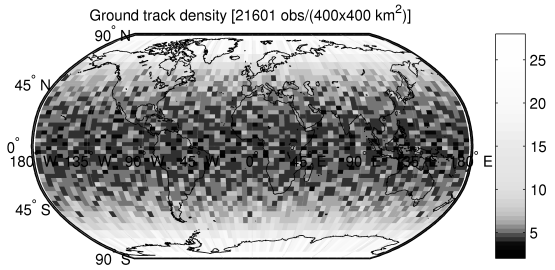

Figure 5.4: Coverage density of satellite's orbit at 576 km

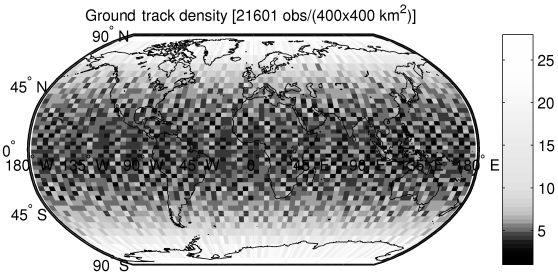

Figure 5.5: Coverage density of satellite's orbit at 574 km

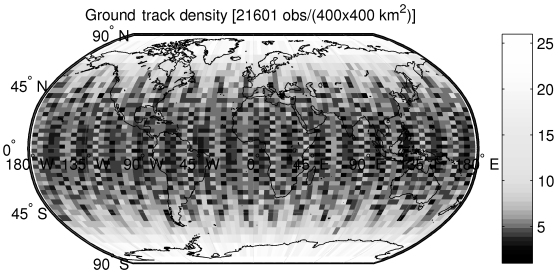

Figure 5.6: Coverage density of satellite's orbit at 572 km

As can be seen from the pictures, the satellite is able to cover almost the entire surface of the Earth within one month period in its initial orbit, and as it decays in its orbit, it would still be able to cover enough groundtrack for measurement purposes.

5.5 Astrodynamic results

This chapter discussed all the possible astrodynamic characteristics of the satellite and it explained how to obtain or determine these characteristics. Table 5.1 shows a summary of all these characteristics.

Table 5.1: Astrodynamic characteristics

Orbit type	Circular, Retrograde, Sun-synchronous
Orbit altitude [km]	580
Orbit inclination [deg]	97.7326
Coverage	Full Earth coverage within a month
Mission duration [yrs]	3
ΔV budget [km/s]	NA
Decay rate [km/3 yrs]	8.89
Lifetime [yrs]	22

6 Payload Design

The satellite payload is responsible for various satellite operations and tasks. Those involve being able to receive GNSS signals with a certain accuracy (defined by TR 3.1, chapter 3), tracking GNSS satellites and coping with non-gravitational accelerations.

To start off, the various occurring measurement errors are identified, and mitigation methods are presented. Then, several COTS GNSS receivers and antennas are described and traded against each other. The final receiver-antenna combination is then subjected to the GNSS link budget, to verify that it the received signal is of sufficient strength. Lastly, a non-gravitational accelerations mitigation method is chosen, which is either implementing an accelerometer or removing those accelerations by means of a numerical model.

6.1 Measurement errors

Measurements of GNSS signals are influenced by several types of (random) errors namely: receiver based errors, satellite based errors and propagation medium errors [47] [11]. An overview of the various error types and corresponding magnitudes is provided in table 6.1.

6.1.1 Receiver based errors

Errors induced in the user receiver are: receiver measurement noise, receiver clock error, multipath error and receiver instrumental bias.

Thermal noise induced by amplifiers, antenna's cables and the receivers all contribute to the random thermal noise induced on the GNSS measurements. Interference from other GPS like signals and quantization noise correspondingly attribute to the receiver measurement noise.

The receiver clock error is an additional parameter in the user position estimation algorithm. Four satellites are required to determine the user position in three dimension as well as the receiver clock error.

Multipath error is caused by reflections from objects in the vicinity of the receiving antenna(s) causing the signal to arrive at the receiver via multiple paths. The phase and amplitude are distorted as the reflected signals are superimposed on the desired direct-path signal. Both code and carrier phase measurements are affected but the magnitude of the error differs significantly. The technique used to mitigate the error can be classified in three categories: pos t-receiver signal processing, pre-receiver and receiver signal processing. Modifying the tracking loop discriminator is a receiver signal processing technique to resist multipath signals. Using a good antenna design which include choke-ring or pinwheel antennas will reduce multipath errors.

Analog hardware within the receiver causes an instrumental bias error due to the frequency dependent transmission delays. The differential instrumental bias is only existent in dual frequency receivers and affects ionospheric delay measurements. Techniques based on Kalman filtering and least squares adjustment methods can be used to estimate the instrumental bias in the satellite and receiver.

6.1.2 Satellite based errors

Errors that originate at the satellite comprise of instrumental bias errors, relativistic effects due to the dissimilar gravitational potential experienced by satellites, satellite clock errors and ephemeris errors.

The L1 and L2 signals propagate through different analog circuitry before digitization entailing that these signals undergo different propagation delays within the satellite causing instrumental bias. Each of the two GPS frequencies have an instrumental bias, the difference between these instrumental biases is known as differential instrumental bias. The satellites differential instrumental biases corrupt the ionospheric delay measurements obtained from a dual frequency receiver. Elimination of instrumental biases must be estimated and mitigated to obtain accurate estimates of the inospheric delay.

The special and general theory of relativity predicts that the clocks used in the GNSS transmitter and receiver are affected by relativistic effects. The GNSS satellite clock would run at a different pace than the receiver clock due to difference in perceived gravitational potential. To compensate for the prescribed relativistic effects, the satellite clock frequency is adjusted to 10.22999999543 MHz before launch. The user receiver is also required to make a correction for the periodic effect that arises due to the assumption of a circular orbit. The elliptical orbit of GNSS satellites cause a time invariant gravitational potential and velocity.

GNSS satellites incorporate highly stable clocks that do not decorrelate spatially, but can decorrelate temporally. An error of about 8.64 to 17.29 ns per day is caused by the drift of the satellites clock. Each GNSS satellite clock is individual analyzed by a master control station to determine the clock error. The station transmits the value of the clock error to each individual GNSS satellite for rebroadcast in the navigation mission. The error for the Coarse/Acquisition (C/A) code pseudorange observations is modelled as a 2nd degree polynomial.

6.1.3 Errors due to propagation medium

The errors induced by delay of the GPS signal as it propagates through the layers of the atmosphere include the ionosphere and tropospheric delay. The tropospheric delay is non-existent for receivers placed in LEO.

The ionosphere is a region in the atmosphere that consists of ionized gases free of electrons and ions extending from 50 to approximately 1000 km. The presence of free electrons in the ionosphere changes the velocity and direction of propagation of the GNSS signals. This effect delays the code phase measurements but advances the carrier phase measurements.

Table 6.1: Overview of various errors and corresponding magnitudes [11]

	Single-frequency	Dual-frequency
Receiver clock error (m)	1.5	1.5
Multipath error (m)	1-5 (code) 0.01 - 0.05 (carrier)	1-5 (code) 0.01 - 0.05 (carrier)
Receiver instrumental bias (m)	-	5.0
Receiver measurement noise (m)	0.5 (code) 0.001 - 0.002 (carrier)	0.5 (code) 0.001 - 0.002 (carrier)
Ephemeris error	1.5	1.5
Satellite clock error(m)	2.59 - 5.18	2.59 - 5.18
Relativistic effects	-	-
Satellite instrument bias	0.55	1.5
Ionospheric delay (m)	1 - 15 (depending on elevation)	-

6.2 Error mitigation methods

This section will specify and discus several methods to mitigate induced errors as discussed in section 6.1.

6.2.1 GNSS protocols

Combining multiple GNSS systems can be beneficial if increased performance is required. The benefits of additional available satellites and their corresponding signals can be classified in terms of continuity, accuracy, efficiency, availability and reliability.[48]

Improved continuity can be acquired due to the independency of the various GNSS systems. There is a possibility that a single system has a global malfunction, furthermore GNSS signals are vulnerable to interference and jamming. This is indeed the reason why nations design and operate their own system to insure independency of other parties. In times of war or heightened tensions, non-military users may be denied from high precision signals. Hence the increased number of signals and frequencies ensures an overall higher continuity and mission probability of success.

The greatest benefit of interest is the increased accuracy obtainable with multiple GNSS signals. The increased number of available satellites means that a certain level of accuracy can be achieved in a shorter time-span. The additional set of signals implies that more measurements can be processed by the receivers positioning algorithm. The accuracy of the position determination will be less subject to the influence of satellite geometry as the Positional Dilution of Precision (PDOP) will be small and constant. The PDOP indicates the accuracy of the 3D GNSS signal based on the number of available satellites and the geometry of their respective positions. Another benefit of combining multiple GNSS signals is the possibility to mitigate effects as multipath and interference. This can be achieved by the implementation of signal selection algorithms, ensuring that only measurements of high quality are processed. This allows one to select a high elevation angle cut-off.

The availability of additional satellites improves efficiency, especially for carrier phase based positioning. The additional satellites will significantly reduce the required time to resolve ambiguities.

Another advantage of using multiple GNSS systems is the improved reliability. The additional set(s) of measurements increases redundancy which can be helpful to identify outliers.

Disadvantages of the additional use of GNSS signals are the increased power consumption and data generation. The data rate will increase by the integer number of additional GNSS signals used.

Quantitatively, experiments have shown that the addition of GLONASS measurements improves geometry (PDOP) and visibility by more than 30% and 60% respectively. These numbers are however deduced using a terrestrial placed receiver. The additional GNSS signals will primarily be beneficial in cases where the receiver is obscured from view and were fast convergence is required. As one is mainly interested in the accuracy achieved in post processing using kinematic POD, fast convergence is not required. Although the faster convergence rate is not beneficial, using multiple GNSS protocols is still beneficial to archive a higher accuracy with higher reliability ensuring a overall more robust solution.

6.2.2 Dual- and single-frequency GNSS receivers

The use of dual-frequency GNSS data transmission and reception is known as a useful tool for Precise Point Positioning (PPP). The dual-frequency receiver operates on both the L1 and L2 frequency band, which enables good handling of ionospheric delays. When compared to the single-frequency alternative (L1 only), this option is technically more enhanced and therefore more expensive. To examine whether a dual-frequency receiver is necessary, or whether the single-frequency receiver suffices, an evaluation on both receiver types is necessary. This section provides a basic elaboration on dual-frequency and single-frequency PPP, a description of reference GNSS receivers, and a discussion on the topic of differencing with multiple GNSS receivers.

6.2.2.1 Dual-frequency GNSS receiver

In PPP ionospheric delays are most often handled by means of a dual-frequency GNSS receiver that forms the so-called ionosphere-free linear combination of L1 and L2 carrier phase and pseudo-range observations [49]. Dual-frequency positioning reaches a centimeter-level accuracy, but unfortunately shows slow convergence towards this final result (20-40 minutes). However, the mission does not require real-time positioning so fast convergence of the receiver accuracy is not necessary.

Furthermore, the aforementioned ionosphere-free linear combination amplifies multipath and receiver measurement errors and is therefore very noisy. Increasing the pseudo-range will increase this noise.

6.2.2.2 Single-frequency GNSS receiver

The formation of the ionosphere-free linear combination of L1 and L2 is not possible via single-frequency PPP, since the single-frequency receivers do not operate on both bands. In single-frequency PPP the ionospheric delays can be handled by using a linear combination of L1 code and carrier phase data, or

by using external data on ionospheric delays (e.g. from the gridded global ionosphere maps). Single-frequency positioning reaches a decimeter-level accuracy, but converges quickly to its best accuracy. But as mentioned earlier, fast convergence is of no important for this mission.

6.2.2.3 Comparison of dual-and single-frequency GNSS receivers

Comparing various dual-and single-frequency receivers, it is concluded that the gain in accuracy of dual-frequency far outweighs its loss in affordability. An overview of the studied receivers, together with the main characteristics, is provided in tables A.1 and A.2 in appendix A.

6.3 COTS GNSS receivers

Recent scientific applications of spaceborn GNSS have relied on dedicated receivers such as Blackjack, GNSS Receiver for Atmospheric Sounding (GRAS) and Lagrange. These receivers can all be characterized by a high level of specialization, limited production volume and demanding qualification program resulting in a price tag in the order of 1 million dollar. This situation causes an increased interest in affordable alternatives for missions where ultimate reliability and space qualification are not required. Research has shown that COTS geodetic GNSS receivers can, with little to no modifications, operate with the increased signal dynamics and environmental conditions of a LEO.

Deutsche Luft- und Raumfahrt (DLR) tested two dual-frequency COTS receivers: Nov-Atel's OEM4-G2L and Septentrio's PolaRx2 and compared them to JPL's IGOR (a follow-on of Blackjack).[17] The COTS receivers both provided accurate code and carrier phase measurements for POD. The use of COTS receivers is therefore ideal for low-cost applications which do require high accuracy positional determination.

6.3.1 Velocity restriction

One modification that is required to use COTS receivers in a space environment is the removal of the Coordinating Committee for Multilateral Export Controls (COCOM). The COCOM limits the operational velocity hence to ensure operability in space this limiter has to be removed. Manufacturers of COTS receivers charge additional cost in the order of $ 1000 for the removal of the COCOM [50].

6.3.2 Ionizing radiation

The main environmental difference between space and Earth's surface is the substantial presence of cosmic radiation in space. This radiation has a large influence on the lifetime of the GNSS receiver and it is therefore an important aspect of the lifetime requirement (see chapter 3 NTR 3-1). Most COTS receivers are not designed to take radiation into account, so in order to use them for space applications they have to be tested. The critical factor for the receiver lifetime is the Total Ionizing Dose (TID), which increases with orbit height. The TID describes the total cumulative radiation over the receiver's lifetime in orbit. Since the satellite will be in LEO, Earth's magnetic field will limit the peak radiation to a low level, so this will not cause severe problems [51][52]. TID testing of IGOR has determined a maximum TID of 12 *krad* before failure occurs, which proved to be enough for a lifetime of several years in LEO. TID tests of COTS receivers, such as OEM4-G2 and PolaRx2@, have resulted in lower TID values: 6 *krad* and 9 *krad*, respectively [51] [52]. OEM4-G2's maximum TID of 6 *krad* results in a lifetime of 2 years in LEO [17]. It is clear that in order to achieve the required lifetime of 3 years, a protective casing should be added to raise the maximum TID to 12 *krad* TID. For TID's of reference single- and dual-frequency GNSS receivers, the reader is referred to tables A.1 and A.2 in appendix A.

6.3.3 GNSS receiver trade-off

With the obtained knowledge from previous sections one is now able to select a GNSS receiver. Following requirement NTR-2, chapter 3, it is determined to only consider COTS receivers in the trade-off. As described in section 6.3, the main advantages of using a COTS receiver are the low power use and mass, the small size and cost, while still maintaining high accuracy compared to space certified receivers. This is in line with the mission philosophy and the CubeSat system. The manufacturers chosen to provide

the receivers are Septentrio and NovAtel. Both have provided receivers for space applications and hence have a flight proven record. Characteristics of their small-sized dual-frequency receivers are collected in table 6.2.

Table 6.2: Dual-frequency COTS GNSS receivers

	OEM615	OEM628	OEM638	AsteRx-m OEM	AsteRx2e OEM
Manufacturer	NovAtel (CA)	NovAtel (CA)	NovAtel (CA)	Septentrio (B)	Septentrio (B)
Frequency channels	L1/L2	L1/L2/L5	L1/L2/L5	L1/L2	L1/L2
GNSS protocols	GPS, GLONASS, Galileo, BeiDou	GPS, GLONASS, Galileo, BeiDou	GPS, GLONASS, Galileo, BeiDou	GPS, GLONASS	GPS, GLONASS
GPS carrier phase measurement accuracy L1/L2/L5 (mm)	0.5/0.5/N.A.	0.5/0.5/0.5	0.5/0.5/0.5	1.0/1.0/N.A	1.0/1.0/N.A
GLONASS carrier phase measurement accuracy L1/L2 (mm)	1.0/0.5	1.0/0.5	1.0/0.5	1.0/1.0	1.0/1.0
Tracking performance ($dB-Hz$):					
Tracking	-	-	-	26.00	26.00
Acquisition	-	-	-	33.00	33.00
Maximum data rate (Hz)	50	100	100	25	25
Mass (g)	29	37	84	47	60
Length $\times$ width $\times$ height (mm)	$71 \times 46 \times 11$	$100 \times 60 \times 9$	$125 \times 85 \times 14.3$	$70 \times 48 \times 8$	$90 \times 60 \times 8$
Operating temperature (°C)	-40 to 85	-40 to 85	-40 to 85	-40 to 85	-40 to 85
Power consumption (W)	1.2	1.3	2.8	0.49	1.5
Antenna LNA power output (VDC)	5.0	5±5%	5±5%	3.3	5.0
Antenna maximum current (mA)	100	100	200	200	200
No. of channels	120	120	240	136	136
Receiver clock error (ns)	20	20	20	10	10
Time to first fix (s)					
Cold start	50	50	50	45	45
Hot start	35	35	35	20	20

The trade-off for the GNSS receiver selection is based on various performance characteristics:

- Capabilities: number of frequency channels and GNSS protocols;
- Carrier phase measurement accuracy: must be minimized to meet requirement TR-3, chapter 3;
- Receiver clock error: must be minimized;

Next to the above-listed characteristics, the receiver mass, dimensions and power consumption must be minimized.

From table 6.2, the main advantage of the NovAtel receivers with respect to the Septentrio ones is the fact that they operate on the L5 frequency channel next to just L1 and L2 (except for the OEM615), and are able to receive Galileo and BeiDou next to just GPS and GLONASS. However, at the moment, only three GPS satellites are broadcasting L5 signals, Galileo is not operational and BeiDou only serves the Asia-Pacific region. Furthermore, the Septentrio receivers can eventually be updated to enable Galileo tracking. Therefore, the extra capabilities of NovAtel' receivers with respect to Septentrio's are not considered highly beneficial for the mission as of yet. In the future, with more L5-broadcasting GPS satellites, Galileo operational and BeiDou expanded to global scale, these extra capabilities will prove their usefulness.

Next to having more capabilities, the NovAtel's L1/L2 GPS and L2 GLONASS carrier phase measurement are 0.5 mm more accurate than Septentrio's. On the other hand, Septentrio's clock error is about 10 ns smaller than NovAtel's. Recalling requirement TR-3, chapter 3, it is concluded that all receivers amply comply with the requirement that the error in center of mass position due to GNSS measurement noise should be smaller than 1 cm, as measurement errors are in the order of mm and clock errors are in the order of ns.

Clearly, selection cannot be based only on the receivers' capabilities and performance characteristics, as all receivers perform sufficiently to comply with the requirements. Therefore, the receivers' masses, dimensions and power consumptions are decisive in this trade-off. With the mass being only 47 g, the critical dimension being 70 mm and the power consumption being only 0.49 W, the AsteRx-m OEM is selected to operate on GES.

6.4 GNSS receiver antenna

The antenna selection starts by an elaboration on several antenna types as each type has its own advantages and disadvantages. After choosing the most applicable antenna type, the final antenna selection is performed. Recalling requirement NTR-2, chapter 3, stating that COTS components should be used where possible, the antenna trade-off considers various reference antennas from different companies.

6.4.1 Antenna types

An antenna can have various shapes and may or may not include electrical components. This section provides a main insight in the advantages and disadvantages of active and passive antennas and discusses relevant antenna shapes, and corresponding sizes.

6.4.1.1 Active vs. passive antennas

An active GNSS antenna contains a Low-Noise Amplifier (LNA) and/or a preamplifier that boosts the signal strength of a weak received signal in order to prepare it for usage by the GNSS receiver. The consequence of using such electrical instruments is that an active GNSS antenna requires power, and therefore needs to be incorporated in the power budget. This directly relates to the main advantage of a passive GNSS antenna that does not use electrical components and therefore does not requires any power. Whether or not the received GNSS signal needs amplification is determined from the GPS link budget, as the potential antenna-receiver combination must yield a tolerant link margin ($>> 3\ dB$ [41]). This is executed in section 6.4.2 using the GNSS link budget provided in section 6.5.

6.4.1.2 Antenna shape

A variety of antenna shapes exists, ranging from parabolic to bionical horn-like, some of which are more applicable to CubeSats than others. For example, parabolic antennas are often used on the ground for communication purposes. This is because parabolic antennas typically yield a high gain (typically between 15 and 65 dBi [41]). Such a high gain is not required for the GNSS receiver antenna, as data rates are relatively low here. Furthermore, parabolic antennas are too large ($\sim m$) for CubeSat applications.

A common antenna for receiving GNSS signals is the patch antenna. This type of antenna is for example used on the BlackJack receiver and is possible to integrate with a CubeSat due to its dimensions, which are in the order of centimeters. The latter in combination with the fact that patch antennas are relatively inexpensive are the decisive arguments for selecting a patch antenna to accompany the AsteRx-m OEM receiver.

6.4.1.3 Reference patch antennas

As mentioned in section 6.4.1.2, the GNSS receiver antenna does not need a high gain, as it has to cope with relatively low data rates. Therefore, a simple, inexpensive patch antenna will suffice. Apart from being inexpensive, a patch antenna is lightweight and easy to integrate with other electronics.

As described in section 6.2.1, making use of GLONASS and eventually Galileo next to GPS shows serious advantages in terms of continuity, accuracy, efficiency, availability and reliability. This translates directly in the requirement that the receiver antenna needs to operate on at least the L1 and L2 frequency band. NovAtel and Antcom provide inexpensive ($\sim 10^3$ euros) dual-band and dual-frequency GNSS antennas for aircraft applications, some of which are provided in table 6.3.

Table 6.3: Reference antennas and corresponding characteristics

	42GOXX16A4-XT-1-1	ACCG5Ant-2AT1	ACCG5Ant-3AT1
Manufacturer	NovAtel (CA)	Antcom (US)	Antcom (US)
Frequency band	L1/L2	L1/L2/L5	L1/L2/L5
Antenna gain @90° (free space) (dBi):			
L1 GPS	3.3	4.1	4.0
L1 GLONASS	−2.7	2.0	3.0
L2 GPS	3.1	0.5	2.6
L2 GLONASS	1.5	−0.8	0.0
L5 GPS	N.A.	−7.0	−3.0
LNA gain (free space) (dB):			
L1 GPS	33	32	33
L1 GLONASS	33	31	33
L2 GPS	35	35	35
L2 GLONASS	35	35	35
L5 GPS	N.A.	35	35
3 dB Beamwidth (°):			
L1 GPS	100	95	95
L1 GLONASS	100	95	95
L2 GPS	105	105	110
L2 GLONASS	100	90	105
L5 GPS	N.A.	105	110
LNA typical power	0.116	0.116	0.116
Noise figure (dB)	3.0	3.0	3.0
Mass (g)	227	156	256
Length × width × height (cm)	$11.9 \times 7.6 \times 2.3$	$6.7 \times 6.7 \times 2.1$	$8.9 \times 8.9 \times 2.2$
Temperature (°C)	−55 to 85	−55 to 85	−55 to 85

Comparing the antennas from table 6.3, it is clear that Antcom's ACCG5Ant-2AT1 is most favourable in terms of mass and dimensions, but hands in antenna gain and beamwidth with respect to its alternatives. In the next session, the three antennas are traded against each other and a final antenna is selected.

6.4.2 Antenna trade-off

First, for each reference antenna, the relevant characteristic values are substituted in the link budget provided in section 6.5. This is to verify whether the potential antenna-receiver combination yields a tolerant link margin ($>>$ 3 dB [41]). The obtained link margins for both the active and the passive case, are collected in table 6.4. Self-evidently, the antenna gain is used for calculation of the passive link margins, whereas the LNA gain is used for active link margin computations.

Table 6.4: Passive and active link margin for the 42GOXX16A4-XT-1-1, ACCG5Ant-2AT1 and ACCG5Ant-3AT1 antenna

	42GOXX16A4-XT-1-1	ACCG5Ant-2AT1	ACCG5Ant-3AT1
Passive link margin (dB)			
L1 GPS	2.46	3.26	3.16
L2 GPS	4.76	2.16	4.26
L1 GLONASS	-2.97	1.73	2.73
L2 GLONASS	3.42	1.12	1.92
Active link margin (dB)			
L1 GPS	32.2	31.2	32.2
L2 GPS	36.7	36.7	36.7
L1 GLONASS	32.7	30.7	32.7
L2 GLONASS	36.9	36.9	36.9

It has to be noted that the free space antenna and LNA gains are used for computation of the link margins. In reality, the fact that the antenna is mounted on a certain ground plane (the satellite) has an effect on the antenna gain. Usually this effect is an increase in gain, but to be on the safe side this is neglected here.

From table 6.4 it is concluded that the two passive Antcom antennas have a high enough sensitivity to successfully receive both L1/L2 GPS and L1/L2 GLONASS. The NovAtel antenna will show deficiencies in receiving the L1 GLONASS signal. Following the tolerant link margin requirement of 3 dB [41], the passive link margins of 42GOXX16A4-XT-1-1 and ACCG5Ant-2AT1 do not satisfy. Antcom's ACCG5Ant-3AT1 does meet the link margin requirement for GPS but not for GLONASS. Therefore the complete passive link margin of ACCG5Ant-3AT1 is not tolerant enough either. This leads to the conclusion that an LNA needs to be incorporated and antenna selection is based on the active link margin.

The active link margins do not vary significantly. Each of the active link margins in table 6.4 yields a very tolerant link budget, as the required link margin is amply met. Furthermore, each antenna requires 0.116 W to achieve this link margin, so no distinction can be made here. However, the 42GOXX16A4-XT-1-1 has a length of 11.9 cm which is difficult to integrate with the CubeSat structure. Therefore a final choice has to be made between the two Antcom antennas. The ACCG5Ant-3AT1 antenna shows a slightly better performance in terms of gain and beamwidth, but is 100 g heavier and ± 2 cm wider than the ACCG5Ant-2AT1 antenna. Based on the latter, Antcom's ACCG5Ant-2AT1 antenna is selected to accompany Septentrio's AsteRx-m OEM receiver.

6.4.3 Antenna lay-out

Figure 6.1 gives an impression of the physical appearance of the ACCG5Ant-2AT1 antenna. This section comments on the antenna phase center and occurring Phase Center Variation (PCV). Additionally, a final note regarding the antenna casing is made.

As previously indicated in the Mid-Term report, a precise knowledge of the position of the antenna phase center is crucial for precise determination of the satellite's center of mass. This is easily explained by the fact that the GNSS signals are received in the antenna phase center, while Earth's gravity acts on the satellite's center of mass. Therefore, knowing the distance vector between those points is vital. The location of the antenna phase center is provided by Antcom and depicted in figure 6.1. It has to be noted that the displayed phase center is not constant and varies with the direction of the incoming signal.

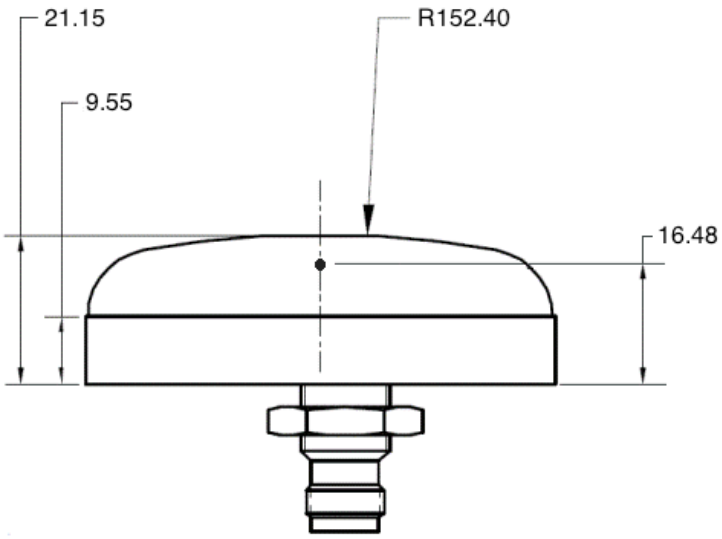

Figure 6.1: Side view of ACCG5Ant-2AT1, including phase center location (dimensions in mm) [2]

As mentioned before, the antenna is initially designed for aircraft applications. Therefore, its casing is aerodynamically shaped and designed for heavy weather it might face. Figure 6.1 shows that the antenna has a spherical casing, which causes a height increase of 10.50 mm. For space flight aerodynamic design is irrelevant and precipitation nor storms occur. Hence, the spherical case can either be replaced by a flat one or removed completely, to decrease the antenna's mass and height and to increase its integrability with the CubeSat.

6.5 GNSS link budget

The GNSS link budget accounts for signal power, noise power and interference power at relevant points in the system. For this analysis the carrier power to noise power spectral density ratio is calculated at the receiver. The link budget is determined for the worst case scenario with given system components, that is the condition were the elevation angle between the GNSS satellite and the receiver satellite is minimal and the slant range maximal.

6.5.1 Numerical model

The link budget that is presented in this section is based on the numerical approach set up by Rouquette [53].

Considering the single zenith mounted omnidirectional antenna, the theoretical radiation pattern is a half sphere meaning that the minimum elevation angle for tracking is 0 °. The orbit simulation tool STK was used to determine the maximum slant range at minimum elevation between receiver and transmitter simulated over a 3 year lifespan.

The carrier power to noise power spectral density ratio or Carrier-to-noise ratio (CNR) is the Signal-to-noise ratio (SNR) of a modulated signal. It can be formulated as dictated in 6.1. It is dependent on the gain and power of the GNSS transmitter, the slant range between receiver and transmitter, carrier wavelength (L1 or L2), receiver antenna gain and receiver system noise temperature.

$$\left(\frac{C}{N_0}\right)_{dB/Hz} = 10\log P_s G_s - 20\log\frac{4\pi R}{\lambda} + 10\log\frac{G_r}{T_s} + 10\log L - 10\log k \tag{6.1}$$

The system temperature 6.2 depends on the reference temperature; which is the exposed temperature of the antenna, antenna noise temperature and the noise figure which is a measure of the degradation of

the SNR. The noise figure is deduced from the antenna manufacturer.

$$T_s = T_a + T_0(NF - 1) \tag{6.2}$$

The antenna noise temperature 6.3 is the temperature of a hypothetical resister of an ideal receiver of the input of an ideal noise-free receiver that would generate the same output noise power per unit bandwidth as that at the antenna output at a specified frequency. It is dependent on the efficiency of the antenna, back to front ratio and the sky temperature. The back to front ratio is the ratio of power gain between the front and rear of a directional antenna. The sky temperature is in this case the cosmic background radiation.

$$T_a = \eta(T_{sky} + R_{bf}T_0) + (1 - \eta)T_0 \tag{6.3}$$

The additional losses 6.4 are dependent on the polarization losses and the reflection coefficient of receiver and transmitter antenna. The polarization match is the ratio between the left and right polarized radiation pattern. The reflection coefficient is the ratio of the reflected wave amplitude to the incident wave amplitude and can be obtained can be obtained using the standing wave ratio specified by the antenna manufacturer.

$$L = p(1 - \Gamma_s^2)(1 - \Gamma_r^2) \tag{6.4}$$

The free space loss 6.5 is computed via the slant range and the carrier wave length.

$$L_p = 20 \log \frac{4\pi R}{\lambda} \tag{6.5}$$

Finally one is able to deduce the link margin 6.6 by subtracting the minimum required CNR for tracking and acquisition, which is a receiver parameter deduced by the manufacturer and the calculated CNR.

$$M_{dB/Hz} = \left(\frac{C}{N_0}\right) - \left(\frac{C}{N_0}\right)_{min} \tag{6.6}$$

Table 6.5: GNSS link budget

Symbol	Discription	I/O	Unit	Value			
				L1 GPS	L2 GPS	L1 GLONASS	L2 GLONASS
P_s	Satellite antenna power	I	dBW	16.5	16.5	16.5	16.5
G_s	Satellite antenna gain	I	dBi	13.8	13.8	13.8	13.8
R	Range	I	m	25350000	25350000	24250000	24250000
c	Speed of light	I	m/s	299792458	299792458	299792458	299792458
f_c	Carrier frequency	I	MHz	1575.42	1227.6	1602	1246
λ	Carrier wavelength	O	m	0.190293673	0.244210213	0.187136366	0.240603899
G_r	Receive antenna gain	I	dBi	4.1	0.5	2	-0.8
T_s	Receive system noise temperature	O	K	853.5	853.5	853.5	853.5
T_a	Antenna noise temperature	O	K	284.5	284.5	284.5	284.5
T_{sky}	Clear sky temperature	I	K	2.7	2.7	2.7	2.7
R_{bf}	Antenna back-to-front ratio	I	-	0.333333333	0.333333333	0.333333333	0.333333333
T_0	Reference temperature	I	K	284.5	284.5	284.5	284.5
NF	Receive noise figure	I	-	3	3	3	3
L	Additional losses	O	-	0.80256	0.8667648	0.8667648	0.8667648
p	Polarization match	I	-	1	1	1	1
Γ_s	Satellite antenna reflection coefficient	I	-	0.1	0.1	0.1	0.1
Γ_y	Receive antenna reflection coefficient	I	-	0.333333333	0.2	0.2	0.2
α	Atmospheric loss	I	-	0.912	0.912	0.912	0.912
k	Boltzmann constant	I	J/K	1.38E-23	1.38E-23	1.38E-23	1.38E-23
L_p	Path loss	O	dB	184.4752696	182.3084801	184.2352683	182.0523789
C/N_0	Carrier power to noise power spectral density ratio	O	dB/Hz	48.2586794	47.15970645	46.73291823	46.11580761
$(C/N_0)_{min}$	Minimal carrier power to noise power spectral density ratio	O	dB/Hz	45	45	45	45
M_{db}/Hz	Link margin	O	dB	3.2586794	2.159706451	1.732918226	1.115807614

It is interesting to note that the manufacturer specified CNR influences the measurement noise hence the obtainable accuracy. If one demands the highest possible carrier phase accuracy a CNR of 45 dB/Hz is required [15], which is a very significant 13 dB higher than what is required for basic acquisition and tracking. Even in this most demanding condition a passive antenna would provide a positive link margin

for GPS and GLONASS. If a LNA is added between receiver and antenna a generous link margin of more than 30 dB/Hz is obtained.

6.5.2 Performance analysis

The achievable positioning accuracy is dependent on the number of satellites that can be simultaneously tracked by the satellite receiver. Research has shown that a reduced number of visible satellites will lower the kinematic orbit precision. With eight or fewer satellites the loss of one or two observations could be critical for the quality of the POD kinematic positions [54].

There is however a downside to measurements taken from GNSS satellites at extreme angles. Besides the lowered received CNR as described in previous section the increased slant range for low elevation GNSS satellites induces a higher ionospheric error, fortunately this error is mitigated via dual-frequency carrier phase measurements.

With the simulation tool STK it was determined that between 10 and 15 GPS satellites could be continuously tracked at minimum elevation.

6.5.3 Effects of Carrier-To-Noise-Ratio

The Canadian CanX-2 triple-CubeSat equipped with a COTS NovAtel OEM4-G2L GPS receiver has yielded sub-par tracking performance due to an unexpected low CNR at the receiver. [55] This had a dramatic effect on the number of satellites that could be tracked simultaneously directly degrading the positional accuracy. The reason for this lower then expected SNR lies in the combination of smaller discrepancies which together resulted in a 5 to 10 dB/Hz lower CNR:

- Close proximity of the antenna, receiver board, and possibly other electronic components causing interference.
- The lacking of proper ground plane.
- The partial blockage of the antenna.
- A lower quality gauge cable as compared to the test setup.

To reduce the risk of analogous problems, the GES will implement the lessons-learned from the CanX-2 mission.

The reduce the risk interference system testing will be executed to determine the need for additional shielding. The selected GNSS receiver does however implement an off-factory Electro Magnetic Interference (EMI) shielding. The position of the GNSS antenna is selected with care to reduce the change of multipath error. The GES GNSS antenna is mounted on the outside body of the satellite bus solving two problems of the CanX-2; the outside surface provides a ground plane, while the ground plane ideally should be 12.7 cm x 12.7 cm specified by the manufacture. Although a larger ground plane is always beneficial [56] the improvement compared to the CanX-2 is very substantial as the latter has almost no ground plane at all due to the sunken antenna placement. The partial blockage of the antenna is prevented by mounting the antenna on the outside of the bus. It may be advisable to make a ground frame to prevent the outer extent of the power plane to go beyond the ground plane see figure 6.2 and figure 6.3. A choke ring will also result in a lower multipath error.

The loss of a gauge cable is directly proportional to it diameter hence weight, this loss is hard mitigate without compromising the mass.

There is also the possibility of interference with the satellites own communication system, especially when using S-band transmitters. [56]. The S-band is in the same frequency region as the GPS signal.

Although on first site the link between GNSS receiver and satellite seems a non-critical factor, several factors can seriously effect the performance. It is recommended to carefully select and experiment with the best elevation cut-off angle to obtain the most accurate position.

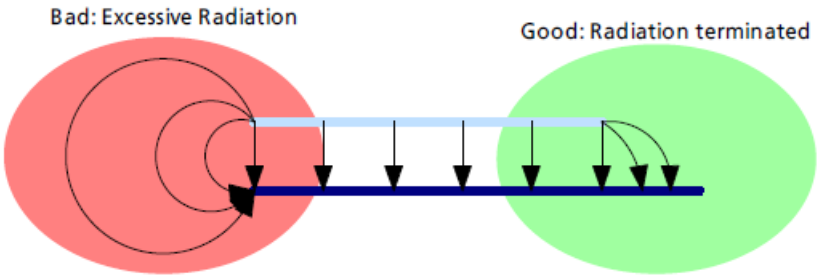

Figure 6.2: Signal and power plane extends lies beyond ground plane extends left side, within right side

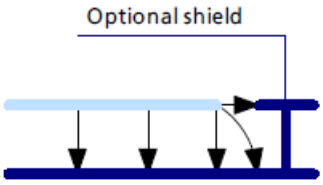

Figure 6.3: Signal and power plane extends with shield

6.6 Coping with non-gravitational accelerations

Non-gravitational forces have a significant effect on the satellite's behaviour. Therefore, coping with non-gravitational accelerations is of vital importance for this mission. Basically, there are three alternatives of recognizing those accelerations, that are: an accelerometer[1], a numerical model[2], and a combination of both. Each alternative will be treated in this section and a final mitigation method will be selected.

6.6.1 Accelerometers

This section will discuss the need and use of accelerometers in a gravity field determination mission. In the past, accelerometers have been used for gravity field determination of both the static and time variable gravity field, as well as for perturbation corrections. The accelerometers of the reference missions are extremely accurate, but also relatively heavy; GOCE's accelerometer system, for example, has a measurement level of $10^{-12} m/s^2$ but a total mass of 150 kg [57]. It is clear that an accelerometer system of this size is not feasible for GES. The mass budget constraints of this mission limit the level of accuracy obtainable. Even when taking recent technological developments into account, GOCE-like levels of accuracy are not reachable. These above-mentioned constraints limit the level of accuracy to a level similar to that achieved by CHAMP's accelerometer ($10^{-9} m/s^2$[57]).The use of this accelerometer on itself for active gravity field determination is not feasible as a higher accuracy is required.

Two potential conventional accelerometers that meet the mission requirements were found: the cub-Satellite Space Three-axis Accelerometer for Research mission (cubSTAR) by ONERA [58] and the Capacitive Accelerometer by SERENUM [59]. Both accelerometers make use of the same principle: a sensor cage with a proof mass in it. The mass acts as a mass in free fall and is kept in between capacitor plates, connected to the satellite bus, that resist proof mass' direction of movement. The voltage difference needed by the capacitor to keep the proof mass in place is measured and used to calculate the corresponding accelerations.

Unfortunately, both accelerometers are still priced far above budget, this led to the consideration of using a less conventional type of accelerometer: the optical MEMS accelerometers. The optical MEMS

[1] With this approach gravitational signals that are not of interests, like for example tidal differences, still need to be taken out with numerically. It is assumed that this is done in order to enable a proper comparison between the accelerometer and the numerical approach method

[2] The term numerical model in this report is used to describe the process of filtering out the GNSS data for non-gravitational disturbance and gravitational signals that are not of interest like for example tidal difference.

accelerometers look promising with a theoretical noise floor of View $8nG/\sqrt{Hz}$; however, they are still under development [60]. Lab testing results are getting better and approaching this theoretical limit. A result of $17nG/\sqrt{Hz}$ has been achieved [60] so far. It should be noted that these test were conducted at a way higher frequency, 1 kHz, than the frequency expected to be measured; 10^{-5} to 1 Hz. Just like the accelerometers from SERENUM and ONERA, a proof mass is used for measuring the displacement, only this time, this mass is measured using optical sensors; an increase in proof mass' mass will result in a higher accuracy [61]. Although the high-accuracy MEMS optical accelerometers are still in conceptual phase, some less accurate versions are already available. These have an accuracy in the $\mu m/s^2-$range. This is the accuracy range required for gaming applications[62], contrary to the desired accuracy for this mission, which is nm/s^2-range.

6.6.2 Numerical approach

This section provides an insight in the use of numerical models to filter out non-gravity related accelerations. The use of numerical methods is still experimental, however, some major improvements have been made over the last few years. Investigations by Ditmar et al. [63] into refinement of static gravity field models from the CHAMP mission discovered that numerical models are able to reduce the noise to the same level as the traditional approach with accelerometers. Further numerical studies [64] have confirmed that the use of an onboard accelerometer is not necessary for precise determination of static gravity field. Unfortunately, the story gets complicated when the time variable gravity field is the topic of interest. In the past the numerical models were considered as not accurate enough for the determination of the time-variable gravity field [64], however, new studies using numerical models have been able to obtain time variable gravity field in the same accuracy range as the ones obtained with accelerometer data [65]. Although, it should be noted that these numerical models are not very reliable as of yet [66]. For the mission at hand the numerical models will suffice for the accuracy requirements, considering the low spatial scale and relative low receiver noise requirements.

6.6.3 Results

A combination of the numerical model and an accelerometer allow validation of the numerical model. Since accelerometers capable of reaching the required accuracy are to expansive and the currently available MEMS accelerometers are not accurate enough, this combination does not form a feasible option.

Using an accelerometer is the traditional approach as it entails significantly less risk and is arguably less complicated. However, with the mission goal of a low cost mission (NTR 3.2, chapter 3), prices of current or future-planned accelerometers are just too high. Recent developments enable development of numerical models that can reach the required accuracy [65]. Depelopment of these models itself already forms an interesting project for students, and since universities are a major group of interest, this is an extra beneficiality. Using the models would also make it possible to prove the use of this new approach, making it easier to use GNSS data of future non-dedicated missions to get higher update rate and lower costs even further. All the above-mentioned reasons lead to the selection of the numerical approached mitigation method for this mission.

7 Subsystem Design

This chapter elaborates on the mission bus design. The design of each subsystem will be explained in separate sections. The AD&C, communications, TTC, C&DH, guidance and navigation, thermal control, power system, structural design, ground segment and launcher selection are presented in sections 7.1 to 7.8 respectively.

7.1 Attitude determination & control

When talking about designing a spacecraft, the Attitude Determination & Control System is one of the inevitable priorities of the design. This system is responsible for orienting the spacecraft in the right direction; any movement of the satellite has to be controlled by the AD&C system. This section discusses the process of selecting the proper AD&C system for the satellite mission at hand.

7.1.1 Requirements on AD&C

Just like any other segments of the design process, the mission will impose some requirements on the AD&C system as well. The requirements listed below will have an affect on the design of the AD&C system.

- TR-3 The error in centre of mass positioning due to inaccurate pointing of the satellite should be smaller than 1 *cm*.
- NTR-1 The minimum operational lifetime should be 3 years.
- NTR-2.1 The operating costs must be kept as low as possible, i.a. by using an autonomous satellite and a cheap ground station.
- NTR-2.3 The mass of the satellite should be as low as possible given the requirements.
- NTR-2.4 Where possible off-the-shelf components should be used.
- NTR-3.2 Where possible the most sustainable materials should be selected for the satellite.

As can be observed, all these requirements impact the design. The minimum operational life will require a system that can operate for that period of time within the power budget, the cost requirement emphasizes that expensive AD&C system products should be avoided, and the low mass requirement mentions that heavy products should be avoided as much as possible. However, the most important and the main driving requirement set for the AD&C system design is the pointing accuracy. The pointing accuracy that needs to be accomplished by the AD&C system depends on the ability of the payload to receive GNSS signals. When selecting the appropriate AD&C system, the combination of all these requirements have to be considered in order to achieve the best decision.

7.1.2 Basics of the AD&C system

The AD&C system consists of two main parts: sensors and actuators. Sensors are used for the determination of the attitude of the satellite and the actuators are responsible for orienting and controlling the motion of the satellite. A list of all possible sensors and actuators for spacecraft are mentioned in

Space Mission Analysis and Design (SMAD) [67]. As it is clear, different sensors and actuators have different accuracies and since pointing accuracy is the main requirement of the AD&C system design, the selection of the proper sensors and actuators is of utter importance. However, when considering these sensors and actuators, two problems arise: one is the fact that the data used for SMAD might be outdated since the technology is improving day by day and finding a reliable source for all these equipments is not feasible; furthermore, searching for all the possible new technologies for sensors and actuators might be very time consuming. The second problem arises from combining these individual components manually on the satellite, especially with such a small size; this will require determining the accuracies of all individual components and determining whether they will satisfy the requirements, plus the cost of combining these individual components will be very high. In order to come up with a solution for these problems, instead of combining the single AD&C system components together, the integrated AD&C system will be considered as an option.

7.1.3 Integrated AD&C

Integrated systems are an attractive alternative to designing and integrating single components. They have the advantage that all components are integrated on one AD&C system board and depending on the manufacturer, the integrated system can be customized if needed. The integrated systems are in development and more and more variations are becoming available. The system is mainly a board with all the sensors and actuators etched on it. Software needed for operations is also provided along with the AD&C system system board. Several companies provide integrated AD&C systems nowadays, Berlin Space Technologies, Maryland Aerospace, and GOMspace just to name a few. Since the integrated AD&C system seems to be the feasible option for the satellite, several different integrated systems will be investigated to determine which one would be the the most proper system. However, in order to do so, the stability and control requirements of the satellite have to be determined and considered.

7.1.4 Stability and control

Stability and controllability of the satellite is what defines the AD&C system; very high stability and control requires very accurate and powerful AD&C system, therefore, in order to choose a proper AD&C system, the stability and control characteristics of the satellite has to be investigated. Once these characteristics are known, a proper system can be chosen, which can satisfy these requirements and is compatible and appropriate for the satellite mission.

7.1.4.1 Control modes

The first step of determining the AD&C system is understanding and defining the control modes of the satellite. During each of these control modes, the AD&C system will have different functions. Below, the various type of control modes of the satellite are listed and described.

Orbit Insertion Controlling the movements during and after the satellite is put into orbit. In the case of this satellite, no attitude control will be required since no rockets or boosters are used.

Aquisition Initially determining the attitude of the satellite and stabilize it if necessary. This can also be used to recover from emergency situations and power malfunctions. At this stage, the satellite is supposed to detumble using the AD&C system.

Normal, On-station This is used during the steady-state mission period. All the activities during this mode will have an effect on the sizing of the AD&C system.

Slew Reorienting the satellite when needed. For this case, the satellite will not need to go through this mode.

Safe This mode is used in case of an emergency and if there is a malfunction within the satellite. This means that the AD&C system might have to use less power than usual.

Special This mode is used in case there is a special case, such as a specific target or eclipse periods.

7.1.4.2 Disturbance torques

During its mission, the satellite will always be exposed and vulnerable to different types of external forces; these forces will exert some torque on the satellite, which the AD&C system should be able to counteract. Sizing the AD&C system critically depends on the value of these disturbance torques. In this section, different types of the disturbance torques will be identified.

Experience shows that at the altitudes between 500 and 600 km, the aerodynamic torque is expected to be the dominant force, with the magnetic field torque following. The gravity gradient highly depends on the shape and altitude of the satellite. Other values of disturbance torques are expected to be 10 to 100 times smaller than these values, so their effect on sizing the AD&C system will be negligible. Figure 7.1 shows typical values of the disturbance torques for a small spacecraft. Therefore, in order to find the maximum disturbance torque induced on the satellite, it will be sufficient to determine the value of the aerodynamic and magnetic torque. However, for future applications, all the disturbance torques will be defined here and the formula regarding the determination of the value of the torque will also be introduced.

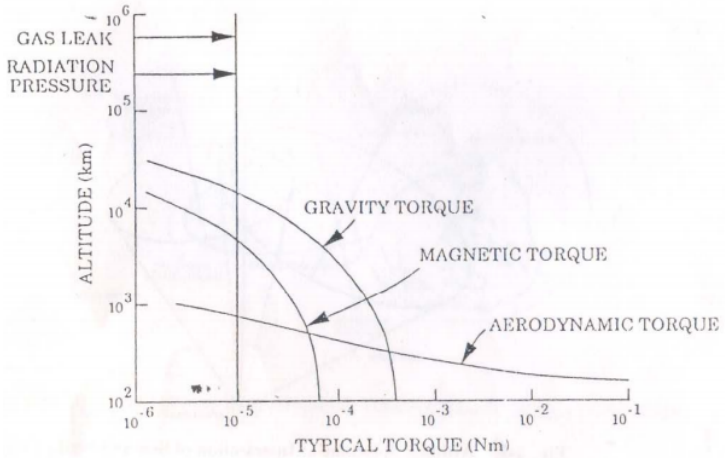

Figure 7.1: Typical disturbance torques for a small satellite as a function of altitude [3]

Gravity-gradient

Unless the axis of the satellite that has the minimum moment of inertia is aligned with vertically with respect to Earth, the satellite will experience force exerted on it by the effect of Earth's gravity pull. This type of torque is a cyclic type torque. In order to calculate the worst case gravity-gradient torque, the following formula will be used.

$$T_g = \frac{3\mu}{2R^3}|I_z - I_y|sin(2\theta) \tag{7.1}$$

In this equation, I_z and I_y represent the mass moments of inertia around the z and y axes respectively and μ represents the gravitational constant of Earth with a value of $3.9860044 \times 10^{14} m^3/s^2$. Since calculating the exact mass moments of inertia will be too difficult, a simple approximation of the moments of inertia will be taken into account by considering the whole satellite as a cube with a mass equal to the total mass of the satellite. By applying the mass moment of inertia for a cube, the approximate value of these inertias can be found. For a cuboid:

$$I_z = \frac{1}{12}m(x^2 + y^2); \tag{7.2}$$

$$I_y = \frac{1}{12}m(z^2 + x^2) \tag{7.3}$$

In these two equations, x, y, and z represent the length, width, and height respectively. Since the base of the satellite is a square, the width and the length of the satellite will be equal. $I_z = 1/12 \times 1.6 \times (0.1^2 + 0.1^2) = 0.00266 kgm^2$ and $I_y = 1/12 \times 1.6 \times (0.1^2 + 0.22^2) = 0.00778 kgm^2$. Although

the Computer Aided Three-dimensional Interactive Application (CATIA) model of the satellite is not completely accurate (due to the fact that all the masses are not inserted into CATIA), it shows that the values for the moments of inertia are within the same range as what is calculated manually. Finally, by assuming a maximum value of 1 for $sin(\theta)$, the worst case gravity gradient torque can be calculated:

$$T_g = \frac{3 \times 398600.44}{2 \times 6958} \times |0.0.00266 - 0.00778| = 9.79 \times 10^{-9} Nm \tag{7.4}$$

Solar radiation

As it is known, light has momentum and when it hits a certain surface, it exchanges momentum with that surface. This exchange of momentum will create a type of disturbance torque caused by the solar radiation pressure, which is a secular type disturbance. Depending on the material, the solar radiation pressure can differ in different spacecraft. The value of the disturbance torque depends on the surface illuminated by then sun and also the reflectivity of the material used on the body of the satellite. The following formulas will be used to calculate the worst case solar radiation torque:

$$T_{sp} = F(c_{ps} - cg) \tag{7.5}$$

$$F = \frac{F_s}{c} A_s (1 + q) cos(i) \tag{7.6}$$

In these two equations, c_{ps} represents the location of the centre of solar pressure, F_s the solar constant ($1376\ W/m^2$), c the speed of light, A_s the surface area, q the reflector factor, and i the angle of incidence.

Magnetic field

This type of disturbance is a cyclic type disturbance and occurs because of the interaction of Earth's magnetic field and the magnetic field created by the satellite. This interaction will exert an external couple on the satellite. The magnetic field torque will be calculated using the following formula:

$$T_m = DB \tag{7.7}$$

In this equation D represents the residual dipole of the satellite and B represents Earth's magnetic field in Tesla. Typical value for the residual dipole can be approximated to be 2 M/R^3 for near polar orbits where M is the magnetic moment of the Earth, $7.96 \times 10^{15} Tm^3$ and R is the radius from dipole centre to the satellite. The typical value of D for a small spacecraft can assumed to be around 0.1 based on SMAD. Using these values, it can be determined that the worst case magnetic disturbance torque for the satellite will be about $4.72 \times 10^{-6} Nm$.

Aerodynamic torque

This secular type disturbance exists due to the interaction of the satellite with air molecules and therefore the existence of drag. Although the air density at such high altitudes is considerably lower than the surface of the Earth, it can still have severe effects on the satellite if it is not taken into account. The following formulas are used to calculate the aerodynamic torque:

$$T_a = F(c_{pa} - cg) \tag{7.8}$$

$$F = 0.5 \rho V^2 S C_d \tag{7.9}$$

In these equations, c_{pa} represents the centre of aerodynamic pressure, cg the centre of gravity, ρ the air density, V the speed of the satellite, S the surface area of the satellite, and C_d the drag coefficient. for the drag coefficient, a typical value of 2.2 will be assumed.

As mentioned before, this value is the most important value in calculating the disturbance torques. All the values for calculating the force can either be calculated or found on research papers or books. The only thing left to be determined is the difference between the centre of aerodynamic pressure and the centre of mass. Finding the exact locations of these two centres will be difficult and requires very thorough applications, however, this value can always be estimated for the worst case scenario. NASA suggests that in order to calculate the worst case scenario for the difference between the centre of mass

and centre of aerodynamic value, a conservative value of one-third of the length of the satellite has to be considered [68]. Based on this estimate, a 2U CubeSat should have a distance of 7 cm between its centre of mass and aerodynamic pressure. A list of values for the calculation of the aerodynamic torque is given in table 7.1. Based on these values an aerodynamic torque of $9.307 \times 10^{-9} Nm$ is determined.

Table 7.1: Values for aerodynamic torque calculation

Parameter	Value
ρ $[kg/m^3]$	2.11×10^{-13}
C_d [-]	2.2
A $[m^2]$	0.01
V $[m/s]$	7569
$c_{pa} - c_{cg}$ $[m]$	0.07

7.1.4.3 Comparison and validity of the disturbance torques

Three different disturbance torques have been calculated in this section. As can be seen, the magnetic torque seems to be the dominating torque for this satellite mission with values within the range of 10^{-6}, while the aerodynamic torque and gravity gradient are within the ranges of 10^{-8} and 10^{-9} respectively. For the gravity gradient, this value seems to be a reasonable value since the satellite is very small and short (in height). This means that the gravity gradient acting on top and the bottom of the satellite will be only very slightly different. Also, the difference between the moments of inertia of the different axes is very low since there is not a huge difference in the length of the axes; this makes the value of the gravity gradient a reasonable value; however, for the other two disturbance torques, it seems that the magnetic torque is more than 100 times higher than the aerodynamic torque.

This is a very unusual situation for a satellite at such a low altitude orbit. In usual cases, the aerodynamic torque is the dominant torque until the altitudes of about 600 km. A few reasons might cause this conflict. First of all, the residual magnetic dipole of the satellite is estimated to be around 0.1 by SMAD, however, in reality this value can be much smaller (10 to even 50 times smaller than this value) since this satellite does not contain any magnetic equipment and its dipole can only be generated by the current passing through the wiring system of the satellite, which will be a very small value. Second of all, the aerodynamic torque is calculated using densities generated from a certain atmospheric model. In other atmospheric models, this value can go up to 10 times higher than the current value. Also, the size of the satellite is very small and its frontal area is only $0.01 cm^2$, so it would be reasonable to have a low aerodynamic torque compared to the typical satellite missions. In general, it can be said that in reality, one would expect a higher aerodynamic torque while expecting a much lower magnetic field torque.

7.1.5 AD&C system selection

Now that all the disturbance torques are known, the integrated AD&C system mentioned in the beginning of the chapter will be examined in order to check whether they are compatible with the requirements on counteracting these disturbance torques. A thorough research on different models of the integrated AD&C system from different companies led to the conclusion of selecting the iADCS-100 as the most appropriate integrated system for the mission, see figure 7.2. Table 7.2 shows the characteristics of this integrated system [4].

The reaction wheels of this integrated AD&C system can generate a torque of $8.7 \times 10^{-}5$, which is 1000 times more than the worst case aerodynamic disturbance torque on the satellite. In order to check whether magnetorquers will be able to counteract the magnetic disturbance torque, equation 7.7 will be used again to calculate the magnetic dipole required on the magnetorquers. Based on the value of Earth's worst case magnetic field of $4.72 \times 10^{-5} Tesla$ and the magnetic disturbance torque of $4.72 \times 10^{-6} Nm$, the required magnetic dipole for the magnetorquer will be calculated to have an approximate value of 0.1 Am^2. The iADCS magnetorquers are capable of having a magnetic dipole of 0.2 Am^2, which is sufficient to counteract the moment created by the magnetic field; furthermore, it was already discussed that in reality, such a high magnetic field torque will not be achieved, and yet the iADCS is still able to

Table 7.2: Integrated system characteristics

Characteristics	iAD&C system	Comments
Size	95 x 90 x 32 mm	2 PC/104 stacks
Mass	250 g	Including baffle and 2mm AL shielding
Power	0.5 W Nominal/ 1.8 W peak	Depending on operation mode
Interface	RS485, I^2 C	
Attitude knowledge	30 arcsec	ST-200 star tracker
Pointing accuracy	« 1°	Depending on intersubsystem alignment
Slew rate	$> 1.5°/s$	For 3U cubesat all axes using reaction wheels
Attitude modes	Target pointing	Using longitude/latitude target coordinates
	Nadir pointing	
	Sun pointing	
	Spin-mode	Max $200°/s$ rotation rate using magnetorquers
	De-tumble	All modes are safe mode recoverable
Actuators and Sensors	3 Reaction wheels	Torque $0.087mNm$, angular momentum $1.5mNms$
	3 Magnetorquers	$0.2Am^2$
	1 Star tracker	30 arcsec accuray, 5Hz update rate
	MEMS sensors	Gyro, accelerometer, magnetometer
	Additional sensors	Plug in capability for GPS and sun sensors

counteract this torque. This integrated system will be constantly dumping momentum and is designed to detumble the satellite within a maximum of a few days after orbit insertion [69].

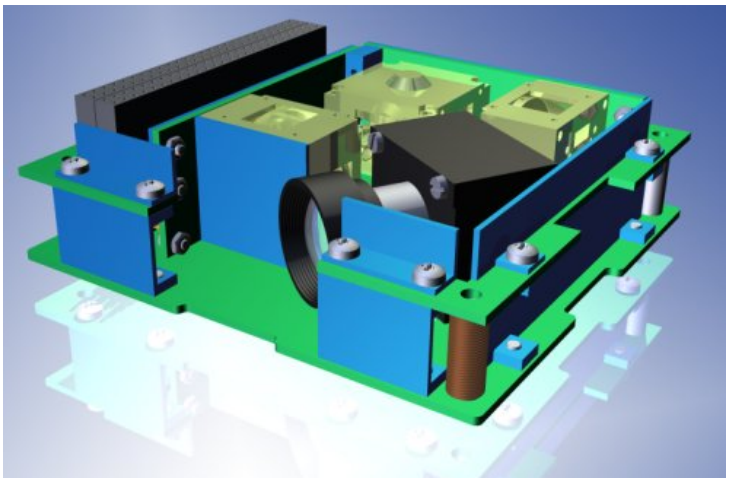

Figure 7.2: iADCS-100 integrated system [4]

7.1.6 Position error

While in orbit, the satellite might not have the exact attitude it is thought it has, therefore the exact position of the GNSS with respect to the centre of mass will be determined with some errors in the roll and yaw axes (the pitch rotation will not have an effect on the distance between the GNSS and the centre of mass). The integrated iADCS is supposed to have an attitude knowledge of 30 arcsec; this means that the satellite might be (1/120)° more or less tilted with respect to any of the axes. The position of the the GNSS with respect to the centre of gravity is [0, 53.775, 56.7] mm. This can be seen in figures 7.3 and 7.4.

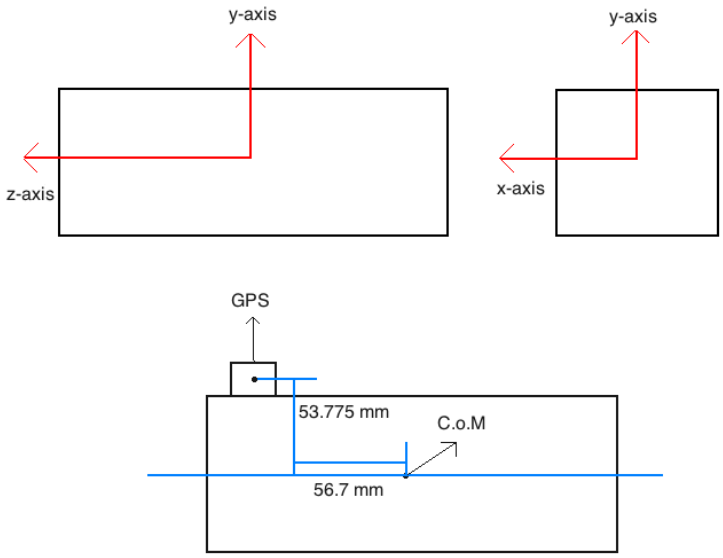

Figure 7.3: Axes of the satellite and the coordination of the GNSS

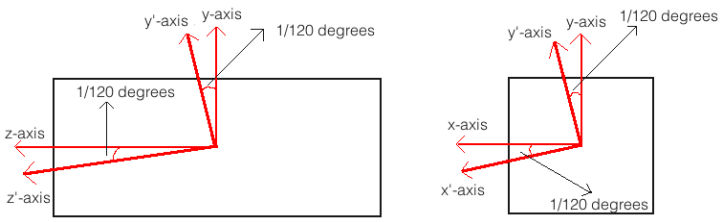

Figure 7.4: Inaccurate pointing knowledge

Using simple geometry the maximum error due to the inaccurate pointing knowledge can be calculated to be $7.82 \times 10^{-3} mm$ and $8.25 \times 10^{-3} mm$ for yaw and roll axes respectively. The calculation can be seen in equations 7.10 and 7.11.

$$\text{Maximum error in yaw axis} = 53.775\ mm \times \sin(1/120) = 7.82 \times 10^{-3}\ mm \tag{7.10}$$

$$\text{Maximum error in roll axis} = 56.7\ mm \times \sin(1/120) = 8.25 \times 10^{-3}\ mm \tag{7.11}$$

7.2 Communication architecture & data handling

The Communication Architecture & Data handling subsystem compromises of downlink and uplink providing a throughput for payload and housekeeping data, and control and operation respectively. The subsystem further distributes, decodes and receives commands while gathering housekeeping and payload data. The classical division of Telemetry, Tracking and Command (TT&C) and CD&H has been omitted in favour of a single subsystem that conducts both functions to obtain a better integrated and optimized solution.

7.2.1 Data rates and volume

The data handling will be executed following the store and forward principle as mostly used by small LEO satellites [41]. This principle relies on storage of data during non-access periods.

The amount of data that is transferred to the ground-station via the downlink depends on the data of interest and the health of the satellite. During normal operation it is chosen to only transfer payload data supplemented by a simple 1 bit true/false health check of each subsystem and critical component. This keeps the amount of data that has to be send over the downlink to a minimum while still obtaining all science data and an indication of the health of the system. During malfunction a diagnostic mode can be activated to provide detailed information such as temperatures, voltages and currents of critical components.

The size of the generated data is furthermore depended on the update rate. For the housekeeping data a refresh rate of 0.1 Hz is found to be a commonly used value for similar satellite missions [70]. The update rate of the science data is dependent on the payload system and intended use. The Septentrio AsterRx-m GNSS receiver has a selectable update rate of up to 25 Hz [15]. Previous gravity exploration missions used a positional update rate of 1 Hz which has found to be sufficient for accurate determination of the long to medium wavelength gravity field [71].
The data output format of the GNSS receiver is defined following the Septentrio Binary Format (SBF). This data block contains several sub-blocks, considering the mission one is mainly interested in the measurement sub-block. For each tracked signal at a particular epoch the pseudorange, carrier phase, Doppler, the CNR and lock-time are put in a measurement set [72]. For each frequency a sub-measurement block is generated, for the tracking of GPS L1 & L2 and GLONASS L1 & L2 this will result in 4 sub-blocks. The size of one block is 4 bytes hence for full tracking of L1 & L2 for both GLONASS and GPS a block of 16 bytes is generated. This information can be used to form a rudimentary telemetry frame for the downlink as depicted by table 7.3.

Table 7.3: Telemetry frame for normal operation

	Data volume [bit]	Data rate [Hz]	Daily data volume [$kByte$]
ADCS status	1	0.1	1.1
EPS status	1	0.1	1.1
UHF/VHF transceiver status	1	0.1	1.1
GNSS receiver status	1	0.1	1.1
CD&C computer status	1	0.1	1.1
ACDS data	32	1	346
GNSS data	128	1	1382
Total data			1734

The amount of data storage required is dependent on the maximum time between access, safety factors for a missed connection and outage time of satellite and/or ground station. As the generated data is relatively low and the mass of (flash) storage neglectable, storage will not be a critical design component. Comparing the data rate in table 7.3 with the amount of storage available as seen in section 7.2.7, it is deducted that several months of data can be stored with the available storage space. One has to keep in mind that the data rate as depicted in table 7.3 does not include detailed housekeeping data, this will however not significantly increase the data volume as the rate of update is low.

A technique to further reduce the necessary downlink data rate is the compression of data. This will however increase the computational work for the CD&H computer increasing the mean power consumption. A variety of data compression techniques have been developed for earth observations applications but are mainly focused on the compression of imagery. There are however several algorithms that can compress (lossy or loss-less) GPS data such as the Hatanaka's method [73]. General purpose file compressors can within reasonable time compress files to approximately 25 "%" of the original file size.

The Data handling block diagram in figure 7.5 describes the data flow and related components of the system. Payload and housekeeping data are stored and processed by the CD&H computer where-after the data for normal operation is forwarded via the downlink to the ground station. At the ground station the received data will be decoded and distributed to the end-users. The ground station sends commands and firmware updates through the uplink to the CD&H computer.

Figure 7.5: Data handling block diagram

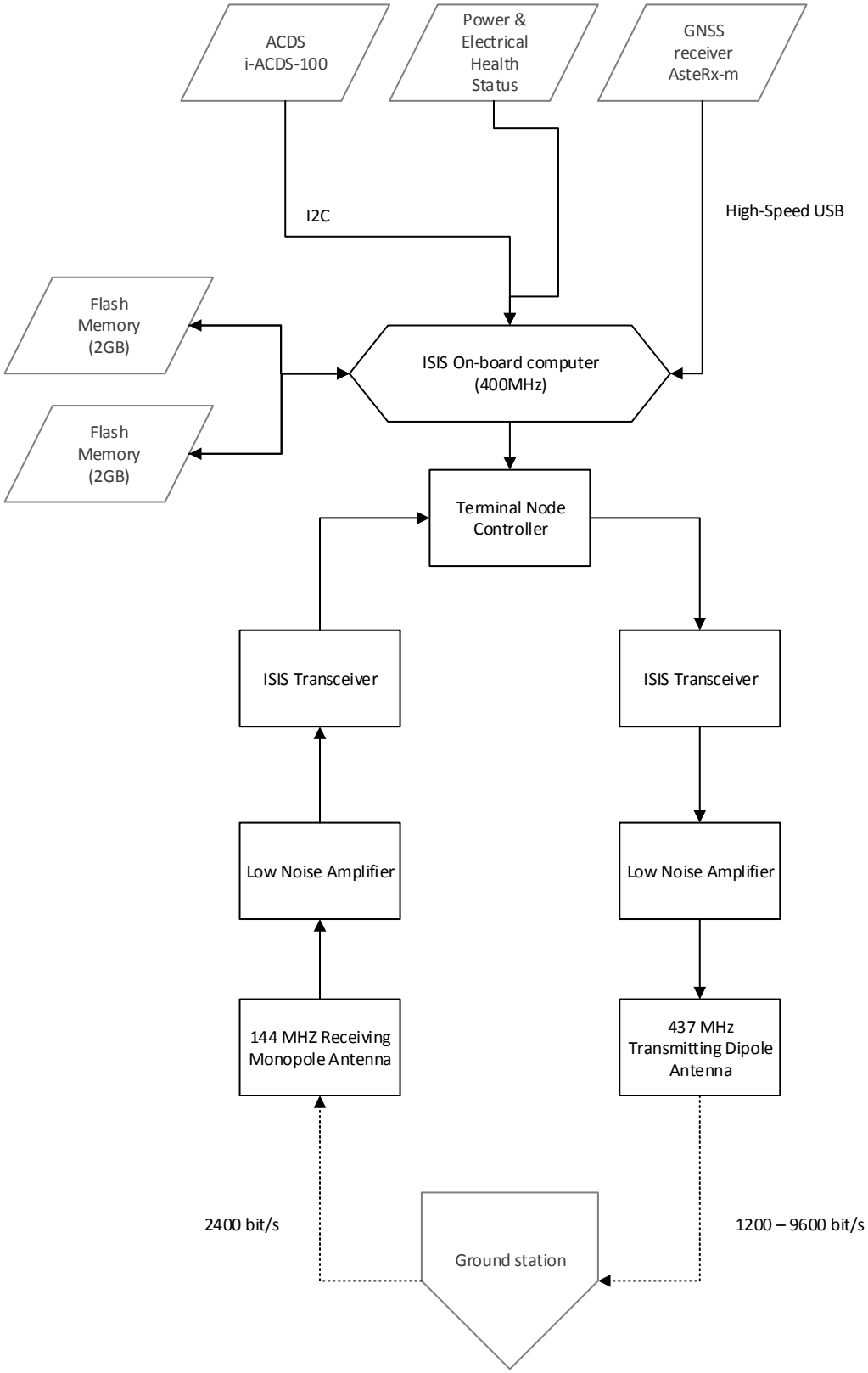

7.2.2 Frequency channel

The frequency band has a profound influence on the achievable data rate of the downlink. High frequency bands such as the S- or X-band are able to allocate high data rates typically used by data driven missions. The data generated by the GNSS receiver is comparatively small for a science system hence a high frequency band is not required for the data downlink. The Very High Frequency (VHF)/Ultra High Frequency (UHF) frequency band is often used by LEO satellites as a cost effective solution requiring a relatively low-cost and simple ground station.[41] The required antennas for the satellite will be in the order of tens of centimetres in size hence perfectly suited for mirco- and picosatellites [41]. The use of the VHF/UHF channel for the up- and downlink respectively can therefore be regarded as the best choice considering the mission profile. The system characteristics can be found in table 7.4.

Table 7.4: TU Delft Ground station parameters [12]

Frequency range [MHz]	432 - 440
Gain [dBi]	15.5
Front-to-back ratio	1.5
Beam-width [deg]	30
VSWR	1.6:1

7.2.3 Ground station and access time

The ground station plays a crucial part in the link budget as it determines the access time. The use of multiple ground stations is beneficial if large amounts of data has to be transferred and/or a continuous command is required. Since neither is essential, a single ground station is sufficient. The location of the ground station has an influence on the access time. In general it is more efficient to use a ground-station near the poles as the access times will be longer [74], hence the data rate can be lowered requiring a less powerful on-board transmitter. In line with Delfi missions it is chosen to use the in-house available UHF/VHF ground station located at the TU Delft campus for practical and economical reasons. Recently completely renovated and optimized to work with the Delfi satellites . The station is located 100 m above sea level and can track satellites from a minimum elevation of $-1°$ [75].

An important aspect for the determination of the communication architecture is the access time between ground station and satellite as this will depict the minimum required data rate hence determining the minimum antenna and transmitter performance. Using the simulation tool STK one is able to simulate the ground track of access over a period of time as can be seen in figure 7.5. Using the access determination tool one is able to calculate the time in view of the satellite from the position of the ground-station. The simulation was run for a period of 3 years, the results can be found in table 7.5. The satellite has 7 to 8 times in view from the position of the TU Delft ground station, the projected access area can be found in figure 7.6

Table 7.5: Access characteristics between Delft ground station and GES

Mean daily access time [min]	79.3
Maximum access time per pass [min]	12.8
Mean access time per pass [min]	9.82
Relative access time [%]	5.58

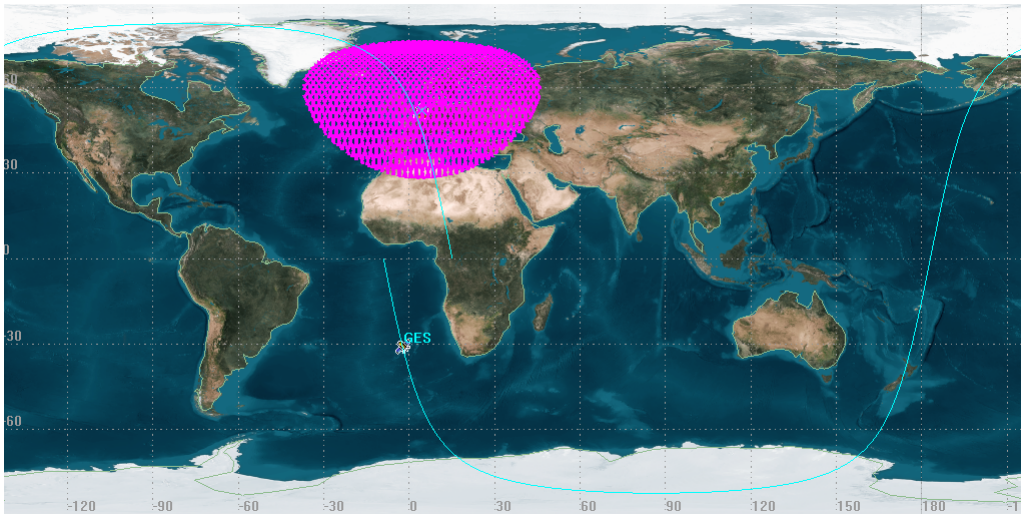

Figure 7.6: Visibility of GES from TU Delft ground station

7.2.4 Transceiver and antenna selection

The selection of the CubeSat system as the primary structure for the satellite offers the opportunity to select COTS components for the communication architecture. These components are specifically designed and tested for the CubeSat system and offer a cost-effective solution. The increased reliability, integrability and simplicity are considered high value factors hence justify the choice to select exclusively CubeSat components for the communication architecture.
The ISIS UHF downlink, VHF uplink Full Duplex Transceiver is currently the only dedicated CubeSat receiver that offers UHF uplink and VHF downlink capabilities [13]. The ISIS transceiver is based on the transceiver used in the Delfi-C^3 satellite and is a single board solution. It is fully compliant to the CubeSat standard and compatible with the ISIS UHF/VHF antenna system. The ground-station at Delft University of Technology is optimized to operate with the ISIS system and has a flight proven record with Delfi missions which operated with similar communication systems. This is a contributing factor to the reliability and sturdiness of the communication architecture. The component characteristics can be found in table 7.6.

Table 7.6: ISIS transceiver specifications [13]

Data rate [bit/s]	1200 - 9600 (UHF) 1200 (VHF)
Transmit Power [W]	0.5
Power [W]	2 (transmitter on) 0.35 (receiver only)
Frequency range [Mhz]	400 - 450 (UHF) 130 - 170 (VHF)
Dimensions [mm]	96 x 90 x 15
Mass [g]	85
Modulation	BPSK (UHF)
Thermal range [C]	-20 +50
Price [$]	8500

The accompanying ISIS antenna system contains tape spring rod antennas. The system is flexible regarding the number of antenna's, the individual length and configuration. Redundant heating elements melt the constricting wires for deployment in space. It is chosen to use a 3 antenna configuration, 1 VHF antenna and 2 UHF antennas. It is chosen to use a dipole configuration for the UHF antenna amplifying

the antenna gain with approximately +3 dB [74]. The dipole configuration uses two identical monopole antennas with the signal of the transmitter applied between the two halves of the antenna. A zenith pointing antenna is avoided to reduce the possibility of induced multipath errors in the GNSS system. The antenna's can be sized following using the relationship between wavelength and antenna length. The length of the rod should be a quarter of the the wavelength. Table 7.7 depicts the characteristics of the ISIS antenna system.

Table 7.7: ISIS antenna specifications [13]

Diameter [mm]	30
Length (cm)	18 (UHF) 50 (VHF)
Power [W]	2 (during deployment) 0.02 (Nominal)
RF Power [W]	2
Antenna gain	-3 (UHF) -5 (VHF)
Mass [g]	100
Price [$]	7250

The positioning of the antenna is constrained due to the placement of the GNSS antenna. To exclude the possibility of multipath induced errors it is decided to keep the antennas below the zenith facing side to prevent disturbance of the GNSS signals.

7.2.5 Link budget

The link budget is based on the numerical model as formulated in SMAD [41]. Table 7.8 provides the description of symbols.

The downlink is sized according to the worst case condition, that is were the distance between satellite and ground station is maximum. The first step in the link budget is the determination of the Equivalent Isotropically Radiated Power (EIRP) at the satellite. The EIRP is the amount of power that a theoretical isotropic antenna would emit to produce the peak power density observed in the direction of maximum antenna gain. It consists of the antenna transmit gain and transmit power, which are component properties, and the line loss and connector loss which can be estimated using SMAD.

$$EIRP_{sat} = P + L_l + L_c + G_t \tag{7.12}$$

The slant range is the distance between satellite and ground station and is dependent on the earth's radius, elevation angle between ground station and satellite, orbit and the orbit height. This equation is only valid for circular orbits.

$$S = R_{earth} * (((\frac{R_{earth} + h)^2}{R_{earth}^2} - (cos(\frac{\alpha}{57.2958})^2)))^{0.5}) - sin(\frac{\alpha}{57.2958}))) \tag{7.13}$$

The space loss is the loss in signal strength due to the path through free space. It is determined via the slant range and frequency of the signal.

$$L_{space} = 147.55 - 20\log S - 20\log f \tag{7.14}$$

The EIRP at ground level is determined by the; transmit antenna space loss, transmit antenna polarization loss, which is the loss due to the ratio between the left and right polarized radiation pattern and the transmit antenna pointing loss. This loss is induced due to the error in pointing.

$$EIRP_{ground} = EIRP_{sat} + L_{pt} + L_p + L_s \tag{7.15}$$

The receiver antenna pointing loss can be estimated by the pointing error and the receiver antenna beam-width, which is the angle between the half power points of the main lobe.

$$L_e = 12(\frac{e}{\theta_r})^2 \tag{7.16}$$

The effective noise temperature is the source noise temperature in an amplifier that results in the same output noise power when connected to noise-free amplifier. It can be equated using the transmission line coefficient, this describes the total power of a wave relative to an incident wave. Further dependence on the sky temperature (cosmic background radiation) and LNA noise temperature.

$$T_n = T_c T_{sky} + (1 - T_c) T_t l + T_{LNA} \tag{7.17}$$

The figure of merit is the quantity used to characterize the performance of the receiver. It can be equated using the receiver antenna gain, the transmission line loss, the effective noise temperature and the receive antenna polarization loss.

$$FM = p + G_r + L_t l - 10 \log T_n \tag{7.18}$$

The signal-to-noise power density has a dependence on the EIRP at the ground station, the receiver antenna pointing loss and the figure of merit.

$$\frac{S}{N_0} = EIRP_{ground} + L_e - k + FM \tag{7.19}$$

Now one is able to determine the energy per bit to noise power spectral density ratio subtracting the system desired data rate from the signal-to-noise power density.

$$\frac{E_b}{N_0} = \frac{S}{N_0} - d \tag{7.20}$$

Finally one is able to deduce the link margin by subtracting the required energy per bit to noise power spectral density to the calculated energy per bit to noise power spectral density ratio.

$$M_{link} = \frac{E_b}{ER_0} - \frac{E_b}{ER_0} \tag{7.21}$$

The uplink is computed in similar fashion as the downlink where the satellite acts as receiver and the ground station as transmitter. As the ground station transmit power is magnitudes higher the overall link budget is far less critical. The resulting numerical process can be found in table 7.8.

Table 7.9: Access parameters for variable data rate

Bit rate [b/s]	Elevation [deg]	Daily access time [s]	Daily data volume [kB]
1200	-1 - 6	1718	257
2400	6 - 16	1202	360
4800	16 - 28	548	328
9600	28 - 90	369	443
Total			1391
1200 (CBR)	-1 - 90	3578	536

Table 7.8: VHF uplink and UHF downlink budget

Ground station parameters								
Symbol	Discription	I/O	Unit	VHF	UHF ($\alpha = -1°$)	UHF ($\alpha = 6°$)	UHF ($\alpha = 16°$)	UHF ($\alpha = 26°$)
f	Frequency	I	GHz	0.144	0.437	0.437	0.437	0.437
P	Transmit power	I	W	75	0.5	0.5	0.5	0.5
P	Transmit power	O	dBW	18.75061263	-3.010299957	-3.010299957	-3.010299957	-3.010299957
L_l	Transmitter line loss	I	dB	-2	-0.2	-0.2	-0.2	-0.2
L_c	S/C Connector, Filter of In-Line swith losses	I	dB	-2.1	-1.9	-1.9	-1.9	-1.9
G_t	Transmit antenna gain	I	dBi	15.5	-3	-3	-3	-3
$EIRP$	Spacecraft EIRP	O	dBW	30.15061263	-8.110299957	-8.110299957	-8.110299957	-8.110299957
Orbit and Path								
Symbol	Discription	I/O	Unit	VHF	UHF ($\alpha = -1°$)	UHF ($\alpha = 6°$)	UHF ($\alpha = 16°$)	UHF ($\alpha = 26°$)
R_{Earth}	Earth radius	I	km	6378	6378	6378	6378	6378
h	Orbit height (circular)	I	km	580	580	580	580	580
α	Elevation angle	I	deg	-1	-1	6	16	28
θ_r	Ground antenna beamwidth	I	deg	21	30	30	30	30
e	Ground station pointing error	I	deg	5	5	5	5	5
L_pt	Ground station antenna pointing loss	I	dB	-0.7	-0.333333333	-0.333333333	-0.333333333	-0.333333333
L_p	Antenna polarization loss	I	dB	-3	-3	-3	-3	-3
S	Propagation path length (slant range)	O	km	2894.703265	2894.703265	2193.273169	1532.197523	1092.353558
L_s	Space loss	O	dB	-144.8493309	-154.4917098	-152.0814833	-148.9659239	-146.0268933
$EIRP$	Isotropic Signal Level at Ground Station	O	dBW	-118.3987182	-168.6020097	-166.1917832	-163.0762238	-160.1371932
Spacecraft parameters								
Symbol	Discription	I/O	Unit	VHF	UHF ($\alpha = -1°$)	UHF ($\alpha = 6°$)	UHF ($\alpha = 16°$)	UHF ($\alpha = 26°$)
k	Boltzman's constant	I	$dBW/K/Hz$	-228.6	-228.6	-228.6	-228.6	-228.6
L_e	Satellite antenna pointing loss	I	dB	-5.5				
p	Satellite antenna polarization loss	I	dB	-3				
G_r	Satellite antenna gain	I	dBi	-4				
L_{tl}	Transmission line losses	I	dB	-0.2	-2.8	-2.8	-2.8	-2.8
T_{LNA}	LNA noise temperature	I	K	0	75.6	75.6	75.6	75.6
T_{tl}	Transmission line temperature	I	K	35	35	35	35	35
T_{sky}	Receiver sky temperature	I	K	600	290	290	290	290
T_c	Transmission line coefficient	O	-	0.954992586	0.52480746	0.52480746	0.52480746	0.52480746
T_n	Effective noise temperature	O	K	574.5708111	244.4259024	244.4259024	244.4259024	244.4259024
FM	Figure of merit	O	dB/K	-31.7934356	-14.18147227	-14.18147227	-14.18147227	-14.18147227
S/N_0	Signal-to-noise power density	O	dB/Hz	72.90784618	45.48318468	47.89341118	51.00897058	53.94800115
d	System desired data rate	I	bps	2400	1200	2400	4800	9600
d	System desired data rate	O	dB/Hz	33.80211242	30.79181246	33.80211242	36.81241237	39.82271233
E_b/N_0	Telemetry system	O	dB	39.10573376	14.69137222	14.09129877	14.19655821	14.12528882
BER	Telemetry system required Bit-Error-Rate	I	-	0.000001	0.000001	0.000001	0.000001	0.000001
(E_b/N_0)	Telemetry system required	I	dB/Hz	11	11	11	11	11
M_{link}	System link margin ($> 3\ dB$)	O	dB	28.10573376	3.691372218	3.091298766	3.196558207	3.12528881

7.2.6 Variable data-rate

If one would design for the worst-case scenario i.e. zero elevation, one obtains a relatively low data rate hence only a low daily data volume can be send through the downlink. Results from the downlink budget indicated that the maximum allowed data rate by the transceiver cannot be achieved at low elevation angles with a positive link margin. To maximize performance a variable data rate should be implemented which increases along with the elevation angle between ground station and satellite during access. The ISIS transceiver allows 4 different data rate settings. For each different data rate the minimum elevation angle is calculated via the link budget with a constant link margin of 3 dB. Using the simulation tool STK one is able to determine the mean daily access time for a constraint range of elevations. The results can be found in table 7.9.

Several interesting observations can be made when analyzing the data presented in table 7.9. Most of the time the access between satellite and ground station occurs at low elevation angles; almost half of the time in view occurs at an elevation angle of 6 deg or less. If one compares the total daily data volume that can be transferred to the ground station one sees a significant performance increase. The

Table 7.10: Link interface subsystems [14] [15]

Manufacturer	Link interface
Septentrio AsteR-m OEM	USB, UART
Clyde Space 2U CubeSat EPS	I2C, CAN
Berlin Space tech iADCS-100	I2C, UART
ISIS UHF/VHF Full Duplex Transceiver	I2C

Table 7.11: CubeSat C&DH computers [14]

	ISIS On Board Computer	NanoMind A712C	Cube Computer
Clock rate [MHz]	400	8 - 40	4 - 48
Data storage [MB]	2x2000	4	2x1
RAM [MB]	32	2	n.a.
Power consumption [mW]	400	312	310
Mass [g]	94	50 - 55	50-70
Price	4300	4750	4500
Interface	I2C, USB, SPI, UART	I2C, CAN, SPI, UART	I2C, SPI, UART

achievable data volume is more that a magnitude higher for the Variable Bit Rate (VBR) implementation as compared the Constant Bit Rate (CBR).

7.2.7 On-board computer selection

In order to maintain and operate the data flows within the satellite a on-board computer is required. The first function of the on-board computer is to process, regulate and store incoming payload and housekeeping data from the GNSS receiver, AD&C system and other subsystems. The second function is the command of the subsystems.

The on-board computer has to provide the necessary interfaces to link with the subsystems. As most of the subsystems are designed using the CubeSat protocal compatibility will not be an issue. The GNSS receiver does however not follow the aforementioned protocol and is designed as a terrestrial instrument. The interfaces of the various subsystems can be found in table 7.10.

The selection criteria for the on-board computer can be classified as follows: available interface protocols, mass, power use, performance, data storage capabilities and cost. Three CubeSat compatible computers were selected, the corresponding specifications can be found in table 7.11.

As the GNSS receiver uses a USB connection for data transfer, the NanoMind A712C and Cube Computer are non-viable options as these components do not support the USB protocol. The ISIS computer offers also a much higher performance with a clock rate and internal memory that is one magnitude higher than the corresponding values for the other two computers. The increased Central Processing Unit (CPU) speed will definitely find its place as fast compression requires high CPU clock speeds. The data storage size of the ISIS computer is significantly higher, but the Cube Computer and NanoMind do provide space for external SD-cards data expansion slots. The mass and and power consumption are marginally higher for the ISIS computer. The ISIS has an additional advantage in the cost department.

Considering the aforementioned observations, the ISIS On board computer is the only valid choice as it is the only computer that supports the USB protocol.

7.2.8 Communications

The communications structure is illustrated by the communication flow diagram in figure 7.7. The communication flow diagram shows the flow of data through the system to and from its environment. The communication flow diagram in figure 7.7 revolves around the CD&H computer. All data flows and commands pass through the computer. The onboard computer includes the CPU and the data storage.

The CPU is divided into three control boards namely the payload control board, attitude control board and subsystems control board. All the control boards within the CPU are connected to each other. Data flow is sketched for the launch, flight duration and ground station processing phase.

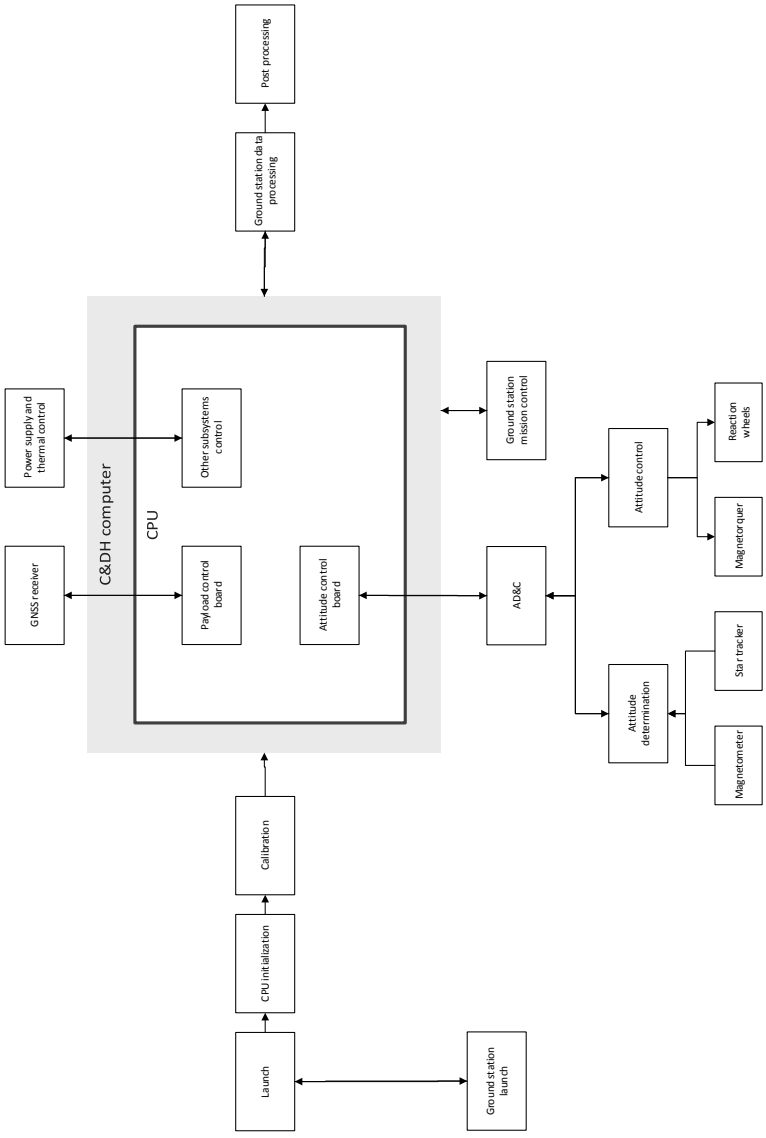

Figure 7.7: Communication flow diagram

7.3 Guidance and navigation

The purpose of the guidance and navigation subsystem of the satellite is orbit determination and control. Since knowing the position of the satellite is highly important for the mission, the payload system covers the orbit determination, see chapter 6. There is no propulsion system onboard to do active orbit control. This means that there is no need for active navigation, as the launcher will insert the satellite in its final orbit. As shown in chapter 5 the orbit is selected to meet the requirements without the need for orbit maintenance, AD&C will be performed by the AD&C system, see section 7.1. Therefore no complementary guidance and navigation system is necessary.

7.4 Thermal control

In the design of the thermal control subsystem several parameters need to be taken into account. Firstly the hot and cold temperature limits of all parts of the satellite need to be registered, for both the operational as well as the survival state. After this the different heat sources and sinks will be listed, to get a clear overview of all adding components. Furthermore the equations used to calculate the thermal control will be given. Finally the results of the calculations and the thermal control system configuration will be presented.

7.4.1 Hot and cold limits

All subsystems (and components) have their own limits concerning temperature. There are hot and cold temperature limits for the operational state, and some systems also have limits for survival conditions in which the systems are not active. The limits of the systems used for the satellite are documented in table 7.12. From the table it becomes clear that the binding hot temperature limit come from the AD&C system, with a hot limit of 40 degrees. The binding cold temperature comes from the battery with a temperature of -10 degrees as the lowest temperature at which the system will work.

Table 7.12: Temperature limits subsystems

	Operational limits		Survival limits	
	hot	cold	hot	cold
iADCS	40°C	−20°C	40°C	−20°C
Solar panels	125°C	−40°C	125°C	−40°C
AsteRx	85°C	−35°C	85°C	−40°C
ACCG5Ant-2AT1	85°C	−55°C	85°C	−55°C
ISIS on board comp.	60°C	−20°C	60°C	−20°C
Battery	45°C	−10°C	60°C	−10°C

7.4.2 Heat sources and sink

For a satellite in a LEO there are four major heat sources: the Sun, the albedo effect, the infrared radiation of Earth and the internal heat of the satellite. Furthermore there is heating by free molecules. The heat leaving the satellite plates is determined to be the radiator heat [76].

Solar radiation The major source of environmental heating for GES is the radiation of the Sun. The solar constant for an Earth orbit varies from 1420 W/m^2 in the hot case to 1360 W/m^2 in the cold case. Solar radiation is experienced by the satellite only by the panels that are directly hit by it, and not during eclipse.

Albedo Albedo is the sunlight that is reflected off a planet or a moon. For GES only the albedo of the Earth is considered. The albedo is given as a percentage of the incident sunlight that is reflected back to space, ranging from 0.23 to 0.30 for the Earth orbit.

Earth Infrared Radiation The Infrared Radiation (IR) of Earth originates from the incident sunlight that is not reflected as albedo. The Earth emitted IR is assumed to be of 218 W/m^2 to 244 W/m^2, for respectively the cold or hot case.

Free molecular heating Free Molecular Heating (FMH) is a form of environmental heating that consists of individual molecules in the outer reaches of the atmosphere bombarding the satellite. For FMH is only significantly experienced up to a height of 180 km GES only experiences it during the launch phase. Therefore FMH was not taken into account for the thermal calculations.

Internal heat The internal spacecraft heat is generated by the different electrical subsystems which will convert some of their power into heat, warming the satellite. The efficiencies of the subsystems are not precisely known but are estimated at 70%. The peak power of the satellite is calculated to

be 5.68 W (see section 7.5), used to calculate the hot case, whereas the average power of 2.995 W is used for the cold case.

Reradiated energy The only heat sinks of the satellite are the radiator surfaces, which reject the heat by IR. The internal as well as the external heat are rejected by the radiator. For GES it is assumed that passive thermal control will be enough, given the radiator surfaces are coated with a finish with a favourable emittance and absorptance. This is based on a simple estimate made for a spherical satellite with a diameter of 25 cm, using the equations shown in subsection 7.4.3.

7.4.3 Thermal equations

The spacecraft needs to be in thermal equilibrium, so the heat that comes in equals the heat that goes out. For GES the heat that comes in exists of internal and external heat ($Q_{internal}$ and $Q_{external}$), and the heat that goes out equals the heat that is rejected from the spacecraft surfaces, i.e. the radiator heat ($Q_{radiated}$), see equation 7.22.

$$Q_{internal} + Q_{external} = Q_{radiator} \tag{7.22}$$

As stated before the internal heat exists of the rejected heat from the electrical subsystems. The external heat has three components as reflected by equation 7.23 (Q_{solar}, Q_{albedo} and $Q_{EarthIR}$).

$$Q_{external} = Q_{solar} + Q_{albedo} + Q_{EarthIR} \tag{7.23}$$

The solar heat can be calculated by the use of equation 7.24. In this equation α represents the absorptivity, I_{solar} the solar flux and A the area of the panel concerned.

$$Q_{solar} = \alpha \times I_{solar} \times A \tag{7.24}$$

The Earth's IR and the albedo are represented by equation 7.25 and 7.26 respectivily. In these equations ε is the emittance of the panel at hand, I_{EIR} is the IR flux of Earth and ρ_{albedo} is the percentage of the sunlight reflected by Earth. Both F_{EIR} and F_{albedo} stand for their respective view factors, which are found for a height of 500 km [77].

$$Q_{EarthIR} = \varepsilon \times I_{EIR} \times F_{EIR} \times A \tag{7.25}$$

$$Q_{albedo} = \alpha \times I_{solar} \times \rho_{albedo} \times F_{albedo} * A \tag{7.26}$$

Now only the equation for the radiator heat needs to be clarified (equation 7.27). Here σ is the Stefan-Boltzmann constant ($5.67051 * 10^{-8}$ W/m^2K^4) and T is the radiator temperature.

$$Q_{radiator} = \varepsilon \times \sigma \times A \times T^4 \tag{7.27}$$

By the use of the above given equations the temperature of the individual panels can be calculated as well as the temperature of the internal system. One could notice that time is not a parameter in the equations at hand, time is neglected for simplicity. This is considered legitimate, for the walls of the spacecraft are very thin, hence the heat can be assumed to go through the panels directly. It is assumed that only passive thermal control is required, based on a first estimate for a sperical satellite with a diameter of 25 cm.

Now an iterative process can be performed by changing the coatings, in order to reach the preferable temperatures. For these calculations the panels of the satellite are numbered, as shown in figures 7.8 and 7.9. The worst hot case as well as the worst cold case are considered. In both cases the spacecraft is assumed to be positioned in a 90° angle towards Earth, and in the worst hot case also a 90° angle towards the sun. This means that panel 1 is the only sunlit panel, and panel 4 is the only panel that receives IR from the Earth and Earth's albedo. Furthermore, the worst hot case is calculated with the peak power found in section 7.5 with an assumed efficiency of 70 %. For the worst cold case the situation in which the satellite is in eclipse is considered, here the only external heat factor is Earth's IR. The power used for the calculations is the average power also with an efficiency of 70 %. The panels are desired to have a small variation in heat, and the system temperature must stay within the limits given in table 7.12.

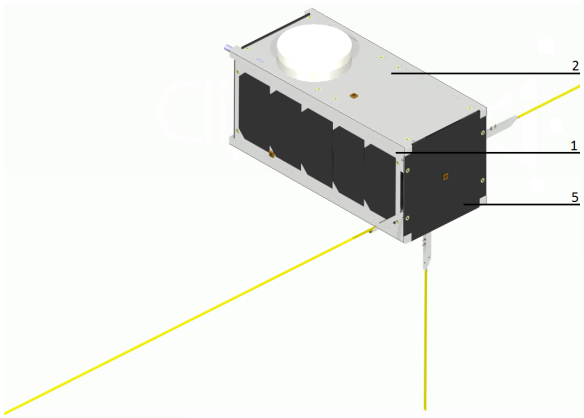

Figure 7.8: Panel configuration 1

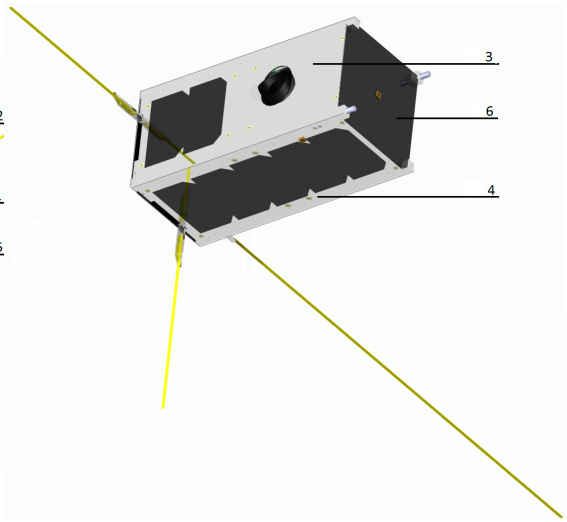

Figure 7.9: Panel configuration 2

One also has to keep in mind that the panels radiate heat onto each other, depending on the viewfactors. The viewfactors from long panel to long panel, long panel to short panel and short to short panel are given in table 7.13 [78]. The energy that one panel does not radiate onto another panel is assumed to be radiated into the internal system of the satellite. The internal components will be covered in a thin layer of epoxy and the inside of the panels will be painted black in order to make them launch proof [79]. Therefore it is assumed in the calculations that the heat radiated from panel to panel will be totally absorbed by the panel it is radiated upon.

Table 7.13: Viewfactors

long to long panel	26.0 %
long to short panel	8.9 %
short to long panel	23.9 %

The thermal expansion is also a parameter to be considered. It must be confirmed that the thermal expansion is not too big as to jeopardize the accuracy of the mission. Equation 7.28 shows how the thermal expansion is to be calculated. In this eqation δL is the expansion, L is the length of the panel, α_L is the material specific thermal expansion factor and δT represents the temperature variation.

$$\Delta L = L \times \alpha_L \times \Delta T \tag{7.28}$$

7.4.4 Results

After the iterative process for finding the most favourable coatings for GES the materials decided upon can be found in table 7.14, the absorptivity and emissivity values for the used coatings are stated in table 7.15. Furthermore, per panel the temperature for the worst hot case and cold case are given. Also the maximum thermal expansion is shown in the table 7.14. It can be seen that the highest thermal expansion is experienced by panel 2, of 0.36 mm, which is an expansion of only 1.8 %. The thermal expansion will not be of critical importance to the mission.

One must keep in mind that panel 1 and 4 are for the most part covered with solar cells to provide power to the system (see section 7.5). Since both panels have five solar cells mounted on, with an area of 0.00269118 m^2, the total percentage of the solar cells on the panels is 67.3 %. Therefore the emissivity and absorptivity of a solar cell is also given in table 7.15. Panel 3 also has two solar cells mounted on its body, which makes the coverage of solar cells on panel 3 26.9 %.

Table 7.14: Panel properties

Panel	Coating	Temperature sunlit	Temperature eclipse	Maximum expansion
Panel 1	White Paint Z-93C55	90.16°C	35.14°C	0.254 mm
Panel 2	Black Paint Chemglaze Z306	0.91°C	−77.92°C	0.364 mm
Panel 3	Black Paint Chemglaze Z306	−20.12°C	−53.56°C	0.154 mm
Panel 4	White Paint Z-93C55	63.45°C	−10.17°C	0.340 mm
Panel 5	Black Paint Chemglaze Z306	42.34°C	−48.33°C	0.209 mm
Panel 6	Black Paint Chemglaze z306	42.34°C	−48.33°C	0.209 mm

Table 7.15: Material characteristics

Material	Absorptance α	Emmittance ε
Solar cell	0.90	0.86
White Paint Z-93C55	0.05	0.66
Black Paint Chemglaze z306	0.92	0.89
Epoxy	-	0.89

The extreme temperatures for the internal components are depicted in table 7.16. Here one can see that the maximum temperature the system can reach is 43.74°C and the minimum is −3.70°C. The mimimum temperature the system reaches does not exceed the tolerance of any of the components. The maximum temperature however does, as the hot limit of the AD&C system lies 3.74°C lower than the temperature that can be reached. The temperature critical part of the ADCS is expected to be the star tracker. The star tracker is located looking towards the stars and away from the sun (see section 7.5.3. Most heat warming up the system will come from the sun. In the performed calculations it is assumed that the entire system will have one equal temperature, however, in reality the temperature will be varying throughout the system. Therefore it is safe to assume that the temperature of the star tracker will actually stay below 40 degrees, as it is located away from the main heat source [74] and looks into cold space. With this assumption the entire system will work with the given thermal control system.

Table 7.16: System temperatures

Situation	Temperature
Hot case sunlit	43.74°C
Cold case eclipse	−3.70°C

7.5 Power system

The power subsystem makes sure that the system is able to carry out its tasks during mission lifetime. The orbit has been chosen such that decay occurs within 25 years without the need of propulsion to de-orbit the satellite. Therefore the satellite has no extra propulsion system. This decreases the power requirement for the system. The power system is collectively called the EPS and can be subdivided into four subsections namely power source, energy storage, power regulation & control and power distribution. First the power budget is constructed. Once the power requirements are determined the power source is designed and optimized. If needed an energy storage is added. Finally, the power distribution and regulation system are selected. This section describes the electrical power system design, the tradeoffs made during this process and the configuration of the power system on the Cubesat.

7.5.1 Power budget

The final power budget can be seen in table 7.17. Peak power is calculated with a safety margin of 15% applied to the quiescent power. This is because a safet factor of 25% is too large for a small satellite as it is almost one fourth of the total mass of the CubeSat. However a safety factor is always necessary to guarantee a margin for the calculations so it is decided to use a minimum safety factor of 15%. The safety factor is kept constant for all subsystems.
The duty cycle is applied to peak power to calculate average power. The duty cycle is 1 for all subsystems except for downlink, which is only operational 4.7% of total orbital period (from table 7.5), battery charging (sunlit period) and battery heater (eclipse period). The battery needs to be charged during sunlit period therefore is included in the power budget. The total power needed to size the power source is power of the system plus the power consumed by the batteries. As can be seen the average power is $2.995W$ and total power is $4.93W$.

Table 7.17: Power budget Gravity Explorer Satellite

Subsytem	Quiescent Power (W)	Peak power (W)	Duty cycle	Average power (W)
Payload	0.6	0.69	1	0.69
TT&C	0.02	0.023	1	0.023
Antenna	0.116	0.13	1	0.133
AD&C	0.5	0.575	1	0.575
Communication	2	2.3	0.057	0.108
EPS	0.1	0.115	1	0.115
C&DH	0.4	0.46	1	0.46
Battery heater	0.22	0.253	0.27	0.068
Battery	0.98	1.127	0.729	0.822
Total	4.93	5.68		2.995

7.5.2 Solar panel selection

For a 3 year earth orbiting mission photovoltaic energy is the most suitable and cost effecient power source [67]. With unlimited solar energy available and low energy demands of the system, due to no propulsion requirements, solar panels will be sufficient and feasible to provide the energy needed during sunlit periods. There are different types of solar cells available. Most commonly available solar cells for CubeSat space missions are triple junction Galium Arsenide Galium Arsenide (GaAs) solar cells with the higest effeciency of 28.3%. This is based on the fact that the COTS solar panels providers found during literature research offer cells made of GaAs. The other available solar cell types are silicon cells, thin sheet amorphous silicon and Indium phosphide [67]. They have lower efficiency than multijunction GaAs cells. With the advent of time and technological improvements higher effeciencies might be achieved. New developments are the Copper Indium Gallium Selenide (CIGS) (compounds made of copper, indium, Gallium and Selenium). These layers can directly be deposited on the substrate using the technique called chemical vapour deposition [80]. They might provide the advantage of lower cost. However, GaAs cells provide the highest effeciency and this will also decrease the surface area required. Also keeping in mind that COTS components should be used as much as possible, most ready made solar panels are triple junction GaAs cells suitable for cubesats. Therefore triple junction GaAs with effeciency of 28.3% are selected.
The solar panel selection from different providers is based upon power provided, cost and mass. This is summarized in table 7.18. The data is for 2U body mounted panels. It can be seen that Clyde Space panels provide the greatest power for the lowest mass and price. The reason for this is that the 2U panels come with the option of 4 of 5 cells in series [5]. Choosing the 5 cell option means that the surface area is utilized as much as possible, leaving little room for other components on the solar panels. These panels are also compatible with cubesat structures. All three providers use triple junction GaAs solar cells from Azur Space with 28.3% effeciency.

Table 7.18: Data for 2U solar panel from different suppliers

	Power (W)	Mass (g)	Price (Euro)
Clyde space [5]	5.21	69	3030
ISIS [13]	4.61	100	3500
Gomspace [81]	4.8	118	4000

The solar panels from Clyde Space contain a high quality PCB substrate with space grade kapton overlay. They include temperature sensors and reverse bias protection diodes. Given that the cells are connected in series, these diodes make sure that if one cell fails due to damage that the other cells are not affected. It is wise to check if the panels have these diodes. If not, then they should be added manually and this will make sure that due to malfunctioning of one cell the entire panel is not lost.
Once the types of panels are selected the power budget can be used to size the panels. This is done using the data sheets provided from Azur space [82] and Clyde space [5]. The average power is used to size the solar panels. Whereas peak power is needed to size the battery.
The orbit is chosen such that while in eclipse the satellite will not pass over the ground station in Delft, therefore no downlink communication occurs during eclipse. The Battery is therefore sized without battery and communication power.
Given the power requirement of P_{av} of $2.995W$ from the power budget in table 7.17 the area of the solar panels can be obtained according to the steps in table 11-34 of SMAD [67]. First the power that must be provided by the solar arrays is estimated with equation 7.29.

$$P_{sa} = \frac{\frac{P_e T_e}{X_e} + \frac{P_d T_d}{X_d}}{T_d} \tag{7.29}$$

where P_e and P_d are power needed during eclipse and daylight, respectively. Similarly the T_e and T_d are the eclipse time and the sunlit period. The term X_e is the path efficiency from solar arrays to battery to individual loads. Whereas X_d is the effeciency of path directly from solar arrays to loads, as no battery is used during sunlit periods. These values can be found from the data sheet of the selected EPS system [83]. It is important to use these values and not the standard values given in [67].
There are two ways to estimate the power output of the solar cells. Method 1 is to estimate the area of the solar array. First the beginning of life power P_{BOL} is calculated with equation 7.30. Here P_0 is the solar flux (1367 W/m^2). It is assumed that the incidence θ angle is zero. The inherent degradation I_d is a function of temperature of the panel and from Azur Space data sheet for solar cells it is 0.259% per degree [82].

$$P_{BOL} = P_0 I_d cos\theta \tag{7.30}$$

The solar panels have to be sized according to the end of life power because at the end of the mission enough power should be available despite life time degradation L_d. For a mission of 3 years the L_d is given by equation 7.31. Here n is the mission lifetime of 3 years.

$$L_d = (1 - degradation/yr)^n \tag{7.31}$$

The end of life power (P_{EOL}) will obviously be smaller than P_{BOL} and even for a small mission of 3 years it is important to consider this, as the calculated array area may differ if not taken into account. P_{EOL} is calculated with equation 7.32.

$$P_{EOL} = P_{BOl} * L_d \tag{7.32}$$

Finally the area of the solar array A_{sa} can be calculated with equation 7.33. The packing factor is not taken into account. This is because the number of cells on the solar array is known and the area is estimated accurately from the Computer Aided Design (CAD) model in CATIA. The number of cells is then changed to see how many cells and hence how many panels are sufficient to meet the power requirements.

$$A_{sa} = P_{sa}/P_{EOL} \tag{7.33}$$

The second method is to directly use the power output of the panels from the provider. It is assumed

that manufacturing losses are taken into account by the provider when giving the power output value. The L_d is applied to this P_{BOL} to obtain the P_{EOL}. Both methods are correct and should give similar values. The second method gives slightly higher power output and will be used because they are the values provided by Clyde space, whereas the method 1 calculations are for personal verification. In table 7.19 the results from method 2 are listed only. Both methods are however carried out in order to check the calculations. The constants used and the results obtained are summarized in table 7.19.

Table 7.19: Power requirements 2U cubesat

P_d (W)	3.00
P_e (W)	2.06
Orbital period (min)	96.20
T_d (min)	70.20
T_e (min)	26.00
X_d	0.86
X_e	0.95
P_{sa} required (W)	4.31
P_{output} Clyde Space (W) [5]	4,19
P_{BOL}	4.19
P_{EOL} (front panel, 5 cells)	3.85
P_{EOL} (Albedo 3 cells bottom panel)	0.53
Total power (W)	4.39

As can be seen from table 7.17 the power provided by the 8 cells is $4.39W$, exactly enough for the power required of 4.31 W. However, the redundant cells also produce power so the total power provided by the two panels (10 cells) is $4.74W$.
The angle of incidence θ is taken to be zero. This is because A_{sa} is not sensitive to slight changes in angle, as can be seen in figure 7.10. However if angle of incidence is much larger then this can have a significant impact on the A_{sa}. In that case the solar panel configuration needs to be optimized with angle. This is not done for GES since it is safe to assume that the attitude of the satellite is stable and maximum solar flux is utilized in the sun-synchronous dawn-dusk orbit.

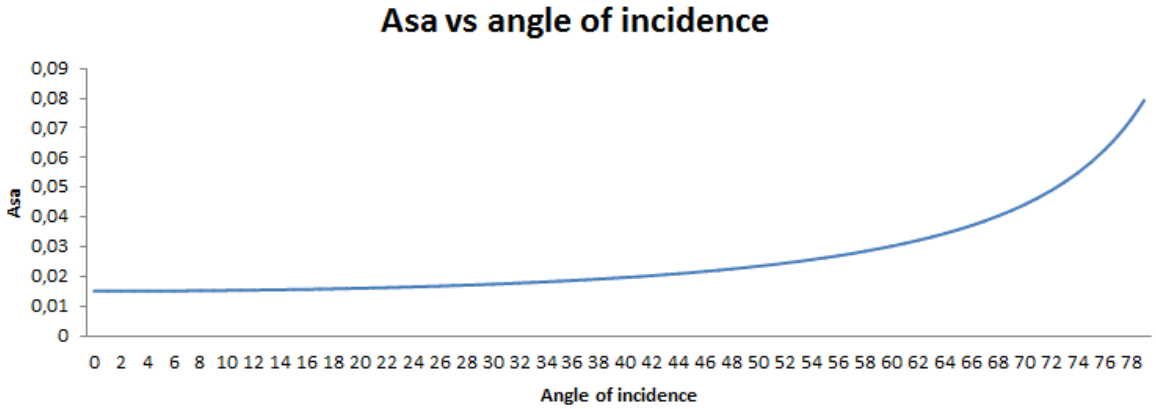

Figure 7.10: Area solar array as a function of angle of incidence

7.5.3 Solar panel configuration

After optimizing the power bugdet and using the methods described in section 7.5.2 many iterations are done before the final number of cells is calculated. Initially the power system was designed for a

3U cubesat. However it turned out that all the components will fit in a 2U cubesat. At some point deployable panels were required due to the fact that one surface would not suffice. With the 2U unit one body mounted panel on front side is not enough. A solution to this is to use panels at the bottom side and utilize the albedo solar flux, assuming that the minimum solar flux from albedo is 23% of the original flux. Using the 5 cell configuration for 2U panels the final design consists of one full 2U panel on the front surface and 3 cells at the bottom, using albedo flux. Therefore 8 cells is the minimum requirement. However a full panel is mounted on the bottom making the 2 extra cells available for redundancy.
The worst case would be if the satellite rotates with its back side infront. To make sure that the system still has enough power a single unit panel is mounted at the back. The albedo flux will also provide power in case the satellite rotates and the back panel (fitted with a 1U bodymounted solar panel)is facing the sun. For a better view of the solar panel configuration see figures 7.8 and 7.9. In case the satellite starts tumbling these extra panel will provide enough power for the system to start generating energy slowly and restarting the AD&C system. At some point the satellite is bound to detumble on its own due to the presence of magnetotorquers in the AD&C. It is assumed that in worst case all systems are shut down except for EPS and CD&H system. If the battery also has run empty (which is unlikely) the solar panels will slowly provide power to restart the system.

7.5.4 Battery selection

In sun-synchronous dawn-dusk orbit the satellite is constantly in sunlight. However, a small eclipse period is possible in certain seasons. This eclipse time is 26 minutes (see section 5.3) and the battery is sized according to this need. Different batteries have been looked at. Conventional lithium ion batteries are normally used in cubesates but the lithium polymer batteries of Clyde Space in figure 7.11 are a cheaper and lighter solution. The battery has a built in heater with thermostat which makes sure that the operating temperature of the battery remains above 0°. The battery heater itself uses power of $0.22W$. This is the power consumption of the battery and heater together. Assuming that the battery only needs warming up during eclipse periods this value is given a duty cycle of eclipse time (0.27) as can be seen in table 7.17.

Figure 7.11: Lithium ion polymer battery from Clyde Space [5]

The battery sizing is done with peak power minus battery power and CD&H power. This is the power requirement during eclipse. The battery power P_{batt} is calculated with equation 7.34:

$$P_{batt} = \frac{P_e T_e}{T_d \eta_{ch} * 0.9} \tag{7.34}$$

Here η_{ch} is the battery charging effeciency of 87% at EOL, given in the paper on polymer batteries from Clyde Space [84]. This gives a battery power requirement of 0.98 W (as shown in table 7.17) and capacity of 1.1 Wh. The Clyde Space Lithium power battery has a 10 Wh capacity and therefore gives 8 times more than the required capacity of 1.1 Wh. A fully charged battery therefore has 8 times more than the capacity required and can be used in peak power demands.

The battery heater is not always on. Therefore it is assumed that only during eclipse when temperatures are lower that the battery heater is needed. Therefore the duty cylce is the percentage of eclipse time to total orbital period (see power budget in table 7.17). In general during operation batteries also produce warmth however the use of polymers in the chosen lithium ion polymer batteries insures that the battery itself does not warm up. This is also the main reason for the higher effeciencies of these batteries. It does mean that the battery temperature needs to be regulated.
Lithium ion batteries have the advantage of higher energy density and wider operating range compared to other batteries (for instance NiCd and NiH2) [67]. The battery life depends upon the Depth Of Discharge (DOD) and the number of charge/discharge cycles. The DOD is the percent of total battery capacity removed during a discharge period. This can be determined by calculating the required battery capacity during eclipse time and assuming that the battery discharges this amount in one cycle. With the charge time of sunlit period it is assumed that the battery is fully recharged during non-eclipse period. The batteries have excess capacity and since the solar panels design is done based on average power, the secondary batteries will be used to meet peak power loads when all components have a duty cycle of 1. This is the case during communication, data downlink, and fully sunlit periods. As mentioned already communuication will not occur during eclipse period so peak power does not occur during eclipse.
Assuming that the battery is used only in eclipse period and experiences maximum eclipse time as mentioned in section 5.3, the battery will experience 1,800 cylces per year or 5,400 cycles in the 3 year period. Given that the battery has been tested for 5000 cycles and the expected lifetime is 35,000 cycles, the battery will therefore suffice the 3 year lifetime requirement. Infact if the satellite continues after the 3 years the battery still can be used.

7.5.5 Regulation and control

The electrical power system selected is the CS-2UEPS2-NB from Clyde Space as shown in figure 7.12. This system provides over-current and battery undervoltage protection. It also uses maximum power point trackers Maximum Power Point Tracking (MPPT). An MPPT is a nondissipative subsystem as it extracts the exact power a spacecraft requires upto the array's peak power [67].

Figure 7.12: Electrical power system for 2U cubesat from Clyde Space [5]

In figure 7.13 the effeciecncy losses in each step of power conversion are given. These are the same losses X_e and X_d mentioned earlier in section 7.5.2. The electrical block diagram in figure 7.13 is based on the block diagram provided by Clyde Space [83]. It gives a detailed overview of the path of energy from the solar panels to the loads. For each solar panel a seperate MPPT is needed. As can be seen in figure 7.13, 3 MPPTs are available which are exactly enough for the 3 panels on GES. In case additional panels are needed an extra EPS or one with more channels has to be added to the CubeSat. The effeciency losses (X_e and X_d) are also included in figure 7.13. The electrical block diagram shows that the solar panels have been connected to earth/ground to get rid of extra static electricity. In case of the satellites this means connecting to the bus/outer structure.

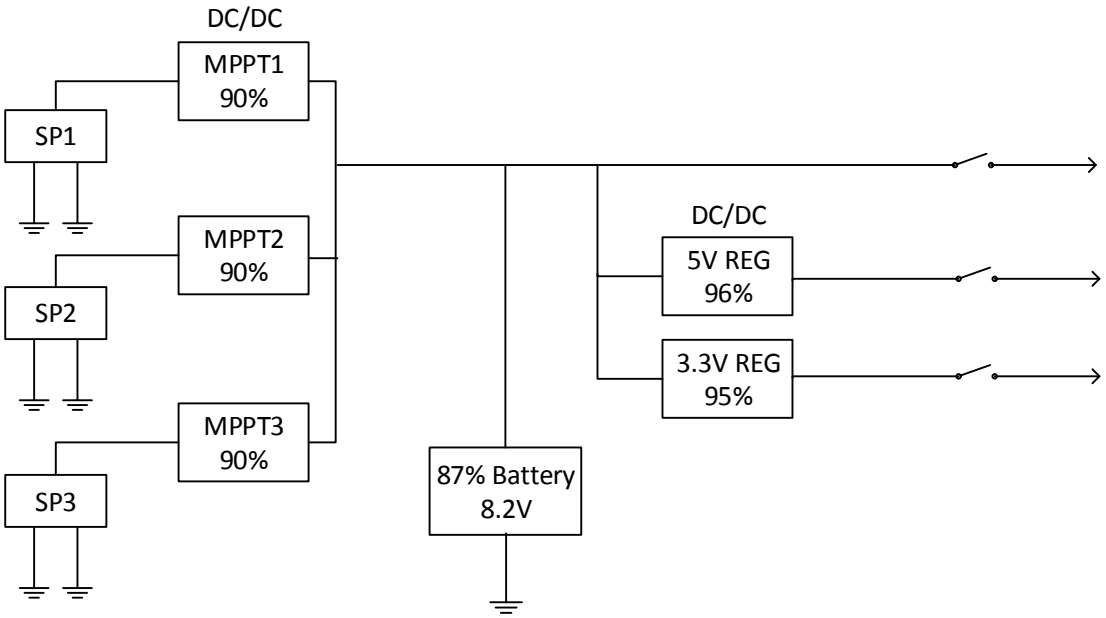

Figure 7.13: Electrical block diagram for 2U EPS system [5]

7.5.6 Power distribution

Clyde space offers a distribution system with 24 on/off switches and overcurrent protection [5]. Overcurrent protection is already present on the selected EPS from Clyde Space. The on/off function is generally also performed by the onboard computer. Therefore no load distribution system is added which saves costs and mass.

7.5.7 Evaluation

The total cost of the the power system is 12,337 *euros*. For a detailed breakdown of the cost break down see table 9.2. For the power system selection use of COTS components has been taken into account. The other option is to create ones own solar cells. This will save costs of manufacturing and will be a much cheaper solution as no labour costs will be involved. However, the use of space grade solar cells from clyde space provide much higher reliability and it is worth it to implement a reliable system in order to improve mission success despite higher costs. This is because manufacturing solar cells requires proper connection of the arrays to the substrate. If this is not done properly there is a chance of the solar cells accidentaly falling off the panel.
The smallest found battery is the one selected. This battery provides 8 times the needed capacity. It would be better to use a smaller battery but an additional one for redundancy. In some cases no battery is used however for safety it is better to add a battery.
The satellite is not rotating therefore dissipating extra energy due to body mounted panels has been ignored. A different configuration for panels can be chosen and optimized for angle of incidence angle however this is beyond the scope of the time available for DSE. It is a recommendation to assume that the angle of incidence may change by a great amount and therefore to optimize the solar panel configuration according to the angle of incidence.

7.6 Structural design

The structure forms the body of the satellite. First, the proper size is selected after which an overview is given of three structures that have been selected as candidates for GES. The three structures are evaluated and the most suitable structure is selected.
Available structures range from a 0.5U size to even 12U. Based on the amount of needed hardware components, it is estimated that a 2U or 3U size is needed. A rough 3D CATIA model was made with both structure sizes to see how all the parts would fit. Although the 3U structure offered more exterior surface for solar cells, the 2U structure was selected because of the lower total mass, thereby reducing launch costs. Three aluminum structures are analyzed and the most suitable chassis is selected.

Pumpkin skeletonized
The most noticeable feature of the skeletonized chassis, see figure 7.14 is the many cut-outs that allow access for hardware connectors such as USB ports and power supply. Other cut-outs are there to save mass or offer access for other systems. Additional panels such as solar panels can be clicked on to the structure with clips. A disadvantage is that it could be difficult to integrate the selected AD&C system with the star-tracker. Additional cut-outs are needed and re-enforcing the structure might be necessary. The same challenge arises when mounting the GNSS antenna on one of the sides. During the assembly process the internal structure can hardly be accessed. Taking out the stacks from the chassis itself is the most easy way of accessing hardware when needed. The price is around 1200 *euro* [85].

Pumpkin solid wall
The main difference of this chassis with respect to the other Pumpkin structure is the solid wall instead of the skeletonized structuring, see figure 7.15. The cut-outs for connectors stay, and additional cut-outs could be made. However, the skin panels form the chassis, which means that large cut-outs will compromise the structural integrity. Next to that, when an error is made with modifying the panels replacing them is going to be expensive. Like the skeletonized version, the price is around 1200 *euro* [85].

ISIS structure
The ISIS 2U structure in figure 7.16 is build differently than the other two. The primary structure consists out of two side frames that are connected to each other with ribs. The ribs carry four rods on which the internal hardware can be attached.

The downside of the ISIS chassis is less volume is available within the structure. However, the skin panels are not the main supporting part and can easily be replaced. Another advantage is that detaching the skin allows easy access to all the internal components. The ISIS chassis has two kill switches and the total mass is 390 *grams*. The price is 2,950 *euro*, which is more than twice the price of the Pumpkin variations.

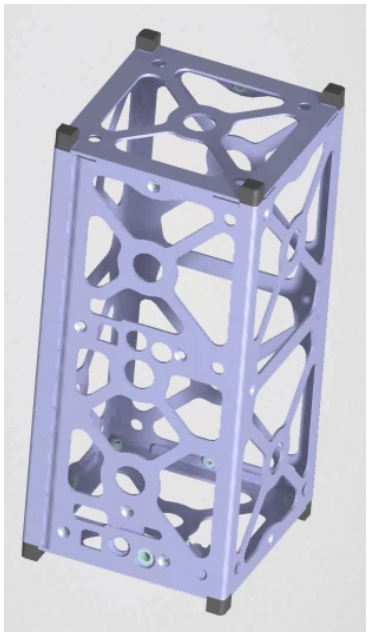

Figure 7.14: CATIA drawing of the pumpkin skeletonized structure [6]

Figure 7.15: Catia drawing of the pumpkin solid wall structure [6]

Figure 7.16: CATIA drawing of the ISIS structure [7]

Structure selection
It is clear that the skeletonized structure can be dismissed due to the inflexibility for cut-outs. The solid wall Pumpkin structure is cheaper than the ISIS structure. However, the ISIS chassis offers better accessibility and more structural reliability when the panels are modified. Therefore the ISIS structure is chosen.

7.7 Ground segment

The ground segment constitutes the ground-based infrastructure necessary to support the operation of the satellite, including the control of the spacecraft in orbit, and the acquisition, reception, processing and delivery of the data [86]. The ground station located at the Technical University Delft is chosen. The selection of the ground station and its properties will be presented in this section.

The measurement data will be transmitted to the ground station during contact time. Once the data is received by the ground station it will be collected, stored and processed to obtain the proper information by the users, this process is out of the scope of this project. In the non-access period the data will be stored in the satellite. For this mission it is not needed to relay data in real-time to the ground. Therefore one active ground station will be sufficient. The low data rate generation produced by the payload system allows one to use a relatively low frequency band as higher frequencies are able to allocate higher data rates. The required UFH antenna size for the satellite is in the order of centimeters. Geographically it is most efficient to use a ground station near the poles as the access times will be longer hence the data rate can be lowered requiring a less powerful transmitter. However, the VHF/UHF ground station located at Delft University of Technology is chosen for practical and economical reasons. In case of failure the ground station located at Eindhoven University of Technology will perform as a ground segment backup [87]. The only cost that the ground segment will have are the cost for the operator, since the satellite is compatible with the equipment that the ground station has. The operator is normally required to be physically present at the ground station at least during the Launch and Early Orbit Phase. For the standard operational phase the operator is often able to capture most passes either automatically or remotely via internet. To keep the cost as low as possible the operator could spend his free time at the ground station, like what is done for the Delfi-n3xt. The station is located at 100 m above sea level

and can track satellites from a minimum elevation of -1 deg. It has a 70 cm crossyagi, circular polarized in use. It tracks satellites in 360 deg Azimuth and 180 deg elevation around this ground station. The primary receiver in the ground station for this is a ICOM IC-910H. Optionally a AOR5000 wide band receiver with QS1R software defined radio on its intermediate frequency output is available [88].

7.8 Launcher selection

From the preliminary cost estimation during the Mid Term Review, it became clear that the launch was the main cost driver. From the total cost estimation the launch cost took up more than 80 % of the total costs. Therefore, it is important to find out if there are cheaper launch options available.

During the design of the total structure, CubeSat measurements are kept in mind to make sure that the satellite can be launched with a certified CubeSat deployer [89]. This saves costs on launch vibrations tests that are not necessary for CubeSats launched within a deployer.

Next to that it creates the possibility to launch the small satellite together with other systems so that the cost of the launch can be split up. Because of the size of the satellite and the popularity of the orbit a piggyback launch can be chosen.

There are commercial companies that offer piggyback launches, one of these companies is Spaceflight [90]. Based on the launch period and destination orbit a launch can be selected and reserved [91] For example, in the second half of 2016 a launch is available to a SSO at an altitude of 500-600km in the United States. A 3U cubesat space can be reserved on this launch for $325.000, that is about 237.625 *euros* with the current conversion rate of 0.73. [92]

Another commercial company that offers piggyback launches is ISIS [93]. The total cost ISIS offer including logistics is about 175,000 - 225,000 *euros* though for a 3U CubeSat of 3-4kg. These costs include the CubeSat deployer, transport and integration with the launcher, but excluding the testing and travel costs of the team [94].

Because the Gravity Explorer Satellite is a 2U CubeSat the launch deployer can be shared with another 1U CubeSat. The launch costs can then be shared, so only 2/3 of 225,000 *euros* remains, that is about 150,000 *euros*.
This is still a lot of money in respect to the other costs of the satellite mission. Therefore ESA can be contacted about the possibilities of launching a university CubeSat. They are known to offer the possibility for students to launch their own satellite as part of a competition [95].

What has to be kept in mind when going for a cheaper option, for example with ESA, that it limits the orbit choice. If no contract is signed with a commercial company the team is dependant on the options that are presented and plans might be delayed.

For now it is assumed that no cheaper options present itself and a launch contract with ISIS will be signed. Thus making the total launch costs 150,000 *euros*.

8 System Characteristics

Now that all subsystems are designed they can be integrated to give shape to the final system. This chapter elaborates on the characteristics of the complete system.

First section 8.1 lists all units carried onboard. Section 7.5.3 shows the integrated system. Finally, section 8.3 elaborates on the manufacturing, assembly and integration plan of the system.

8.1 Spacecraft system characteristics

Every subsystem has been designed in chapter 7 and the electronic units have been selected. This section combines all subsystems to form the complete list of electronic units carried onboard. With this list the system integration can be started in section 7.5.3. Table 8.1 shows this complete list of components.

Table 8.1: Electronic units carried onboard

Component	Specification	Dimensions
Payload		
GNSS receiver	Antcom G5 Antenna	$r = 66.8\ mm$, $h = 21\ mm$ [96]
GNSS antenna	Asterx-m OEM	$70 \times 48 \times 8\ mm$ [97]
AD&C system		
Integrated system	BST iADCS-100	$95 \times 90 \times 32\ mm$ [69]
Tracking, Telemetry & Command		
Full duplex transceiver	ISIS Full Duplex Transceiver	$96 \times 90 \times 15\ mm$ [98]
Deployable antenna system	ISIS Deployable Antenna System	$98 \times 98 \times 7\ mm$ [99]
Command & data handling		
On board computer	ISIS Cube Computer	$96 \times 90 \times 10\ mm$ [14]
Thermal system		
Coating	White Paint Z-93C55	$0.01309\ m^2$
Coating	Black Paint Chemglaze z306	$0.05462\ m^2$
Power system		
Battery (including heater)	Clyde Space CS-SBAT2-10	$96 \times 90 \times 16\ mm$ [100]
Electrical power system	Clyde Space CS-2UEPS2-NB	$96 \times 90 \times 12.7\ mm$ [101]
Body mounted 2U panel	Clyde Space SP-L-S2U-0031-CS	$216.6 \times 83 \times 1.6\ mm$ [102]
Body mounted 2U panel	Clyde Space SP-L-S2U-0031-CS	$216.6 \times 83 \times 1.6\ mm$[102]
Body Mounted 1U panel	Clyde Space SP-L-S1U-0002-CS	$110.85 \times 83 \times 1.6\ mm$ [103]
Structure		
2-Unit structure	ISIS 2-unit	$100 \times 100 \times 227\ mm$ [7]

To illustrate the mutual relations and interactions of the components in table 8.1 a block diagram is presented in figure 8.1.

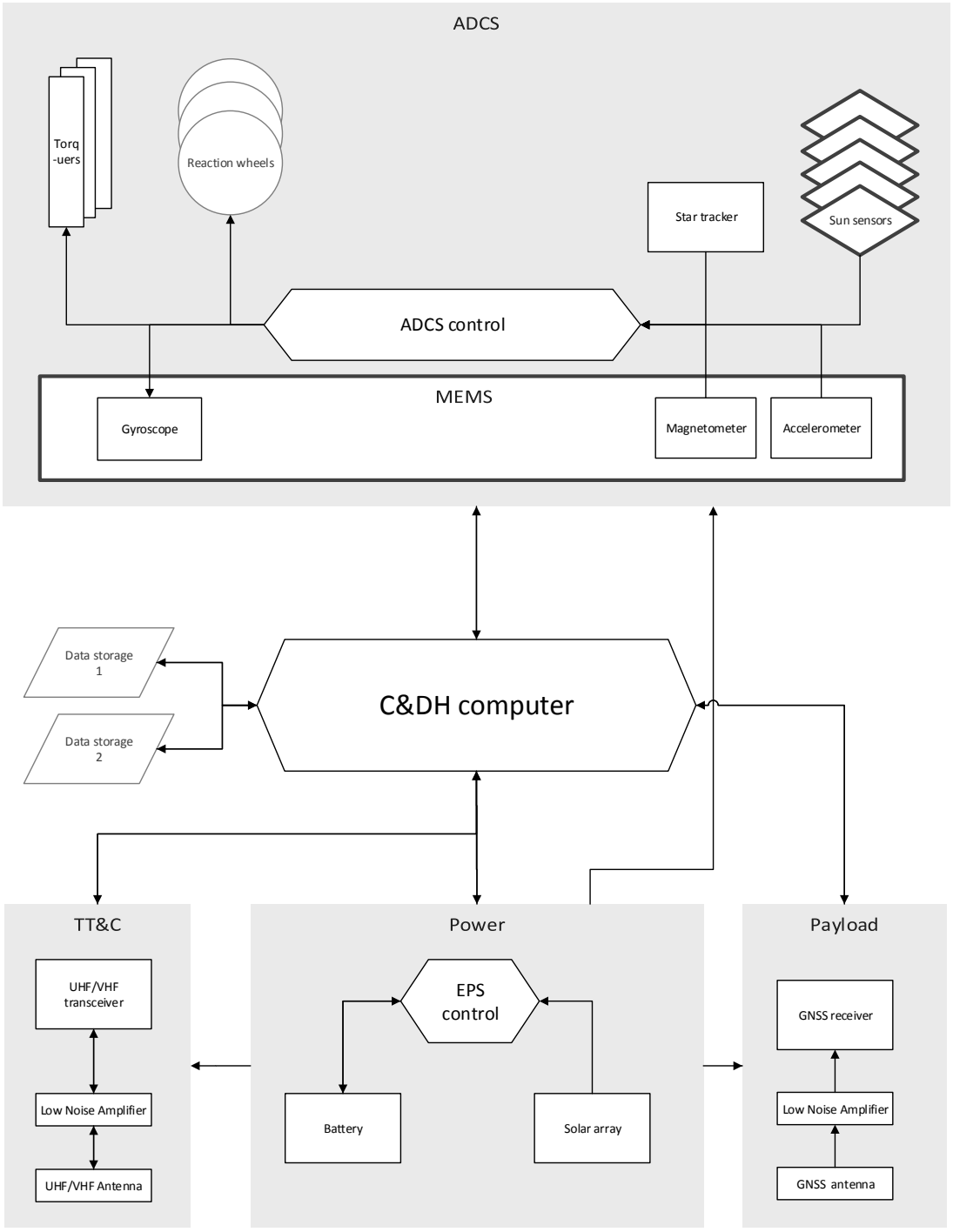

Figure 8.1: Hardware block diagram

8.2 Configuration and system integration

System integration entails the process of combining the selected systems and components in such a way that the most optimal design is created. A configuration plan is made to include the requirements of different departments. Afterwards a 3D-model is made to verify the requirements and resulting conflicts are solved. The final result is given at the end of this section.

8.2.1 Requirements and freedom of configuration

The requirements for the configuration are set by payload, communication, AD&C system, power and thermal control. These are formulated such that components can already be selected, integrated and leave room for flexibility.

Payload

- the CubeSat shall have a GNSS antenna and GNSS receiver on board
- the GNSS antenna shall be mounted on the top side, opposite to Earth
- the GNSS antenna shall be free of any obstacle that can interfere with its received signals

These payload requirements have a high priority because the success of the GNSS system determines the success of the whole mission. Therefore, the position of the antenna is therefore not negotiable and interference must be kept to a minimum.

Communication

- the CubeSat shall have the specified UHF/VHF antenna on board
- the CubeSat shall have the specified On Board Computer

The communication antenna and receiver do not have a fixed position according to the requirements. The antenna has four strings of which two vertical mounted strings can be considered redundant.

AD&C system

- the CubeSat shall have the specified AD&C system on board.
- the star-tracker shall be pointed away from the Sun and Earth.
- five sun-sensors shall be mounted on each side of CubeSat, except for the side where the star-tracker is mounted.

The star-tracker determines how the AD&C system component shall be positioned in the satellite structure. The four stack rods are not evenly spaced, see section assembly, therefore the therefore the AD&C system can only be positioned in one way assuming the front side flies in a constant direction.

Power

- a 2U sized solar panel with five cells shall be mounted on the Sun side of the CubeSat.
- a 2U sized solar panel with five cells shall be mounted on the Earth side of the CubeSat.
- a 1U sized solar panel with two cells shall be mounted opposite to the Sun.
- the specified EPS and battery shall be included in the CubeSat.

The requirements of the power section is largely determined by the needed power to run operations in the Sun and during eclipse. The solar panels are selected based on redundancy and energy radiating from the Sun and Earth.

Thermal

- the panels facing the Sun and Earth shall be coated white
- except for the panels facing the Sun and Earth, other panels shall be coated black

The two thermal requirements take into account the heating and cooling of the satellite during sun and eclipse time. The solar panel configuration is already taken into the thermal calculations.

Other requirements

- the mass of the CubeSat shall be kept to a minimum.
- components mounted on the exterior are allowed to have a height of less than 9 mm.

The mass must be kept to a minimum to deal with the launcher costs. A 2U sized satellite for example is more convenient than a 3U size. The space allowance between the satellite exterior and launch-pod is 9 mm. However, a small clearance margin is preferred to allow assembly tolerances.

8.2.2 Final configuration

To verify the dimensions and volume of the satellite, CATIA is used. Next to that the program visualizes how all the components are installed with respect to each other. The external dimensions can be found in figure C.1. Appendix D shows a selection of exterior views. This section starts with the three main conflicts that came from the different requirements. The exterior configuration is discussed afterwards, followed by the interior configuration.

Solved Conflicts
Inputs from each department were evaluated and applied during system integration. Some conflicts had to be solved that were caused by structural and requirement aspects. A solution had to be found for three main conflicts.
The GNSS antenna has a height of 9.55 mm while the outer clearance between the pod and the CubeSat is 9 mm. A cavity is made of 1 mm deep in the outer panel such that the needed clearance is now 8.55 mm. See figure D.4.
One of the UHF/VHF antenna strings could interfere with the GNSS antenna. As a solution, one of the deployable antennas is detached. See figure D.5. The consequence of this action is a loss of redundancy for ground communication. However, daily operations are not influenced.
The standard 2U CubeSat panels do not cover the sides of the UHF/VHF antenna that is mounted on top. Panels are elongated and cut-outs are made to let the UHF/VHF antenna deploy its antennas in space. See figure D.6. The side panels have to be customized during the manufacturing process.

Exterior configuration
A 2U structure is selected to house all the systems. Cut-outs have been made in the outer panels to make way for sensors and antennas. The UHF/VHF antenna can only be mounted on the front or rear side of the satellite. The front is chosen to allow easy access during assembly. The GNSS antenna is positioned away from the UHF/VHF antenna to keep interference at a minimum. Sensors are mounted on the outside of the satellite. The star tracker is located opposite to the sun away to avoid being blinded. On the other panels, a total of five sun sensors are installed. Three solar panels are mounted on the structure. Two 2U-sized panels are located at the sunlit and Earth side. One 1U-sized solar panel is positioned opposite to the sun, next to the star tracker. The distance between the outer end of the star tracker and the skin panel is 5.5 mm, which is within the tolerance of 9 mm. The exterior is shown in figure 8.2.

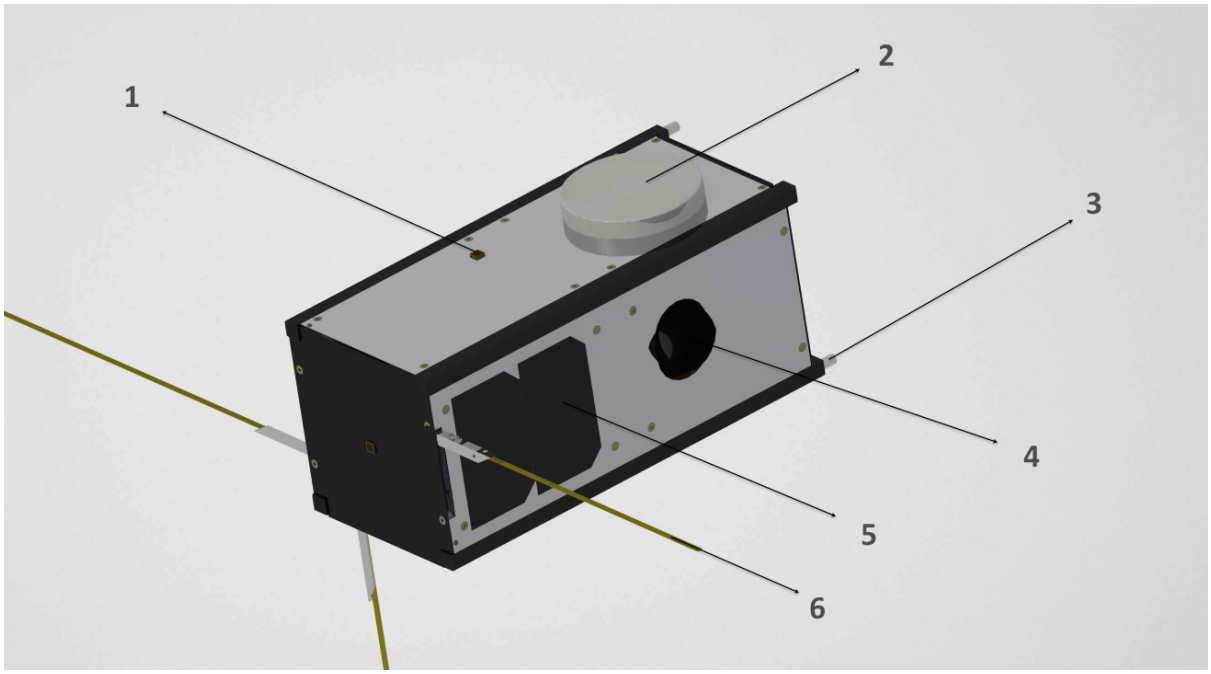

Figure 8.2: Exterior of GES

The following exterior components are indicated:

1. sun-sensor
2. GNSS antenna
3. kill switch
4. star tracker
5. solar panel (1U)
6. UHF/VHF antenna

Interior configuration
Internal modules are attached with stacking rods. The interior is set up such that the center of mass lies in the middle or moves slightly towards the AD&C system and GNSS antenna. Although module groups such as the GNSS antenna/receiver and UHF/VHF antenna are positioned as close to each other as possible to avoid unnecessary complications, the battery and electronic power system are separated to centralize the center of mass. The AD&C is mounted as close to the centre of the structure as possible without letting the star tracker touch the structure. The interior of GES is shown in figure 8.3.

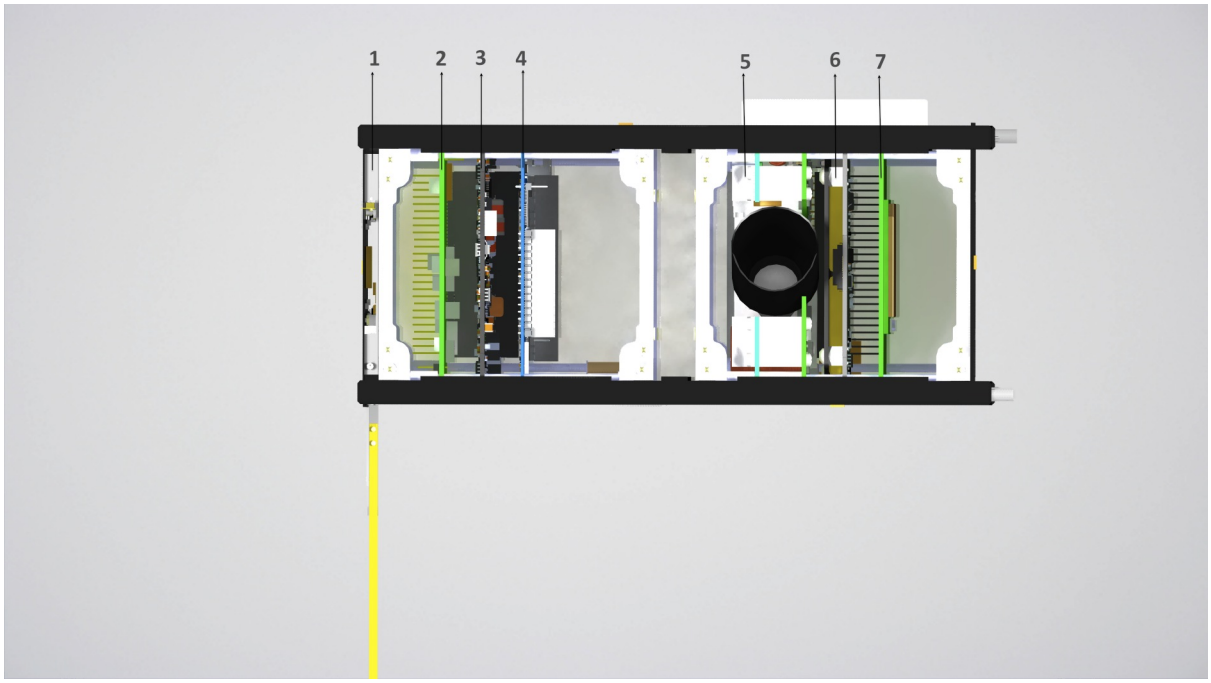

Figure 8.3: Side view with internal hardware

The following internal hardware components are indicated:

1. UHF/VHF antenna
2. UHF/VHF receiver
3. Electronic Power Unit
4. On Board Computer
5. Attitude Determination & Control Unit
6. battery
7. GNSS receiver
8. GNSS antenna

8.3 Production plan

This section presents an overview of the satellite's manufacturing, assembly, and integration plan. This plan describes the procedures, activities, and tests that will be done on the satellite and all its components before it can be launched. It is really important to understand the production plan since it can significantly influence the cost and time budget. Before a production plan can be made, all the constitutive parts of the satellite have to be known. From the smallest to the largest these parts are [104]:

- **Piece parts:** the smallest fundamental parts of any device. These include individual parts such as resistor, integrated circuit, bearing, or housing.
- **Components:** any part that can function individually as a unit, such as an antenna, a battery, or a power control unit.
- **Assembly:** functional group of parts, such as an antenna feed or deployment boom

- **Subsystem:** the combination of components and assemblies that can be considered a satellite subsystem, such as thermal control, AD&C.

8.3.1 Manufacturing and assembly

Once the data for all the constitutive parts of the satellite is gathered, the project goes into the manufacturing phase. During manufacturing, all the pieces, components, assembly pieces, and subsystems have to be prepared. Furthermore, for a manufacturing plan all the facilities (such as laboratories and clean rooms), methods of manufacturing, precautions and information about the personnel have to be defined. Once all the information is complete, the manufacturing process begins.
For GES all components are already sub-assembled and are ready to be mounted on the satellite. First the assembly of the structure will be discussed, after which possible modifications will be considered.

Assembly of the structure
The piece parts of the structure are shown in figure 8.4.

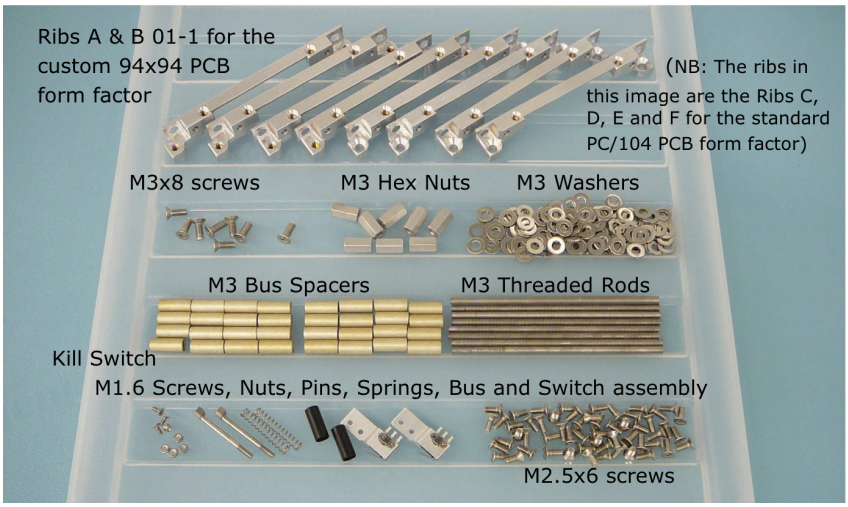

Figure 8.4: Parts needed for the structure [8]

The stack is prepared on an assembly jig as shown in figure 8.5. First two bottom ribs are place on the jig after which the threaded rods can be inserted into the outer holes of the rib. A washer is placed over each rod followed by the first module. In the pictures this is shown as a simple PCB. The bus spacers ensure that there is enough space between each module. The same process is repeated for each module until a stack height of 82.4 mm between the outer modules interfaces are reached. The upper ribs can then be placed on top of the first stack. For GES, two stacks are build up.

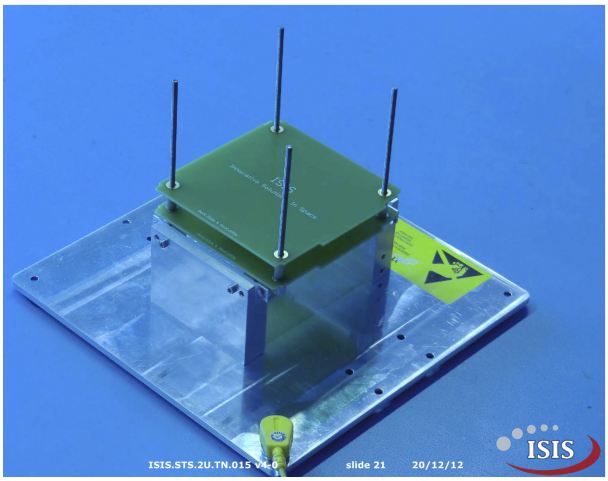

Figure 8.5: The jig with a small stack of PCB's [8]

The kill switch is made of a button, spring and a guide pin, see figure 8.6. Note that the proper functioning of the kill switch must be checked. If faulty mounted, the satellite might not activate in space.

Figure 8.6: Kill switch parts [8]

To integrate the stacks in the primary structure, the first side-frame is placed on top of a 2U sized horizontal assembly jig, see figure 8.7. A ground cable must be attached to the side-frame to limit the build-up of static electricity. The two stacks can now be placed on the side-frame after which the second side-frame can be placed on the stacks. The two side-frames can now be screwed on the stack ribs. After this the side exterior panels are mounted. The bottom panel follows. Cut-outs in the exterior panels have to made for the star tracker, sun sensors and GNSS antenna.

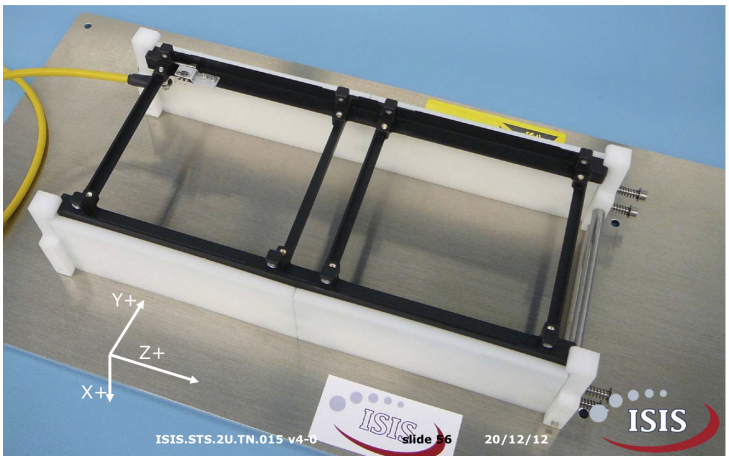

Figure 8.7: Horizontal jig with the sideframe [8]

The horizontal and vertical assembly jig can be used to place the structure, allowing easy access to all the systems. For example, the UHF/VHF antenna can be placed on top of the structure by using the vertical jig. On top of the UHF/VHF antenna a skin panel with the sun sensor is mounted. The GNSS antenna is mounted with the help of the horizontal jig.

Modifications
One of the strings on the UHF/VHF antenna must be detached on the side where the GNSS antenna is mounted to avoid potential interference. The GNSS antenna is already shortened and is delivered by the manufacturer as such. The GNSS antenna itself however must lower another 1 mm to have enough clearance between the satellite exterior and the launch pod. This is done by milling a 1.5 mm aluminum panel such that it looks like the panel in figure 8.8. All side panels need to be elongated to cover the UHF/VHF antenna and cut-outs at the end are needed to let the antennas deploy in space. The solar cells are 4 mm thick and therefore the panels hosting the solar cells must be milled. Additional cut-outs are applied for sun sensors.

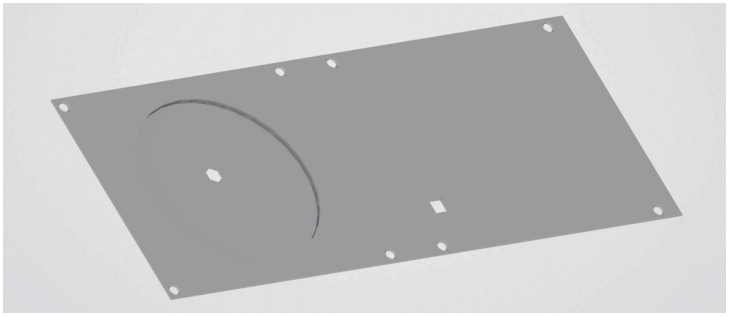

Figure 8.8: The panel on which the GNSS antenna is placed

8.3.2 Quality assurance

Quality assurance is the process of the verification of the production procedure and it includes the planning, personnel, facilities and manufacturing. Personnel and volunteers should be qualified and all facilities used for the production of GES are tested. As for the manufacturing process itself, all the sub-assemblies and components of are purchased as a complete product. Attention is spend on how suppliers of facilities and components verify the quality of their components.

8.3.2.1 Quality tests

The entire satellite system as well as the material used for the system have to go through some tests before they can be validated for operation. These tests include: vibration test, shock test, thermal test and radiation test. GES could be vulnerable to vibrations and shocks during launch and orbit insertion. Therefore, in order to verify the strength of the material, vibration tests of different frequencies ranging from 20 to 2000 Hz will be necessary. After doing the vibration test, a shock test will be performed. This is optional for GES because of the use of deployers during the launch of the satellite. Afterwards, different components of the satellite will be mounted on a base plate and put inside a vacuum chamber and using conductive coupling of the base plate and radiative coupling to chamber walls, the satellite can go through the temperature cycles it will experience during its mission. Once this test is done, the satellite can be tested for radiation. Once again, this test will not be necessary, but it is beneficial to have an understanding of the endurance of the components in a radiation environment.

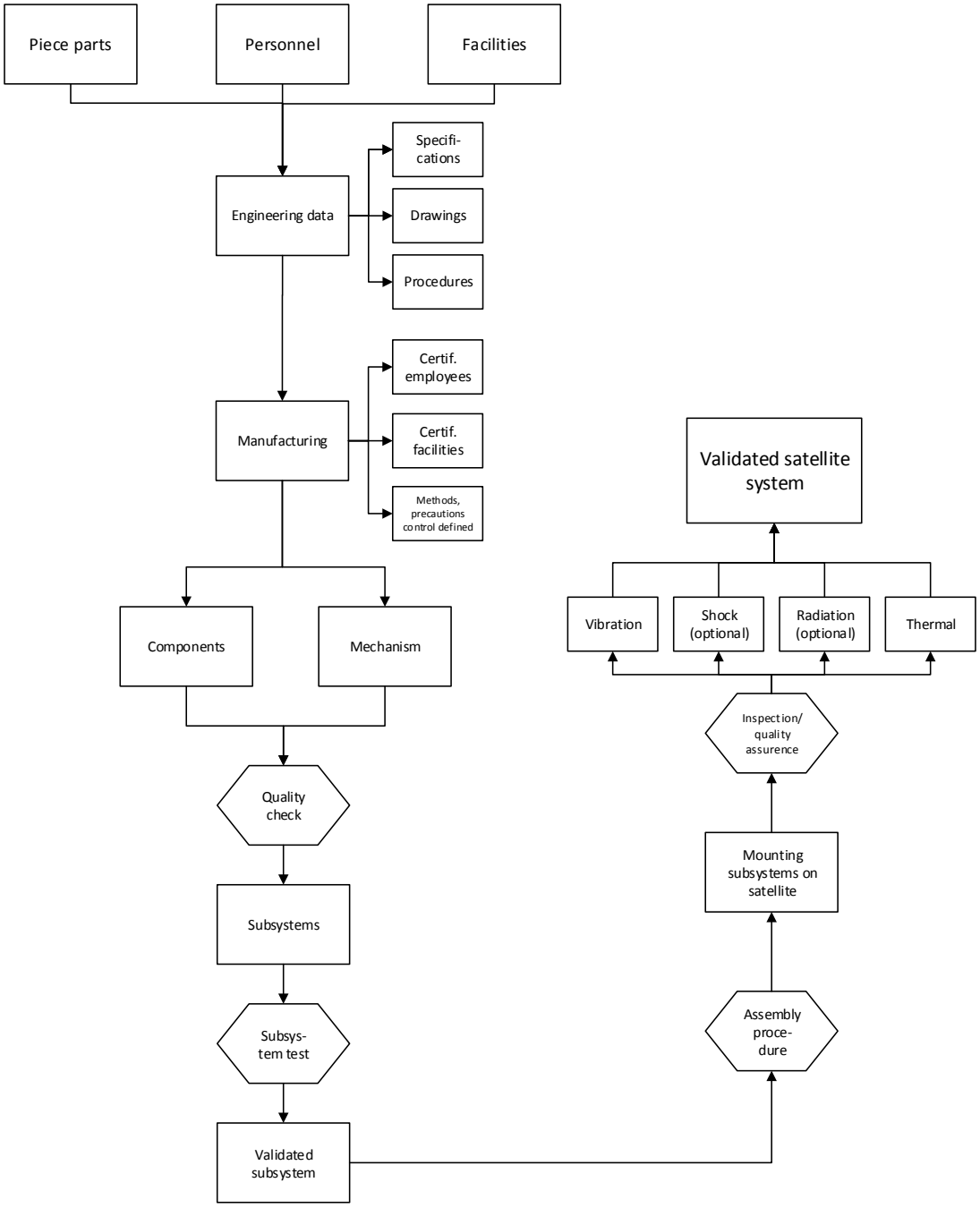

Figure 8.9: Production plan

9 Budget Breakdown

Every action taken in each phase of the mission will have an effect and contribution to the entire mission design, therefore, recognizing all the resources and understanding their effect on the mission is of utter importance. In order to have a general view on this matter, a so called "budget breakdown" has been done. This breakdown explains the effect of different resources on different aspects of the mission. During the budget breakdown, all the effective factors are recognized and after investigating each of these factors, a budget will be presented for those different aspects of the mission, namely ***the satellite system budget, financial budget, time budget,*** and ***reliability budget***. Figure 9.1 shows a graphical representation of the budget breakdown.

The satellite system budget is presented in section 9.1, with a focus on the mass budget of the satellite. The power budget has already been presented in section 7.5. Next section 9.2 shows the financial budget with a cost breakdown structure. The time budget has been discussed in the production plan and will be elaborated on in chapter 15 linking the mission time to the operations and logistics. Finally the reliability budget will be explained in chapter 11 together with the maintainability, availability and safety.

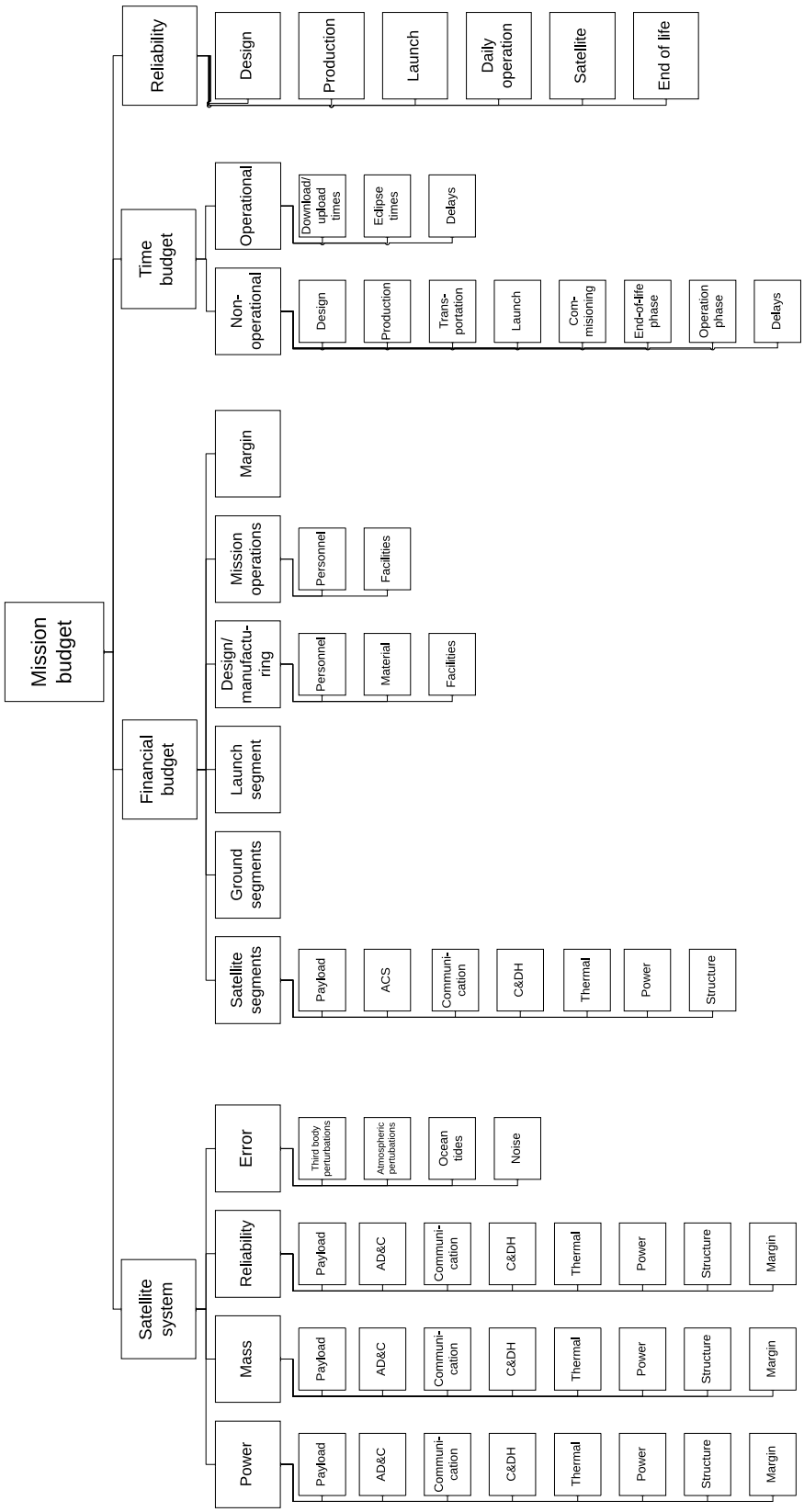

Figure 9.1: Budget breakdown

9.1 Satellite system budget

The satellite system budget mentions all the budgets that have been considered within the satellite; these budgets include the mass budget, power budget, reliability and error. As can be seen, reliability is both an individual budget and also a part of the satellite system budget. The reliability of the system will be explained in chapter 11. For the power and mass budgets, all the subsystems of the satellite, such as the payload, communications, command and data handling etc., are taken into account. The power budget has been presented in section 7.5, therefore only the mass budget is discussed in section 9.1.1. The other budget that is taken into account is the error budget. The error budget is specifically dedicated to the errors that will occur during the operation of the satellite.

9.1.1 Mass budget

The mass budget consists of different categories based on the satellite subsystems. For each subsystem the components are listed with their mass. A margin of 10% is added to account for uncertainties and integration hardware [105]. Table 9.1 shows the total mass budget for GES.

Table 9.1: Mass budget

Component #	Mass [g]
Payload	
GNSS receiver	47
GNSS antenna	156
AD&C system	
Integrated system	250
Tracking, Telemetry & Command	
Full duplex transceiver	85
Deployable antenna system	100
Command & data handling	
On board computer	70
Thermal system	
Coating	negligible
Power system	
Battery (including heater)	103
Electrical power system	87
Body mounted 2U panel	69
Body mounted 2U panel	69
Body Mounted 1U panel	42
Structure	
2-Unit CubeSat structure	390
Margin (10%)	147
Total	1,615

9.1.2 Error budget

The error budget contains the errors of the measurements done by the satellite. Therefore, any other errors occurring during other phases of the mission such as design imperfections are irrelevant to this budget. This budget describes the unwanted factors during the measurements of the gravity field. These errors include third body perturbations due to the gravity of the moon and the sun, atmospheric perturbations, tidal waves (which is an indirect effect of the third body gravity fields), the location of the centre of mass, and noise. All these errors have to be taken into account once the measurements are done. It is notable to say that other sources of errors also exist during the mission, but their effect is so small that they can be considered as negligible.

Third body perturbations
Once the satellite is put into its orbit to measure the temporal changes in gravity field, the gravity field of Earth is not going to be the only influencing factor; the gravity of the moon and the sun also put forces on the satellite and these two bodies will change the deviations of the satellite in its orbit. This will create an error in the produced data, however, since the gravity fields of the moon and the sun are fully known and there are models that accurately describe them, this type of error can be easily eliminated.

Atmospheric perturbations
The existence of the atmosphere will interfere with the data producing errors in the measurements. Since these perturbations are not easy to calculate accurately, a certain maximum error will be assumed to exist due to these perturbations when analysing the data.

Ocean tides
The gravity fields of the moon and the sun are also responsible for the existence of the ocean tides. The height of the water on the surface of the Earth changes during the day due to the existence of the high and low tides. These tides will be problematic for the data especially if the satellite only passes certain places with the same type of tides every day. This is discussed in section 5.2.

Noise
This type of error exists in any measurement device and it always has to be taken into account. Using special techniques and advanced devices, this error can be minimized as has been discussed in chapter 6.

9.2 Financial budget

The financial budget gives an estimate on how much the cost of the satellite will be. In order to do so, all the aspects of the mission are investigated to get an overview of the money spent on each part. Firstly, the satellite itself is considered, which means all the subsystems of the satellite are studied in detail to give an estimate on the money spent on subsystems. Next to the budget for the satellite, several other factors are taken into account, which include ground segment, launch, design and manufacturing, mission operations and margin. The ground system budget includes the cost of all the interactions and operations done from the ground station to the satellite such as the cost of receiving data and using the computers etc. Design and manufacturing of the satellite is another contributing factor to the financial budget; this includes the cost of the materials, the facilities, and also the personel. Similar to the design and manufacturing, the mission operations are also taken into account with respect to personel and facilities.

Design and manufacturing
The design phase covers the project definition and initiation where a working group is put together. If the working group consists of students there will be no expenses for student labour [106]. The manufacturing process has been simplified because of the selection of COTS components. The use of these components saves development costs. The costs of these components are listed under satellite segment.

Every satellite has to be tested before it is launched. Vibration and shock testing, thermal vacuum testing and electromagnetic testing can be done to ensure the satellite will survive launch and the space environment. Vibration and thermal testings are mandatory, while the other tests are optional. To save costs, only the mandatory tests are performed. The specific cost of testing is unknown, so these costs are taken into account in the margin.

Satellite segment
The satellite segment consists of the 2U CubeSat with all components. Table 9.2 lists the mass of each component and the total satellite mass. The prices given in dollars are converted to euros with a conversion rate of 0.73. For further calculation and reference the total of 94,801 *euro* is rounded off to 100,000 *euro*.

Table 9.2: Satellite segment cost

Component	Cost [euro]
Payload	
GNSS receiver	7500 [96]
GNSS antenna	441 [97]
AD&C system	
I ntegrated system	45,000 [69]
S un sensors	7,000 [69]
Tracking, Telemetry & Command	
Full duplex transceiver	8,500 [98]
Deployable antenna system	4,500 [99]
Command & data handling	
On board computer	4,300 [14]
Thermal system	
White paint	662 [107]
Black paint	994 [107]
Power system	
Battery (including heater)	1,214 [100]
Electrical power system	3,202 [101]
Body mounted 2U panel	3,312 [102]
Body mounted 2U panel	3,312 [102]
Body Mounted 1U panel	1,914 [103]
Structure	
2-Unit structure	2,950 [7]
Total	94,801

Launch segment
The launch segment is the most costly segment of the mission, but by selecting a piggyback launch these costs are downplayed as discussed in section 7.8.

Ground segment & mission operations
The ground segment consists of the facilities, equipment, software, logistics, management, system engineering and integration. The facilities and equipment of the ground station selected can be used for free by students from the Delft University of Technology [75]. If a student team will operate the satellite mission as volunteers with educational purposes, no labour expenses will have to be made.

The same principle can be applied to the mission operations. Personnel training, mission operations, command, communications and control can be done by students. If the software allows it even scientists can participate in the operations. With a good user interface scientist can contribute to the operations.

Margin
Because there is an uncertainty in the cost-estimate presented before and also the fact that the costs can grow due to unforeseen technical difficulties, a margin is applied. Typically the margin is 20% for major programs [108]. Keeping in mind that some of the costs are unknown, for example the manufacturing, testing cost and potential supervising, this relatively large margin will be applied for this small program.

From the costs mentioned above, a final financial budget can be calculated. The results are shown in table 9.3.

Table 9.3: Financial budget

Segment	Cost [euro]
Design and manufacturing	unknown
Satellite segments	100,000
Launch segment	150,000
Ground segment	0
Mission operations	0
Margin (20%)	50,000
Total	300,000

GES is definitely a low-cost mission compared to its reference missions; GRACE-1, GRACE-2 and GOCE. This can be concluded from table 9.4 showing the total cost of each mission.

Table 9.4: Total mission cost compared to reference missions.

Mission	Cost [euro]
GRACE-1	93,000,000 [26]
GRACE-2	327,000,000 [28]
GOCE	350,000,000 [25]
Gravity Explorer Satellite	300,000

9.3 Time budget

A time budget is made to see how many hours are needed. Based on this amount, a certain number of students can be invited to work on the project. Table 9.5 shows an overview of the estimated hours.

Table 9.5: Time budget

	Time (hrs)
Project definition and initiation	
Research and design	1600
Project organization and management	700
Spacecraft production	
Production, programming and testing	1000
Logistics	400
Launch phase	
Launch	100
Orbit initialization	60
Daily satellite operations	
Contact time	1600
Margin	1100
Total	6560

Except for the launch phase, the hours are roughly based on the gannt chart in appendix E. It is assumed that until launch, 5 students work effectively 3 to 5 hours per day. For the launch and initialization more hours per day are needed to guide the process. The contact time of GES is 79 minutes per day. Based on this number it is estimated that 1.5 hours are needed per day to monitor the satellite. This includes uplink and downlink activities. Additionally, a time margin of 20% is taken to allow for unforeseen problems.

10 | Technical Risk Assessment

In this chapter the technical risks that might occur during the mission are assessed. In the first section the mission is analyzed based on the possible malfunctions that can occur during the mission. These risks are detected and evaluated. For every risk, a definition is provided and a solution to mitigate the risk is given in the form of closure criteria [109]. In the second section the risks are presented in a risk map.

10.1 Risks

Risk management is important for a successful mission. It will save cost, and prevent common failures, therefore the implementation of a technical risk assessment is needed. The possible risks are categorized into general mission and subsystem risks.

10.1.1 General mission risks

The risks of this mission that can occur in general are listed below.

1. **Schedule problems**
   Risk statement: Given that the project has schedule problems, there is a probability that the entire mission will be rushed at different design phases.
   Context statement: When the project is not properly scheduled the time will increase and the end date of the project will be delayed.
   Closure criteria: Important is to create a learning event at selected critical events in the lifetime of the project. Scheduling the impact of mitigation of the risks will reduce the risk of rushing through the project [110].
2. **Exceeding cost resources**
   Risk statement: Given that there is an unforeseen cost growth, the budget will run out prematurely, leading to the mission not being able to be performed, or being delayed.
   Context statement: Unforeseen technical difficulties can lead to cost growth. This can be problematic when there are limited resources available that cannot be exceeded.
   Closure criteria: Minimize the chance that cost resources are exceeded by applying a generous margin [110].
3. **Launch failure**
   Risk statement: Given that the rocket fails during launch, the satellite will not reach its intended orbit.
   Context statement: If the launcher has trouble with generating enough power the launch will fail.
   Closure criteria: In 2012 the failure rate was 1 in 15.6 launches [111]. The launcher risk would be mitigated by carefully selecting a launcher with a high success rate. Since this satellite will be launched as a piggy-back launch the choices are limited, keeping in mind that this is a low cost mission.
4. **CubeSate deployer failure**
   Risk statement: Given that the CubeSate deployer is not working properly, there is a possibility that the satellite will not be deployed.
   Context statement: The deployer is mounted to the launcher and carries the satellite into orbit

and deploys it once the proper signal is received from the launch vehicle.
Closure criteria: The chosen deployer, the ISIPOD CubeSate Deployer, has been accepted for functional, vibration, and thermal cycling tests, furthermore it is qualified for mechanical shock and thermal vacuum tests. This system has been used for other missions, therefore it becomes very reliable [112].

5. **Space debris impact**
Risk statement: Given that space debris interferes with the satellite's orbit, which will effect the pointing requirement at an altitude of 580 km, there is a very small possibility that the satellite will be damaged in such a way that it is not functional anymore.
Context statement: Assessing risk due to smaller debris or objects is hard because they are difficult or impossible to track. Larger debris are detectable, but the impact will be more severe.
Closure criteria: At the chosen altitude there will hardly be any harmful collisions with debris in the coming 200 years [113]. Hence, no further action is taken to mitigate this risk.

10.1.2 Subsystems risks

The risks of this mission that can occur within any of the subsystems are listed below.

6. **Attitude determination and control failure**
Risk statement: Given that any of the attitude determination and control subsystem elements will not function anymore due to wear, and/or the environmental atmosphere, there is a possibility that this could lead to a failing mission.
Context statement: The attitude determination and control takes care of the position of the satellite, this subsystem is necessary to achieve the desired attitude. It monitors and modifies the attitude of the satellite to meet requirement TR-3.1. The systems has five sunsensors, three reactionwheels, three magnetorquers, and one startracker.
Closure criteria: The chosen system has a software frame which will minimize the risk of software failures. Also it has several devices which can be used for redundancy, and therefore will reduce the risk of failure as well [114]. Furthermore, this system has an ISS-certified startracker, and is already been used for other missions like Aalto-1, which makes it more reliable [69].

7. **Solar panel failure**
Risk statement: Given that a solar panel will not function, there is a possibility that the system does not receive enough power, and therefore the mission fails.
Context statement: The operational lifetime of the mission is directly linked to the electrical power of the satellite. The solar panels obtain the electrical energy that the system needs. If for some reason the satellite will rotate, and therefore the solar panel will not face the sun anymore, the satellite will not receive solar energy. Also if a single solar cell fails, the received power for the system reduces.
Closure criteria: The chosen solar panels are environmentally tested by the manufacturer. Hence the risk of failure is minimized by the approval of tested hardware. Nevertheless, failure of the power subsystem is still one of the main failures of space missions [115]. Therefore, to prevent that the satellite will not receive solar energy, two solar cells are mounted on the bottom of the satellite for redundancy. The solar panels contain several solar cells, and due to bypass diodes the panels still function if one single cell fails [30].

8. **Battery malfunction**
Risk statement: Given that battery malfunction will take place, there is a possibility that the system does not get sufficient power to function.
Context statement: The battery provides power to the system during eclipse times. If the battery does not work during this time, the satellite will not be able to function. Furthermore battery degradation can occur due to radiation.
Closure criteria: In case the battery does not work anymore, the system should go into full-safe-mode when entering an eclipse. This is the software redundancy which have to be added to the system, since the system the will not get any power. If this would happen the effect would be that there are no measurements obtained during the eclipse time. The chosen battery for this mission is space flight proven, so the possibility that this would occur is very small. Furthermore, the verified

cycle life in accelerated life test is 5000 cycles, and the expected life cycles are 35000 [30]. If battery degradation would occur this would not cause any trouble over the minimum operational life of 3 years. Since for this mission the battery life cycle is lower that the tested 5000 cycles, see section 7.5 about the power subsystem.

9. **Communication failure**
   Risk statement: Given that the antenna for the up- and downlink will not deploy after launch, there exists the possibility that the communication with the groundstation will not be optimal.
   Context statement: The antenna is necessary for the communication with Earth. In order to receive all the data measurements this antenna is needed.
   Closure criteria: This satellite has one dipole and one monopole configuration. If one of the antennas will not deploy, the communication is still working but only not optimal. Since data storage is onboard no data measurements could get lost.
10. **Onboard computer failure**
    Risk statement: Given that onboard computer failure occurs, there is a possibility that the measurement data will not be (correctly) stored for further use due to the hostile space environment.
    Context statement: The satellite is exposed to radiation in space which can cause damage to the components of the satellite and can cause memory errors.
    Closure criteria: By using a COTS computer, which has been qualified for spaceflight, the risk of hardware failure is minimized. Furthermore, software failures are human based errors which can be fixed as well. According to a study from M. Tafazoli in 2009, only 8 % of the failures, which occurred during operational phase, were due to human error [115].
11. **Structural failure**
    Risk statement: Given that structural failure occurs, there is a possibility that components will get loose, and therefore not function perfectly anymore.
    Context statement: The structure supports all components of the satellite, during launch and operational phase. The chance of manufacturing flaws is very small but possible, since it is build by people.
    Closure criteria: During the manufacturing process several safety checks will take place. This will minimize the risks of manufacturing flaws. Furthermore, the satellite should undergoes a vibration test. Hence, the satellite will be able to survives the heavy vibrations during launch, and reach safely the orbit.

10.2 Risk map

In order to get a clear view of which risks are most important and need to be assessed, a risk map is produced as displayed in figure 10.1. On the vertical axis of the risk map the likelihood is displayed and on the horizontal axis the impact of the risk. The different levels of both variables are stated below.

Likelihood

1. Not likely
2. Low likelihood
3. Likely
4. Highly likely

Impact

1. Negligible
2. Marginal
3. Critical
4. Highly critital
5. Catastrophic

The different risks are given a number, and based on their level of likelihood and impact they are placed in the risk map. These ratings were made based on current knowledge and insight. Below is shown which number corresponds to which risk. One can see three different kind of grey colors in the map; risks in a the darkest area are serious risks for which actions need to be taken, the lightest grey color risks need to be monitored closely and a plan to asses them needs to be ready and for the risks in last area no immediate action needs to be taken.

1. Schedule problems
2. Exceeding cost resources
3. Launch failure
4. CubeSate deployer failure
5. Space debris impact
6. Attitude determination and control failure
7. Solar panel failure
8. Battery malfunction
9. Communication failure
10. Onboard computer failure
11. Structural failure

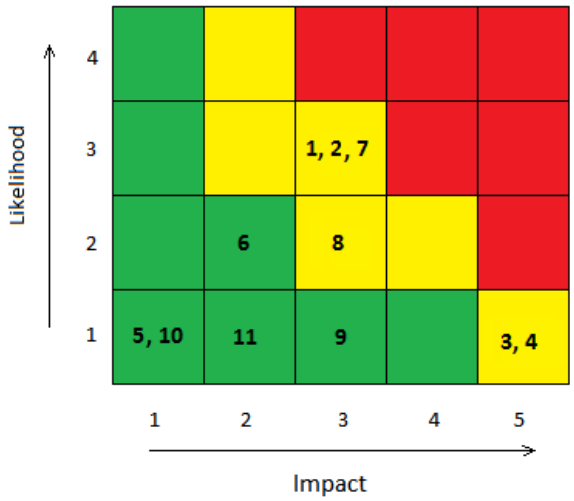

Figure 10.1: Riskmap

11 Reliability, Availability, Maintainability & Safety

This chapter contains the reliability, availability, maintainability and safety analysis (RAMS) that is integrated in the design, in sections 11.1, 11.2, 11.3 and 11.4 respectively.

11.1 Reliability

Reliability is defined as the probability that a device will function without failure that impairs the mission over a specified time period or amount of usage [116]. Because the satellite cannot be repaired in space, it is very important to create a highly reliable system. The reliability of a system can be calculated by examining the failure rates of each component or subsystem during space flight or launch. Unfortunately, most of these failure rates are unknown at this stage and thus it is not possible to calculate the specific reliability of the satellite system. Therefore a statistical method is used to give an indication of the reliability.

Based on a study from 2009 on all satellites launched between January 1990 and October 2008, a statistical estimation can be made [117]. In this study the failure data of 1584 satellites is gathered to show the reliability of the system over time and the culprit subsystem that caused the failure. Figure 11.1 illustrates the results from the reliability study. From this graph can be seen that the average reliability for a satellite with a lifetime of 3 years is 0.962.

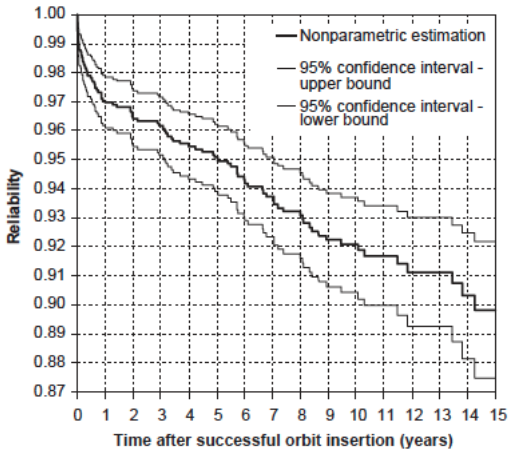

Figure 11.1: Satellite reliability with 95% confidence intervals.

Next to the total reliability of the satellite system, the specific subsystem that caused the failure has been studied. Figure 11.2 shows the percentage of contribution to the satellite failure for a number of subsystems. After 3 successful years in orbit the subsystems that mostly cause failure are the TT&C and thruster/fuel. The Gravity Explorer Satellite does not have thrusters or fuel, so the TT&C is the subsystem most likely to fail. This has been taken into account in the design by using COTS components.

The antenna and GNSS receiver have been tested together before and are designed for cubesats. The risks associated with the TT&C are covered in chapter 10.

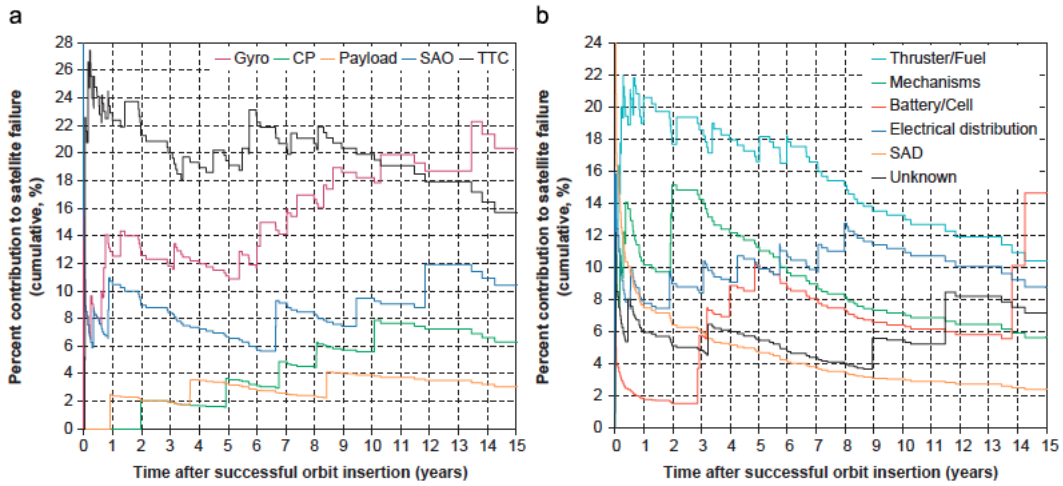

Figure 11.2: Relative contributions of various susbsystems to satellite failure.

The satellite has several redundancy elements in order to achieve the mission requirements. To keep it as a low cost mission, it is not possible to add all of the devices onboard as redundancy. Since studies like [115] showed that failure of the power and AD&C subsystems are 59 % of the total failure which can occur during the operational phase. Therefore, it is chosen to only have the power and the AD&C subsystems as part of the redundancy. The AD&C subsystem has 5 sun sensors for redundancy. For the power subsystem this includes several extra solar cells, namely 2 cells on the side opposite to the sun of the satellite for redundancy. Furthermore, for the safe mode 1U of solar cells are added to the long side of the CubeSat which does not face the sunny side.

11.2 Availability

Availability is the quality of a device or system for being at hand when needed [118]. This can be split up in two considerations; availability of components for production and availability of the satellite in service.

The system consists mostly of off-the-shelf components. These components are readily available and do not need to be designed, constructed or tested. The availability of these systems depends on the delivery time of the suppliers.

Since parts of the satellite segments cannot be replaced during operation in space, the availability in service is closely related to reliability. Another aspect of availability involves the available time to transfer data. This depends on the location of the ground station and the satellite telemetry segment. The contact time has been described in detail in section 7.2.

11.3 Maintainability

Maintenance is a very important factor in every mission and therefore needs evaluation. Maintainability is defined as the ease and speed with which any maintenance activity can be carried out on an item of equipment [118]. The satellite can not be accessed for maintenance on the system when it is in space, but some aspects can be considered to maintain the system.

The first aspect is the attitude maintenance, which is secured by the AD&C system. The preservation of the correct attitude is an essential part of the mission, as an off-orientation can result in loss of data. The AD&C is a self-contained system and therefore is expected to perform sufficient.

Furthermore, the health status of all satellite components needs monitoring. In case of failure of a system, with build-in redundancy, the redundant part should be activated. If not, the system will fail or the system will have to operate without the failing part.

11.4 Safety

The most important part of safety is protecting human life, public property, and the environment [119]. Safety condiserations consist of the risks that might occur during the design, production and operational lifetime of the satellite. It is desired to avoid unacceptable levels of such risks. Different aspects of safety are involved in every project, these are: safety management, safety assessment, safety engineering and safety assurance.

Safety management is important when it comes to studying and planning the activities needed to minimise the risks. To identify, asses, minimise and control all risk and make sure they are part of the risk management, safety management is brought into play.

Safety assessment contains the analysis of the system as a whole. It consists of the identification, control and verification of the risks and the failure scenarios. The risks and failure scenarios of the gravity exploration satellite have been identified and analysed in chapter 10.

Safety engineering is the implementation of safety in the design and operation from a technical and organisational point of view. In the design of the gravity exporation satellite safety has been considered for different aspects.

- To avoid human loss or injuries it is important that safety measurements are taken during the production process. Safety management of this phase is the most critical in protecting human life, because during the other phases of the mission personnel is not in direct danger if something with the satellite would go wrong.
- The most critical phase for the satellite and the other payloads around it is the launch and deployment. The selection of a certified cubesat deployer downsizes these risks and keeps the public property safe.
- When the satellite is in operation it is important to keep the satellite and the satellites around it safe by avoiding collisions. A collision can be catastrophic for a satellite and creates a lot of space debris, which must be avoided. GES does not have a propulsion system, so cannot move out of the way, but with monitoring other satellites can be warned if they are moving right at GES and potentially a collision can be avoided.
- Finally, to make sure everyone on Earth is safe from the satellite and no debris is created at the end-of-life, the satellite burns up in the atmosphere. So there is no trace of the satellite left in the environment in the end.

Safety assurance consists of the monitoring of the other safety aspects. It is important to check if they have been implemented correctly to make sure the final safety assessment is correct. This can not be done at this stage of the design, but becomes important when the design is implemented.

12 | Sustainable Development Strategy

Sustainability is an integral part of the design philosophy. The definition of sustainable development as defined in the *Brundtland report* (WCED, 1987) is used as a reference:

> "Development that meets the needs of the present without compromising the ability of future generations to meet their own needs [120]."

In this chapter both the way sustainability is taken into account in the design and the way the system contributes to sustainability are discussed. In the end a comparison with other satellite missions is made.

12.1 Approach with respect to sustainability

From a sustainability point of view, the cloud of space debris surrounding Earth is one of the largest occurring problems in space engineering and astronautics as it has been ever-growing since the launch of Sputnik 1 in 1957. This has been noted by many scientists and received global awareness in 2002, when the Inter-Agency Debris Coordination Committee (IADC) adapted space debris mitigation guidelines to counteract this problem. The guidelines focus on four aspects [121]:

1. Limitation of debris released during normal operations
2. Minimization of the potential for on-orbit break-ups
3. Prevention of on-orbit collision
4. Post-mission disposal

To make sure the Gravity Explorer Satellite meets the guidelines some considerations have been made. First of all there are no objects intentionally released by the satellite or destructed. Unintentionally released objects and accidental break-ups are minimized by using space certified COTS components. These components have been tested in space before without causing failure. On-orbit collisions will have to be limited by the ground station operators who keep track of the satellite and the objects around it. For GES the issue of post-mission disposal is reflected in the requirements; stating that the satellite shall re-enter within 25 years (NTR-3.1) and must burn up entirely (NTR-3). Minimizing the satellite's 'debris time' is seriously strived for. Therefore iterations on the orbit altitude have been done to optimise the height for decommissioning, such that the satellite decommissions within the limit without needing additional propulsion, thus saving costs.

The use of COTS products is not only promoted for their reliability, but also because it saves time and production efforts. These COTS components can be developed in large quantities and used for multiple purposes, thus development investments and tests can be decreased. By skipping the development phase the use and waste of materials can be reduced. This is related to requirement NTR-3.2, stating that where possible the most sustainable materials should be used.

Besides the fact that choosing a piggyback launch is effective for saving costs, it also minimizes the pollution and energy consumption of GES. Using a launcher for multiple missions reduces the amount of launchers needed, thus total pollution is narrowed. Minimizing the system mass and size is not only good for cost saving but less energy is needed to get the satellite into space and more room is available for other missions.

12.2 Contributions to sustainability

Apart from the satellite itself being sustainable, its mission outcome is also used for sustainable purposes. This means that by measuring the gravity changes over time, the movement of water on Earth's surface can be visualized, which makes it possible to observe ice melt, sea-level rise and groundwater extraction.

> The average rate of ice loss from the Greenland ice sheet has very likely substantially increased from 34 (-6 to 74) Gt/yr over the period 1992 to 2001 to 215 (157 to 274) Gt/yr over the period 2002 to 2011 (United Nations, 2013) [122].

The melting ice causes a rise in the sea-level as well as some changes in the ocean currents, which affects the living conditions for marine organisms. Next to that water absorbs more heat from the sun than ice would; this is a real threat to the environment and a sustainable future, that can be quantified with this mission. To get a grasp on the current situation and predict the future, precise measurements are needed.

With a small low cost satellite that is able to obtain precise measurements of the gravity changes over time, this data becomes available to universities, research institutes, and commercial companies. This will hopefully contribute to raise global awareness, inform policymakers and help realize a sustainable future.

13 Performance

This chapter will discuss and analyse the performance of the satellite mission by first presenting a performance analysis table in section 13.1. Later on, a Requirement Compliance Matrix will be provided and elaborated on in section 13.2. Finally, in section 13.3, a sensitivity analysis will be performed to measure the robustness of the satellite with respect to changes in different parameters.

13.1 Performance analysis

The characteristics of the different parts and subsystems of the satellite together create the performance characteristics of the satellite. It is important to be familiar with what the performance of the different parts of the satellite. All these performances have been discussed thoroughly during the report. This section presents table 13.1, showing the performance analysis of the satellite and it will direct the reader to the appropriate section for more information on the performance of any part or subsystem.

Table 13.1: Performance analysis of GES

Subsystems	Comments	Reference
ADCS	iADCS-100, Berlin Space Technologies	7.1.5
Reaction wheels	0.087 mNm torque, 1.5 $mNms$ angular momentum	7.1.5
Magnetorquers	0.2 Am^2	7.1.5
Pointing accuracy	« 1○	7.1.5
Power		
Solar panels	Gallium Arsenide triple junction capable of delivering 4.74 W	7.5
Batteries	Lithium ion polymer batteries providing 10 Wh energy	7.5
Thermal		7.4
Maximum temperature	43.7°C using white and black paint coatings	7.4
Minimum temperature	$-3.7°C$ using white and black paint coatings	7.4
TTC, CDH		
UHF antenna	Downlink budget of 3 dB	7.2.5
VHF antenna	Uplink budget of 22 dB	7.2.5
Visiting frequency	Ground station contact 7 to 8 times per day, total time of 79 minutes	7.2.3
GPS	Comments	Reference
Type	AsteRx-m OEM	
Phase measurement accuracy	1mm/1mm L1/L2	6.3.3
Tracking	26 dB-Hz	6.3.3
Acquisition	33 dB-Hz	6.3.3
Maximum data rate	33 Hz	6.3.3
Operating temperature range	−40 to 85°C	6.3.3
Orbit	Comments	Reference
Type	Dawn-dusk SSO	5.2
Orbit decay	8.8 km within 3 years	5.1
Mission duration	22 years	5.1
Coverage		
Ground track	Full monthly coverage	5.4
Spatial scale	1667 km	13.1.1
Eclipse	Maximum of 26 minutes	5.3

13.1.1 Spatial scale

One of the top level requirements states that the spatial scale should be 1000 km or less, see section 3.1 **TR-1**. The spacial scale is limited by the combination of the noise of the GNSS receiver and the influences of hydrological signal on the gravity field, represented using spherical harmonics. In order to verify the spatial scale requirement for this mission, the GNSS receiver noise at 20 degrees should be lower then the gravitational hydrological signal strength because the required 1000 km spatial scale correspondent to 20° on the spherical scale. The GNSS receiver noise was estimated by rescaling the receiver noise of the proposed iridium payload, see figure 13.1 the top doted line [123]. This scaling was done in order to take into account the following differences:

1. The receiver noise of the proposed iridium payload modelled in figure 13.1 is fore 24 satellites not one. The noise was scaled up with a factor $\sqrt{24}$.
2. The modelled receiver noise in figure 13.1 is done for a receiver with a position error of 2 to 3 cm [123], the selceted reciever for this mission has a (radial) position error off 1 cm. The noise was scaled down with a factor 2.5.
3. The noise modelled is for just one month, this mission is planed to be at least 3 years long. Them noise was scaled down with a factor $\sqrt{36}$.
4. The iridium configuration flies at altitude of 750 km[124], while this mission flies at altitude of 580 km. Since this differences will have a very small impact on the signal [125] it is neglected.

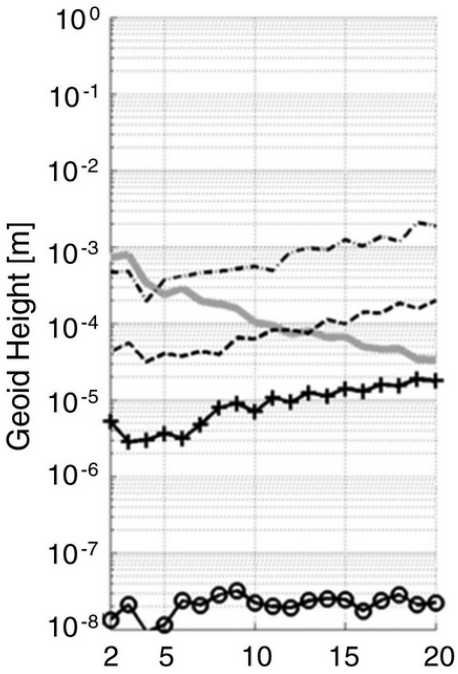

Figure 13.1: Iridium GNSS receiver noise (the top doted line is the one of interested).

The influences of hydrological signal on the gravity field is given as function of the spatial scale in a spherical harmonic function of degrees in figure 13.2. This figure represents the annual variations of the hydrological signal worldwide. This also means that the figure is an average, for example, the variation in signal amplitude in the Amazon basin will be much bigger then that of the sahara desert.

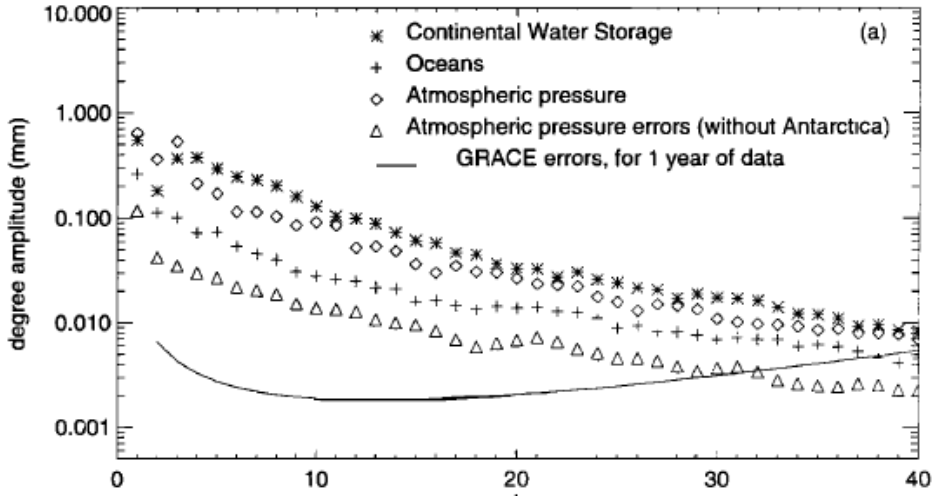

Figure 13.2: Degree amplitudes for the annually varying component of the geoid

Considering the values for 20 degrees in the two graphs results in a value in the noise plot of 2 mm, which becomes 0.7 mm after rescaling; this also results in value for the hydrological signal (more specifically the one from continental water storage) of $0.06mm$. It is clear that noise is bigger than the signal, so the required spacial scale is not met. Based on the two figures, a spatial scale for this mission of around 12 degree can be found, which represents a value of 1667 km.

It should be note, however, as already mention above, the signal is on a global range. For the Amazon basin with a stronger signal variation, for example, the spatial scale will be much better. Other parameters that were ignored that could influence the spacial scale in a positive way are the increasing global coverage due too the lower attitude of this mission. More data points will result in lower noise. An increased sample rate of this receivers compared to the proposed iridium one, might be helpful as well. In conclusion, it might be advisable, for future references, to have more detailed studies to make a noise figure of the selected mission in order to get a more accurate estimate of the spatial scale.

13.1.2 Lifetime

For some components the lifetime can be calculated at this stage, but not for all. Therefore, the lifetime of these components is discussed and then a statistical indication for the complete mission is given.

The most critical component is the GNSS receiver. Because this receiver model is not space certified it is not designed to withstand the hostile space environment. Without radiation protection it will not survive 3 years. Therefore, a shielding will have to be designed to secure the lifetime requirement. The design of the shielding is beyond the scope of this project.

The lifetime of the AD&C system is 5 years [74], and thus not critical. The lifetime of the battery has been calculated in section 7.5 and showed not to be critical as well.

For the other components the lifetime is unknown, therefore, a statistical model will be considered.

The expected exact lifetime of the total satellite cannot be calculated, but an estimation can be extracted from the relation between the actual and design lifetime based on past reference missions. A graphical representation of the relation between the actual and the design lifetime of remote sensing satellites is given in figure 13.3. From the graph can be concluded that the planned lifetimes are generally 5 years or less but the data indicates actual lifetimes that are significantly longer than required. Therefore, it can be assumed that GES will meet the lifetime requirement of 3 years.

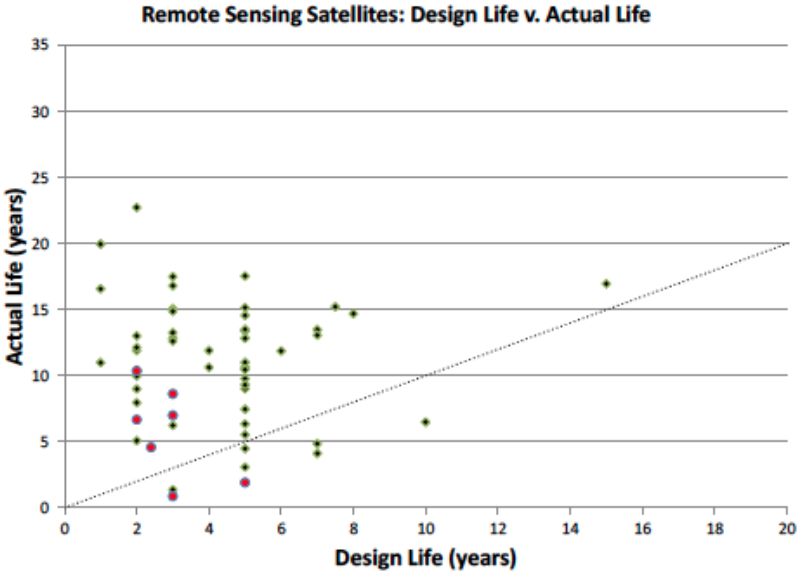

Figure 13.3: Actual versus design life of remote sensing satellites [9]

13.2 Requirements compliance matrix

Now that the final satellite configuration is determined, verification on whether or not it actually meets the requirements presented in chapter 3 is needed. This section provides a link between the aforestated requirements and the satellite's performance characteristics by means of the Requirements Compliance Matrix (RCM) presented in table 13.2. A check box is included to indicate whether or not a specific requirement is met by the system performance.

Table 13.2: RCM of GES proposal

Technical requirements			
Requirement	Content	Compliance	Reference
TR-1	Observations of yearly mass transport must be at a spatial scale of 1000 km or less	✓/✗	
TR-1.1	The ground track must ensure a spatial scale of 1000 km or less	✓	Section 5.4
TR-1.2	The altitude must ensure a spatial scale of 1000 km or less	✓	Section 5.4
TR-1.2	The GNSS receiver accuracy must ensure a spatial scale of 1000 km or less	✗	Section 13.1.1
TR-2	Measurement principle to be used is the tracking of navigation satellites	✓	Chapter 6
TR-3	Center of mass positioning error due to inaccurate pointing should be smaller than 1 cm	✓	Section 7.1.6
TR-4	Center of mass positioning error due to GNSS measurement noise should be smaller than 1 cm	✓	Table 6.2
TR-5	Entire Earth must be covered within a month	✓	Section 5.4
Non-technical requirements			
Requirement	Content	Compliance	Reference section
NTR-1	Minimum operational lifetime should be 3 years	✓	Section 13.1.2
NTR-2	Satellite mission costs should be minimized where possible	✓	Section 9.2
NTR-2.1	The operating costs must be kept as low as possible	✓	Section 9.2
NTR-2.2	Orbit selection is partly cost-driven	✓	Section 9.2
NTR-2.3	Satellite's mass should be minimized where possible	✓	Section 9.2
NTR-2.4	COTS components shall be used where possible	✓	Section 9.2
NTR-3	Satellite must be eco-friendly	✓	
NTR-3.1	The satellite must re-enter within 25 years after EOL	✓	Section 5.1
NTR-3.2	Satellite's material is sustainable where possible	✓	Section 7.6

13.3 Sensitivity analysis

Knowing the system's sensitivity to variations in major parameters is of vital importance, as it identifies those characteristics that are critical for the mission. Furthermore, in reality, the occurring characteristics will inevitably vary from the designed and computed ones. Therefore, this section provides an insight

in how various system features change with varying system parameters. Those parameters involve orbit height and inclination, pointing accuracy and knowledge, and power losses. Sections 13.3.1 to 13.3.6 describe how the system behaves as a result of a changes in these parameters.

13.3.1 Sensitivity to orbit height

Throughout the mission, a deviation in actual orbit height from designed orbit height might occur. From figures 5.2 – 5.6, section 5.4, it is concluded that variations in orbit height in the order of kilometers do not affect the coverage density significantly. With a calculated decay of 8.8 km during the required 3 years operational lifetime (requirement NTR-1, chapter 3), eventual deviations in orbit height will not cause the coverage density to vary such that the Earth coverage requirement of 1 month is harmed (requirement TR-5, chapter 3).

The operating temperature does not change with an orbit variation in the order of kilometres. The orbit's synchronicity also does not change with an orbit height variation in the order of kilometres, and the SSO is maintained.

13.3.2 Sensitivity to orbit inclination

As for the orbit height, minor deviations in the orbit inclination will not harm the Earth coverage requirement. However, the inclination must remain such that a near-polar orbit is maintained.

The orbit synchronicity is very sensitive to changes in orbit inclination. Section 5.2 explains that the chosen altitude of 580 km yields an inclination of 97.7° for the Sun-synchronous orbit. A deviation of this inclination causes the eclipse period to increase over time. Naturally, the moment where this deviation occurs is critical. An initial deviation in the order of 0.01° or more causes a catastrophic eclipse period increase over the several operational years left. If, on the other hand, this deviation occurs more towards the end of operational life, the increase in eclipse period will be less catastrophic.

On its turn, increase in eclipse time both decreases the operating temperatures and the power extracted from the solar panels. The former is simply explained by the fact that the more the satellite spends in eclipse, the more it cools down. The latter is caused by the fact that solar panels need to face the Sun for optimal power extraction, which is not the case during eclipse. The results of these phenomena will be elaborated on in sections 13.3.3 and 13.3.4.

13.3.3 Sensitivity to temperature

As described in section 13.3.2, a result of a changing the orbit inclination causes the system's temperature to drop. On its turn, this temperature change affects the performance of several instruments. Table 7.12 shows the operating and survival temperature limits (hot and cold) of the various instruments, and table 7.16 shows the system temperatures for various cases. The hot case sunlit temperature of 43.74°C is not critical in this case as this number is computed for minimum eclipse period. The possible deviation in orbit inclination causes an increase in eclipse period over time, resulting in a decrease in cold case eclipse temperature. If this temperature decreases from the current −3.70°C to a value of −20°C the iADCS, the ISIS on board computer and the battery approach their cold operational limits.

13.3.4 Sensitivity to power losses

The power system produces 5.55 watt hour in normal operating conditions. In case of power loss that does not exceed 0.34 watt, it can be compensated by the fact that the system produces more power than needed. Larger power loss results in the loss of some functionality. Depending on the situation, safety mode can be entered in hope of restoring the system to normal conditions. If the system is permanently damaged depending on the situation it can be decided to drop GLONASS tracking by the GNSS receiver saving 0.1 watt from the power consumption but losing some precision. Other more drastic measures can be taken like switching of the GNSS receiver for part of the orbit period to save power for example.

13.3.5 Sensitivity to pointing accuracy

The pointing accuracy of the fully functional design is less the 1°. However, if for some reason, this accuracy cannot be achieved, it would not make a big impact in the mission due to the fact that the

GNSS antenna is not very sensitive regarding its pointing direction; the order of accuracy required for the GNSS antenna is in the order of tens of degrees). The other affected subsystems such as power, communication, and thermal are not very demanding either. Since the integrated AD&C system has backup for every axis due to the existence of both magnetorquers reaction wheels, and also the fact that pointing accuracy requirement of all the subsystems is very low, results in the fact that pointing accuracy will not be critical.

13.3.6 Sensitivity to attitude knowledge

The attitude knowledge of the spacecraft in normal operation mode is 30 arcsec. Every loss in attitude knowledge accuracy is directed loss in position accuracy. A small loss in attitude knowledge will not be that crucial. The current contribution of the pointing knowledge to the position error is 8.25 μm see section, 7.1.6. As long as the contribution of pointing knowledge error does not exceed the 60 μm it will not impact the most critical requirement the spacial scale. This means that attitude knowledge should be at least 216 arcsec.

14 | Verification & Validation

In this chapter the verification and validation of the system is explained. Throughout this chapter, the following definitions of verification and validation are maintained. Based on NASA, 2008 [126]:

Verification The process of determining that a model implementation accurately represents the developer's conceptual description of the model and the solution to the model.

Validation The process of determining the degree to which a model is an accurate representation of the real world from the perspective of the intended uses of the model.

The first section covers the verification and validation of the used models in this report. Followed by the validation of the measurement data.

14.1 Verification and validation of models

In this section the used models are verified and validated. The STK software has been used to calculate the maximum contact time in section 7.7. Also this program is used to determine the orbit decay and lifetime, see chapter 5. The thermal model has been used in section 7.4, and the link budget in section 7.2.

STK
This STK is a commercial toolkit which is used very often in the space community. The Analytical Graphics Inc. (AGI) handles its own verification and validation [127]. Therefore it is a very valid and accurate model to use.

Thermal model
For the thermal calculations a model was created in the form of an Excel sheet. This model was verified by performing the calculations by hand for one particular value and checking if this corresponds to the value given by the model. This was done for all the important steps, confirming that the model does perform the calculations wanted.

The validation of the thermal model was done by comparison to the design phase values of the Delfi N3xt mission. This mission was chosen because it is a comparable CubeSat mission, also flying in a sun-synchronous nearly circular LEO at a height of 600 km, with an almost equal inclination of 98.8 degrees [128]. The lowest temperature Delfi N3xt reaches in eclipse is -15 degrees, for GES this is -3.7 degrees. The highest temperature of Delfi N3xt is 35 degrees, GES has a highest temperature of 43.7 degrees [129]. These temperatures are very similar, only the temperatures of GES seem to be about 9 degrees higher. This difference is insignificant enough in order to regard the thermal model used for GES as validated.

Link budget
The sizing of the communication architecture and GNSS system was conducted via a numerical link budget. Both simulations are adjusted versions of pre-divined models.

The link budget of the communication architecture was set up following the procedure as found in SMAD [41]. The input parameters were set up for direct insertion of antenna gain and transmit power. The model was verified using the numerical examples as found in SMAD [41].

The GNSS link budget was based on a model by AXONN [53]. This model contained some errors which which were uncovered during the verification process and were adjusted accordingly. An numerical example by AXONN was used to verify the model.

14.2 Verification & validation procedures

In chapter 13 the verification of the system has been done. All the requirements were checked if they have been achieved. As discussed in chapter 2 there are several missions that have some kind of similarity with this mission. CHAMP, GOCE, and GRACE also measured temporal gravity changes of the Earth. These missions all make use of accelerometers, see chapter 6. For this mission no accelerometer has been implemented in the system, and therefore a numerical model needs to be used in order to achieve nearly the same accuracy. The obtained measurement data from the satellite will be validated against the already available data of these missions. This would be one way to proof that this mission is a successful one. For the comparison of the data, first the numerical model needs to filter out the non-gravitational forces. The development process of this model is outside the scope of this project.

15 | Project Design and Development

The project design and development logic shows the logical order of activities to be executed in the post-DSE phase of the project. The first section presents the activities that have to be done. The Cost Breakdown Structure (CBS) contains the cost elements of these activities, which is shown in the last section.

15.1 Post-DSE phases

In this report the first detailed design of this mission is presented. The first step after this project is to find funding in order to continue this mission. In the budget breakdown in chapter 9 a good overview of the cost and planning is given. The second step is to review the detailed design from the DSE project, followed by applying the recommendations into the new full scale development. The recommendations are written in chapter 16. This includes developing software and testing it. When the improved detailed design is finished, the production phase starts. This includes ordering the subsystem components and manufacturing the satellite. A launch date needs to be selected. Once the satellite is launched, the operational phase starts. This means that the satellite is measuring the temporal gravity changes and sends its data to the ground station were in-service support is provided. This data needs to be given to the involved scientists, which means that a website needs to be build to distribute the data. The end of the mission will be when the satellite burns up in the atmosphere and all the data is processed. An overview of this process is presented in figure 15.1. For an indication of the time frame a Gantt chart is made, shown in Appendix E.

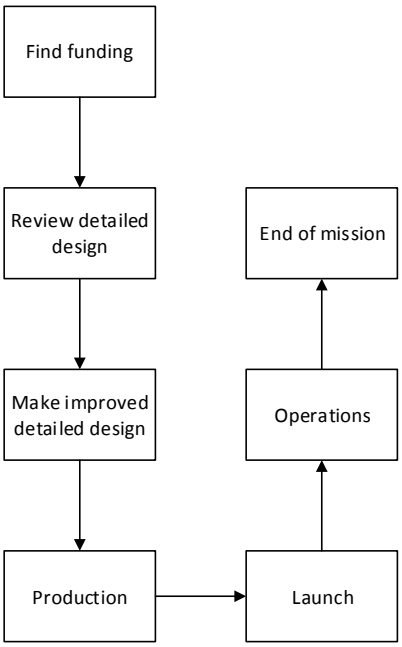

Figure 15.1: Post-DSE project design and development logic

15.2 Cost breakdown structure

A cost breakdown structure is presented for the post-DSE project activities in this section. Figure 15.2 identifies all elements that contribute to the overall development and production cost of the system, for which the first detailed design has been produced in this report. The total cost of the mission are divided into tree main part: research and development, investment, and operations & maintenance.

15.2.1 Research and development

Research and development is divided into four parts: program management, advanced research & development, engineering design, and equipment development & test. The program management task includes finding funding for the mission. Advanced research & development, and engineering design has been already done in this report. For the post-DSE project activities these parts can be reviewed. Equipment development & test consists of engineering & qualification of models, and the test & evaluation.

15.2.2 Investment

The investment is divided into the manufacturing, construction, and initial logistic support cost. The production of the satellite is covered by the manufacturing and construction. All the other parts needed in order to build the satellite are presented in the initial logistic support.

15.2.3 Operations and maintenance

The operations and maintenance includes operations, maintenance, system/equipment modifications, and system phase-out & disposal. All parts that cover the operation of the mission are presented in operations. The technical data obtained from the measurements is categorized in maintenance. Modifications in software are only possible, which follows under system/equipment modification. The system phase-out & disposal will not have any extra cost, since the satellite will burn up in the atmosphere.

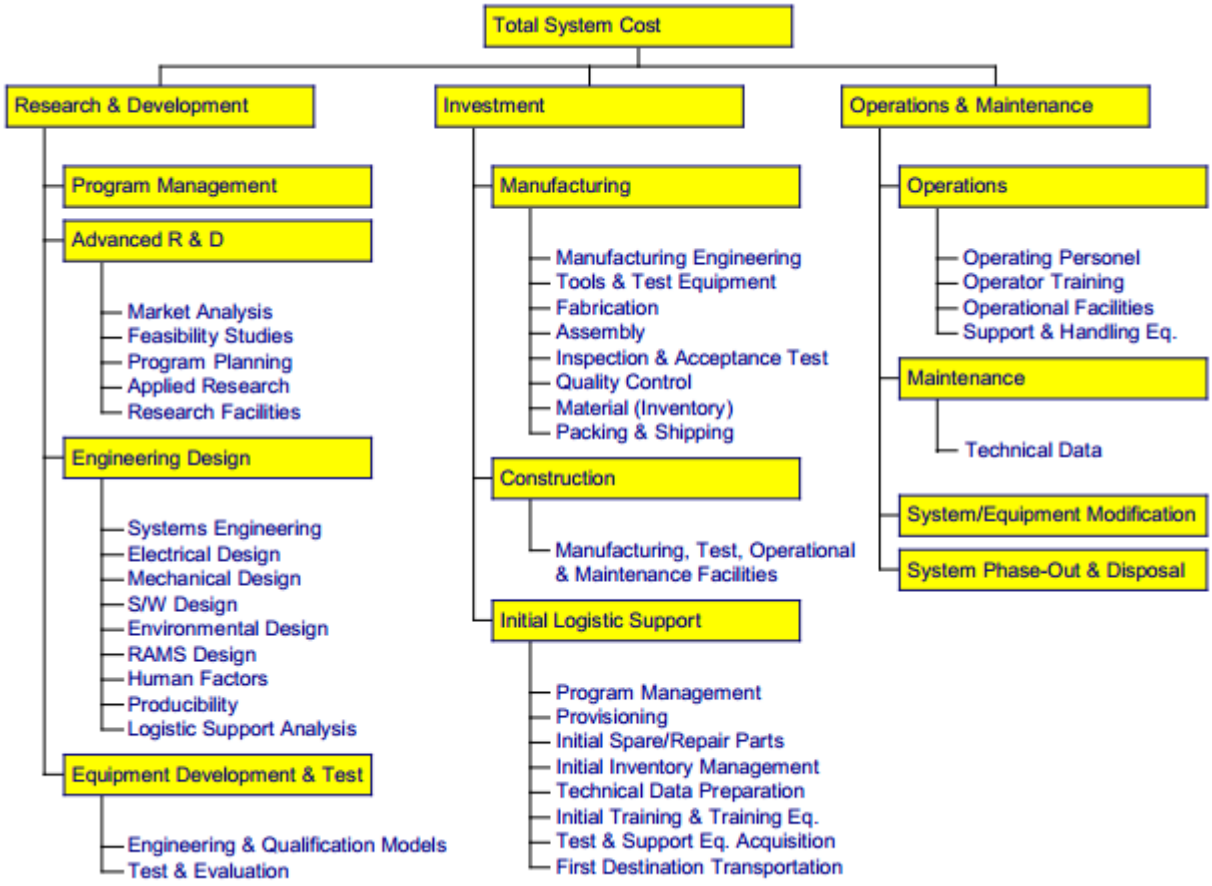

Figure 15.2: Cost breakdown structure of the post-DSE project activities, [10]

16 | Conclusion & Recommendations

The final report presents the detailed design of the GES mission, including all subsystems, the system integration, the orbit, and the steps to be performed in the future. The next two sections will describe the conclusion and recommendations.

16.1 Conclusion

The main purpose of this report was to present the detailed design of the GES mission. All subsystems necessary to perform this mission were considered, designed, and sized. Also the orbit type was decided upon, and the total cost of the mission was estimated.

The orbit type is chosen to operate in a dawn-dusk sun-synchronous orbit. This type was chosen as it provides an almost constant lightning and thermal condition. The inclination of the orbit is 97.7 degrees, giving an almost circular retrograde orbit. The height was selected based on the groundtrack; at 580 km height the whole Earth is covered within a month which is deemed necessary to measure temporal gravity changes while still meeting the end-of-life requirement of 25 years. This height additionally ensures that the ground track requirement is still met even after orbital decay during the 3 year life time. This orbit can be considered popular hence more and cheaper launch options are available.

The launch selection was based on cost, as it is the highest cost driver, and a piggy-back launch was chosen as it is the most cost-friendly option. For the communication a ground station needed to be selected. The in-house ground station location on the campus of the TU Delft was chosen, the satellite will pass over the station seven to eight times a day.

The payload includes a terrestrial state-of-art dual-frequency GNSS receiver by Septentrio with a carrier-phase measurement error of less than 1 mm meeting the required measurement noise error of less than 1 cm. The performance of this receiver is at similar level as the space certified receiver used by previous gravity explorer missions at a fraction of the cost while size, mass and power usage is kept at a minimum. Compared to these earlier missions, the use of additional satellite navigation systems such as GLONASS and Galileo allows for a higher accuracy and more robust solution. The higher update rate of the receiver means that a higher number of data points can be acquired hence a higher resolution is obtained as compared to forgoing missions. The GNSS antenna is a critical component and is a determining factor in the amount of GNSS satellites that can be simultaneously tracked which influences the achievable accuarcy. The received signal strength is an additional factor that influences the accuracy. Careful placement on the GES bus ensures that the radiation pattern remains unaltered and is able to receive all signals from visible GNSS satellites up to a zero degree elevation with the required signal strength for maximum accuracy. With the above described design solutions it is expected that the GES will have a superior performance regarding precise orbit determination as compared to forgoing gravity explorer missions.

The AD&C system was selected to be the iADCS-100. The data handling within the satellite is performed by an on-board computer, the ISIS computer proved to be the only one viable for the GES mission. After calculations it was found that the thermal control can be maintained by only passive control, i.e. the use of coatings. White as well as black coating will be used. The power supply to the system will be extracted from the Sun, by placing five body mounted solar cells on the Sun-facing plate as well as on the Earth facing side (using the albedo). All subsystems fit perfectly in a 2 unit CubeSat, which will be used to house the system.

Although the spatial scale is 667 m larger than required, the achieved spatial scale is far better then any mission solely flying a GNSS receiver. The the maximum pointing knowledge accuracy of GES is

8.25 μm. This satisfies the pointing error requirement, which states that the error in centre of mass positioning due to inaccurate satellite pointing is allowed to be 1 cm.

The total mission cost is estimated to be 300.000 *euros*, several magnitudes less than forgoing gravity explorer missions.

The GES can be classified as a low-cost mission that generates geodesy science data with significant precision contributing to a better understanding of climatological changes and variations on earth, crucial knowledge considering the vulnerability and human dependency on earth.

16.2 Recommendations

In this section the various recommendations made for the continuation of the GES project are listed. A distinction is made between recommendations regarding improvement of the current design and recommended future areas of study.

16.2.1 Improvement of current design

Below, the recommendations regarding improvements of the current GES design are described.

Specific reliability It is recommended to make a better estimate of the specific reliability of the mission, based on the failure rates of the several subsytems. Up to now this is calculated by the use of reference missions. By using the failure rates of the selected subsystems the reliability will be more mission specific.

Orbital characteristics More investigation needs to be done concerning the orbit decay and the satellite's lifetime. STK has several parameters that influence the orbit decay. One of the parameters is the atmospheric model, for which STK has different options for the atmospheric model to choose from. For LEO this is one of the main perturbations that the satellite has to deal with. Furthermore, an iterative process should be made between the orbital altitude and the power subsystem. The eclipse time follows from the chosen altitude, which then results in a specific type of battery. Due to the limited time during this project, this iterative process has not yet been made.

Thermal model For the calculations of the thermal subsystem it is recommended to use a more precise model. Now the temperatures have been determined assuming it would be constant per panel. A more precise model will be able to obtain the thermal conditions based on node calculations. The temperature will be calculated for different points on the satellite resulting in a more accurate thermal subsystem. Furthermore, the temperature within the satellite can be determined for each subsystem separately when using such a precise thermal model.

Manufacturing cost For the cost estimate made in this report the manufacturing costs were not seperately considered, but included in the margin. For a more accurate cost estimation in the further development of the project it is recommended to investigate the likely costs accompanying the manufacturing phase. Also it is recommended to look for opportunities to get a student discount or free testing possibilities.

Calculating the disturbance torques The disturbance torques for the mission were calculated using approximations and simplifications, these calculations were therefore not accurate enough and leaded to unrealistic values for the torques. In order to avoid this, some values need to be exactly calculated, such as the moments of inertia (which were calculated using a simplification of assuming a cuboid), the residual magnetic dipole of the satellite, and the exact location of the center of aerodynamic pressure (which was assumed to be one third of the length of the satellite). For the magnetic torque some accurate magnetic field models can also be used to determine Earth's exact magnetic field.

Structural loads during launch Due to the limited time of the project the structural loads have not been taken into account. The satellite structure has been used for space applications Therefore the structural loads during operations are assumed not to be a problem. However, it is recommended to model the structural loads during the launch phase, for these loads could be critical for the structure and the satellite components.

Battery of satellite The chosen battery of the satellite fulfills the requirements of the power subsystem. This battery has more than enough capacity, which is not used by the system. One can find out if it is also possible to have another battery with less capacity. Also if it is possible to have two smaller batteries where one is for redundancy.

Antenna PCV As mentioned in section 6.4.3, a determination of the exact antenna phase center location is critical. How this point varies can be determined through testing. Once the PCV is known as a function of the direction of the incoming signal, the exact location of the phase center (and therefore the exact location of the center of mass) can be modeled at any moment in time.

Software So far the software applications on the mission were not taken under consideration. However, onboard the satellite software will be used to manage the communication, attitude determination and control, power supply, and data handling. Also this sofware needs to be interconnected, to ensure a uniformly working satellite. Therefore it is recommended to investigate the software possibilities and implement them into the satellite system.

16.2.2 Further areas of study

Next to recommendations on the current design, the group encountered some configuration possibilities that fall outside the current design concept. These are listed below.

Non-relevant accelerations In section 6.6 three methods of identifying non-relevant accelerations have been described, one of which has been selected. However, extra study in this field can be executed, investigating the options of including a plasma density meter. Plasma density meters are known to be simple and cheap, and can be included to validate numerical models for atmospheric density and drag.

Coverage time Throughout the GES design process, the requirement of Earth coverage within a month has been taken as reference. However, beneficial results of decreasing this coverage time in terms of spatial scale and mission uniqueness might be explored and implemented.

Number of satellites Assuming university budgets are in the order of 1 mln. euros, the final financial budget as presented in section 9.2 indicates that the GES mission is highly promising. The extremely low mission cost might allow for increasing the number of satellites to two or more. In case investigation points out that the resulting increase in mission performance is significant, universities or other institutions might be willing to finance the expanded GES mission.

Joining other missions The final GES design offers two possibilities of integration with other missions:

1. Add payload from other mission to GES. The 2U CubeSat structure provides more than enough space for the necessary components of the GES mission, leaving some space.
2. Add GES payload to other mission. As the GNSS receiver and antenna are small, lightweight and do not require a much power, they can possibly be integrated with satellites of other mission.

Satellite laser ranging Considering the scientific goal of GES, laser ranging ground stations possibly offer their services for free. For payload validation purposes, it is useful to investigate the possibilities of applying satellite laser ranging to GES.

Tidal model contributions Section 5.2 discusses the fact that a SSO passes over the same point on Earth at the exact same times, repeatedly. The downside of this is that the satellite always measures the same tidal error. An upside might however be, that this error can be used as a contribution to the existing tidal models.

A Characteristics for Various GNSS Receiver Types

Table A.1: Dual-frequency GNSS receivers for space applications [16] [17]

Manufact.	Receiver	Chan	Ant	Power Mass	TID (krad)	Missions
Laben (I)	Lagrange	16×3 C/A,P1/2	1	30 W 5.2 kg	20	ENEIDE, Radarsat-2 GOCE
General Dynamics (US)	Monarch	6-24 C/A,P1/2	1-4	25 W 4 kg	100	
JPL (US) / BRE (US)	BlackJack / IGOR	16×3 C/A,P1/2	4	10 W 3.2/4.6 kg	20	CHAMP, GRACE, Jason-1/ COSMIC, TerraSAR-X
Alcatel (F)	TopStar 3000G2	6×2 C/A,L2C	1			Under development; PROBA-2
Austrian Aerospace (A)	Inn. GNSS Navigation Recv.	Up to 36 C/A,P1/2	2		>20	Under development; SWARM
BRE (US)	Pyxis Nautica	16-64 C/A,P1/2 L2C,L5	1-4	20 W 2.5 kg		Under development
NovAtel (CA)	OEM4-G2L	12×2 C/A,P2	1	1.5 W 85 g	6	CanX-2; CASSIOPE
Septentrio (B)	PolaRx2	16×3 C/A,P1/2	1 (3)	5 W 190 g	9	TET

Table A.2: Single-frequency GNSS receivers for space applications [16]

Manufact.	Receiver	Chan.	Ant.	Power Mass	TID (krad)	Missions
Alcatel (F)	TopStar 3000	12/16 C/A	1-4	1.5 W 1.5 kg	>30	Demeter, Kompsat-2
EADS Astrium (D)	MosaicGNSS	6-8 C/A	1	10 W 1 kg	>30	SARLupe, TerraSAR-X Aeolus
General Dynamics (US)	Viceroy	12 C/A	1-2	4.7 W 1.2 kg	15	MSTI-3, Seastar, MIR, Orbview, Kompsat-1
SSTL (UK)	SGR-05	12 C/A	1	0.8 W 20 g	>10	
	SGR-20	4×6 C/A	4	6.3 W 1 kg	>10	PROBA-1, UOSat-12, BILSAT-1
DLR (D)	Phoenix-S	12 C/A	1	0.9 W 20 g	15	Proba-2, X-Sat, FLP, ARGO, PRISMA
Accord (IND)	NAV2000HDCP	8 C/A	1	2.5 W 50 g		X-Sat

B | Coverage Density Figures

The following figures describe the passage of the satellite from each altitude and longitude seen at an area of 100 by 100 km. As can be seen, the minimum number of observations occur near 0 latitude and longitude, so special attention should be given to these areas during the orbit design.

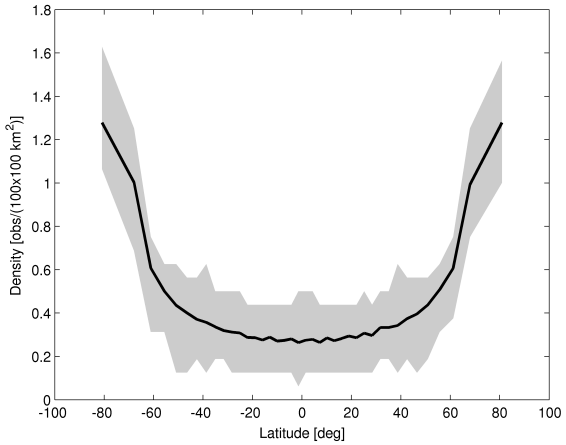

Figure B.1: Observation density in each lattitude at 572 km

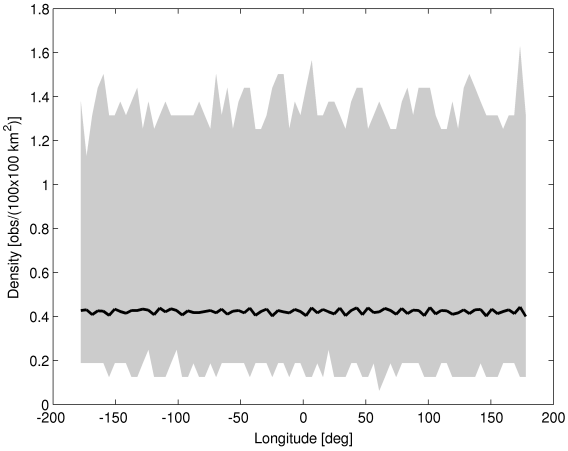

Figure B.2: Observation density in each longitude at 572 km

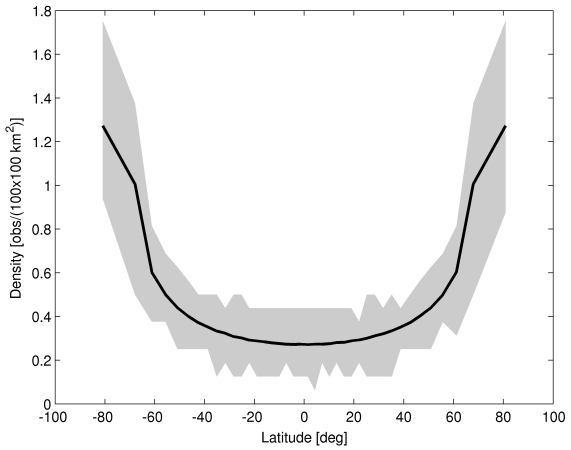

Figure B.3: Observation density in each lattitude at 574 km

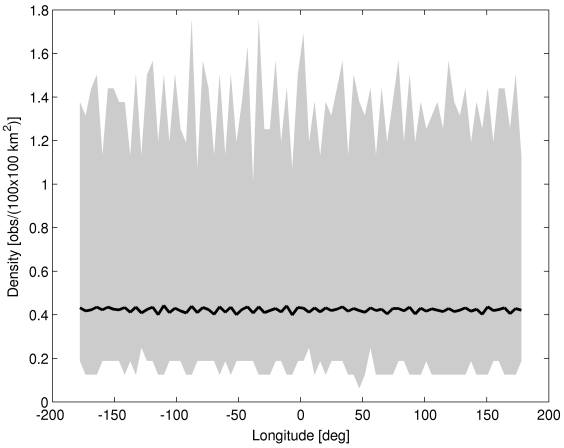

Figure B.4: Observation density in each longitude at 574 km

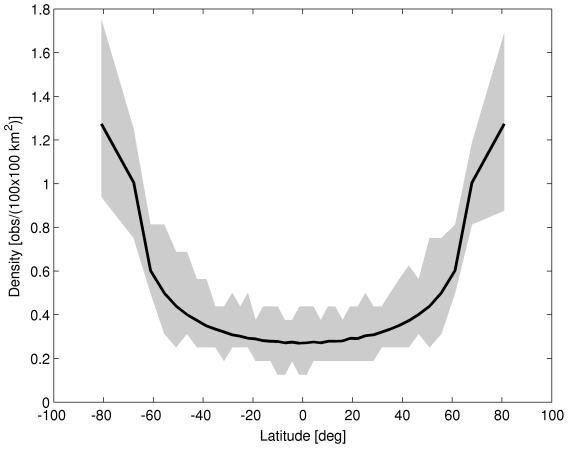

Figure B.5: Observation density in each lattitude at 576 km

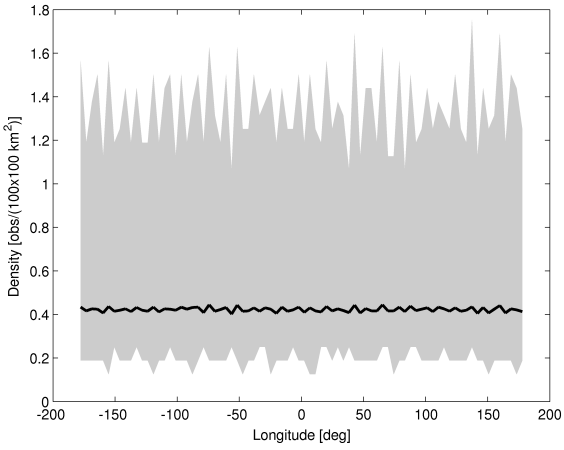

Figure B.6: Observation density in each longitude at 576 km

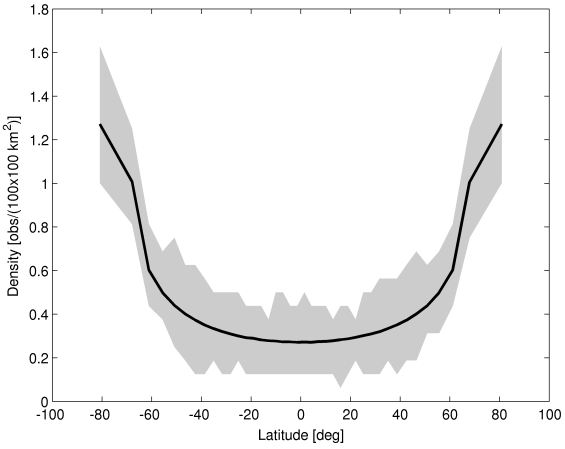

Figure B.7: Observation density in each lattitude at 578 km

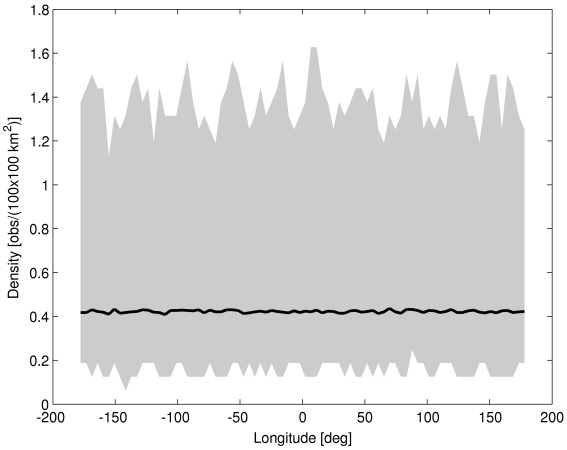

Figure B.8: Observation density in each longitude at 578 km

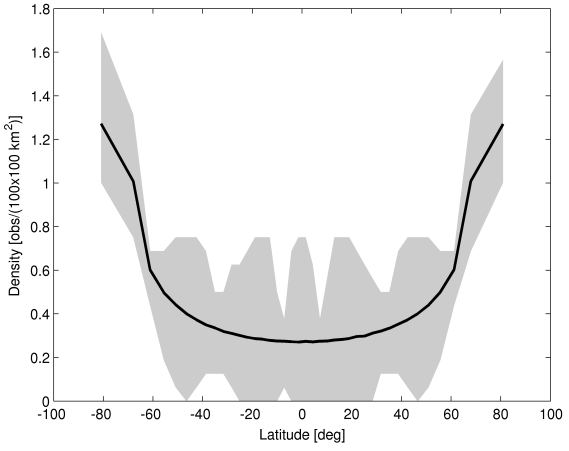

Figure B.9: Observation density in each lattitude at 580 km

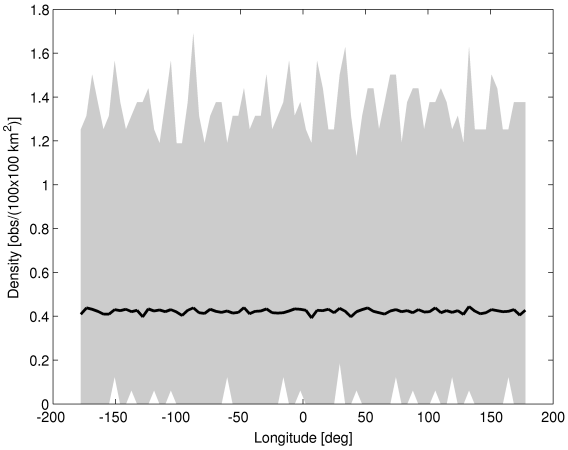

Figure B.10: Observation density in each longitude at 580 km

C 2D Representation

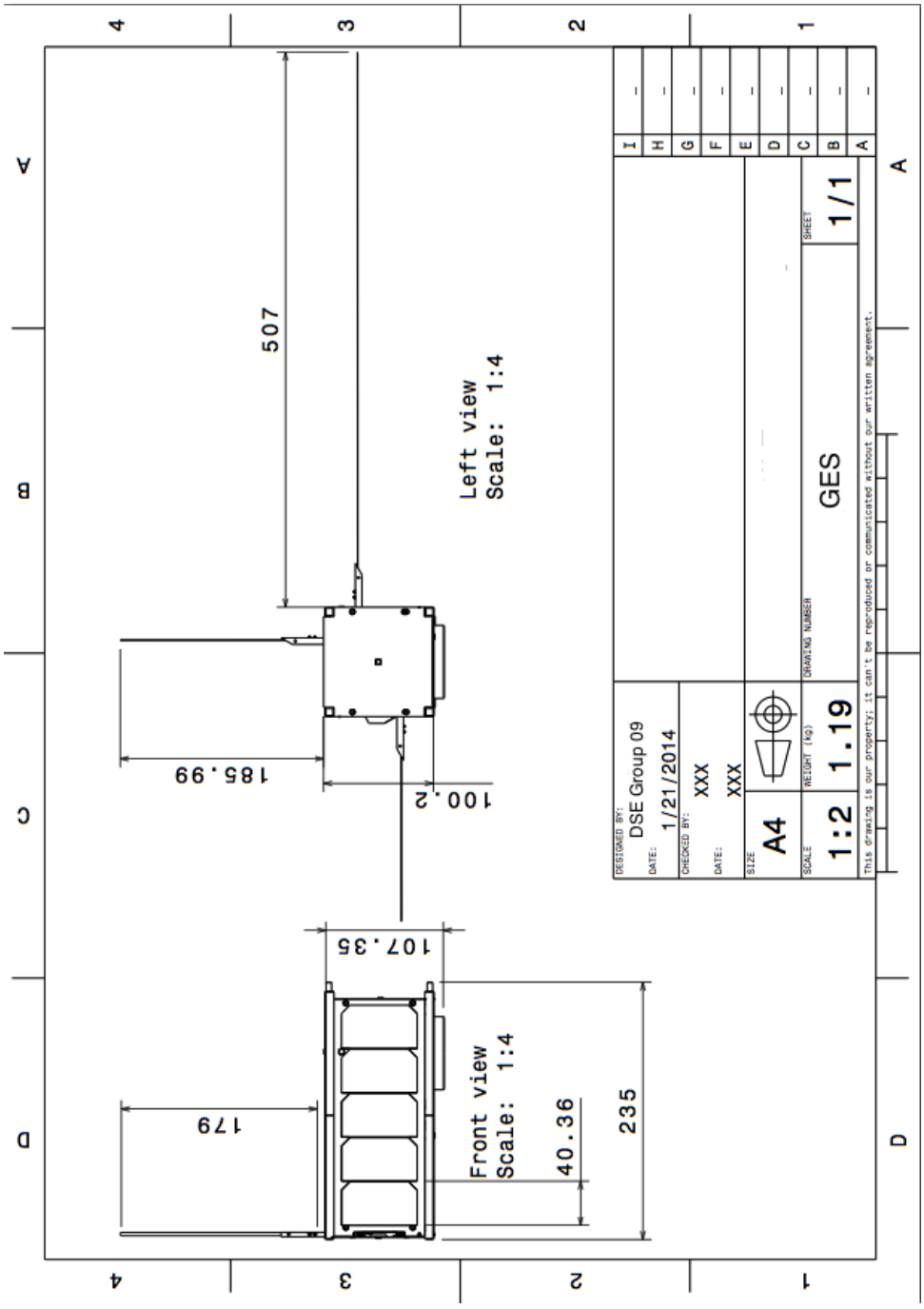

Figure C.1: 2D CATIA drawing of GES

D | 3D Representation

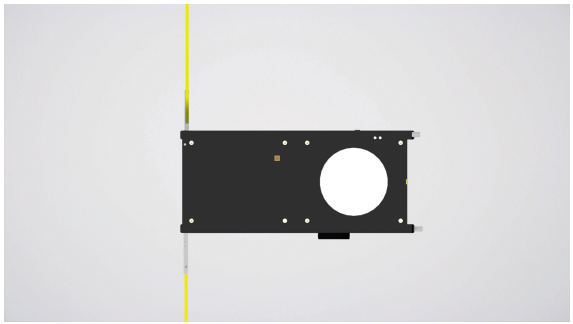

Figure D.1: Top view

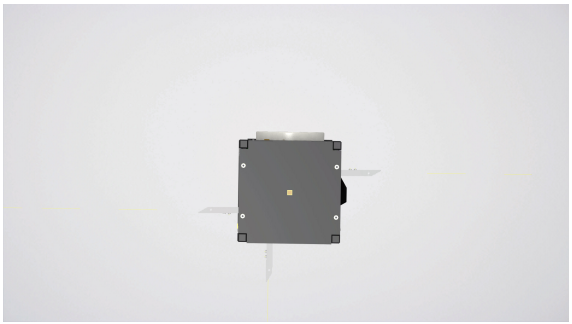

Figure D.2: Front view

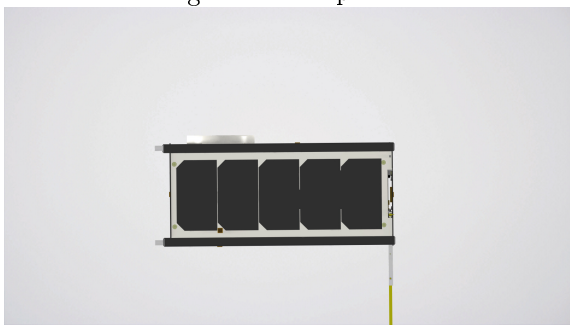

Figure D.3: Side view (facing the Sun)

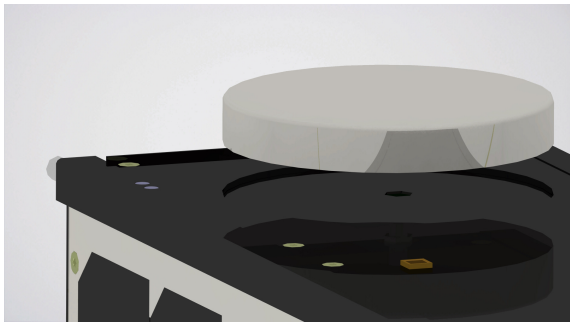

Figure D.4: GNSS mounting

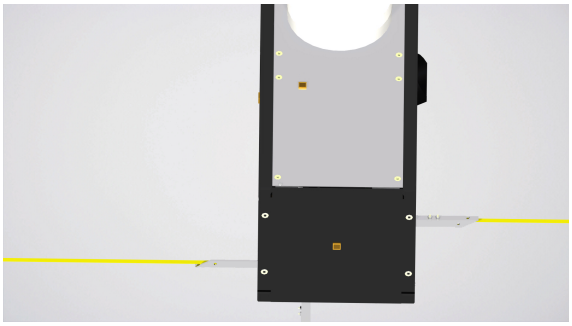

Figure D.5: Detached antenna

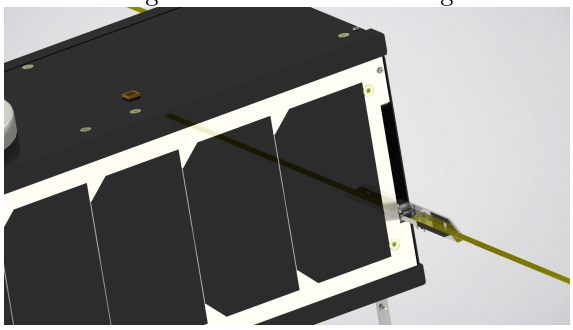

Figure D.6: Deployable antenna cut-out

E | Gantt Chart Post-DSE

The Gantt chart for the period post-DSE project is presented. The Gantt chart, provided in figure E.1, shows a standardized diagram that contains the planning of the mission. This chart gives an overview of all the tasks that have to be performed in order to make this a successful mission. An estimation of the duration of the different tasks is also made.

Figure E.1: Gantt chart Post-DSE project

F Logbook

Table F.1: Logbook

Part	Team member(s)
Preface	Céline
List of Figures & Tables	Daan, Sander
List of Abbreviation & Symbols	All
Abstract	Evelyne
1. Introduction	Ariadad, Céline
2. Market Analysis	
Market segmentation	Erik
Developments in the space sector	Erik
Competitors	Erik
Business model	Erik
Cost analysis	Erik
SWOT analysis	Erik
Resulting mission types and applications	Stephanie
Technology	Bushra
Vision	Bushra
3. Requirements	Evelyne
4. Mission Overview	Céline
5. Astrodynamic Characteristics	
Decay and end-of-life	Stephanie
Sun-synchronous orbit	Ariadad
Eclipse time	Ariadad
Coverage density	Ariadad
Astrodynamic results	Ariadad
6. Payload	
Measurement errors	Fabian
Error mitigation methods	Fabian, Daan
COTS GNSS receivers	Fabian, Sander
GNSS receiver antenna	Daan
GNSS link budget	Fabian
Coping with non-gravitational accelerations	Sander
7. Subsystem Design	
Attitude determination & control	Ariadad
Communication architecture & data handling	Fabian
Guidance and navigation	Céline
Thermal control	Evelyne
Power system	Bushra
Structural design	Erik
Ground segment	Stephanie
Launcher selection	Céline
8. System Characteristics	
Spacecraft system characteristics	Fabian, Céline
Configuration and system integration	Erik
Production plan	Ariadad, Erik
9. Budget Breakdown	
Satellite system budget	Céline, Ariadad
Financial budget	Céline
10. Technical Risk Assessment	Stephanie
11. Reliability, Maintainability, Availability & Safety	
Reliability	Céline, Stephanie
Availability, Maintainability, Safety	Céline
12. Sustainable Development Strategy	Céline
13. Performance	
Performance Analysis	Ariadad
Requirements compliance matrix	Daan, Sander
Sensitivity analysis	Daan, Sander
14. Verification & Validation	Stephanie, Fabian, Evelyne
15. Project Design & Development	Stephanie
16. Conclusion & Recommendations	
Conclusion	Evelyne, Fabian
Recommendations	All
Appendix A	Daan
Appendix B	Ariadad
Appendix C.1	Ariadad
Appendix D	Erik
Appendix E	Stephanie
Bibliography	All

Bibliography

[1] Guerra L., "Cost Estimation Module, Space System Engineering," NASA's Exploration Systems Mission Directorate, January 2014.

[2] National Geodetic Servey, "Antenna Calibrations," http://www.ngs.noaa.gov/ANTCAL/, January 2014.

[3] Kumar A., "lecture 5 Disturbance," `http://www.ae.iitm.ac.in/~amitk/AS3010/ProfSSK/05_Disturbance.pdf`, Department of Aerospace Engineering Indian Institute of Technology Madras.

[4] Technologies, B. S., "iADCS, Intelligent Attitude Control for Cubesats," `http://www.berlin-space-tech.com/fileadmin/media/BST_iACDS-100_Flyer.pdf`.

[5] Clyde space, "Small satellite solar panels," `http://www.clyde-space.com/cubesat_shop/solar_panels/2u_solar_panels/79_2u-cubesat-side-solar-panel`, Jan 2014.

[6] CubeSat Kit, "CubeSat Kit CAD Models," `http://www.cubesatkit.com/content/design.html`, Jan 2014.

[7] ISIS, "2-Unit CubeSat Structure," `http://www.cubesatshop.com/index.php?page=shop.product_details&flypage=flypage.tpl&product_id=2&category_id=1&option=com_virtuemart&Itemid=66`, Jan 2014.

[8] Innovative Solutions In Space BV, *Assembly Manual ISIS 2-Unit CubeSat Structure*, 2012.

[9] George Fox, et. al., "A Satellite Mortality Study to Support Space Systems Lifetime Prediction," *Aerospace Conference, 2013 IEEE*, 2013.

[10] Curran R., Verhagen W., "Design for Product Support & Life Cycle Cost," Lecture Systems Engineering & Technical Management Techniques, 2012-2013.

[11] Coias J. M. M., *Attitude Determination Using Multiple L1 GPS Receivers*, Master's thesis, Universidade Tecnica de Lisboa, 2012.

[12] Antenna Systems, Inc., *M2 Antenna Systems, Inc.*, 2011.

[13] ISIS, "Cubesatshop," `http://www.cubesatshop.com/`, 2006-2013.

[14] ISIS, "ISIS On Board Computer," `http://www.cubesatshop.com/index.php?page=shop.product_details&flypage=flypage.tpl&product_id=119&category_id=8&option=com_virtuemart&Itemid=75`, Jan 2014.

[15] Septentrio nv, *AsteRx-m*, 2013.

[16] Montenbruck O., Markgraf M., Garcia-Fernandez M., Helm A., "GPS FOR MICROSATELLITES STATUS AND PERSPECTIVES," 6^{th} *IAA Symposium on Small Satellites for Earth Observation*, April 2007.

[17] Montenbruck O., Wiliams J., "Performance Comparison of Semicodeless GPS Receiver for LEO satellites," Tech. rep., DLR, March 2006.

[18] OECD, *OECD Handbook on Measuring Space Economy*, OECD Publishing, 2012.

[19] Jolly C., "The space economy at a glance 2011," http://www.oecd.org/sti/futures/space/48301203.pdf, Directorate for Science, Technology and Industry.

[20] Easton R., "Who invented the Global Positioning System?" http://www.thespacereview.com/article/626/1.

[21] Dinerman T., "Financial risk analysis for the space industry," http://www.thespacereview.com/article/1151/1.

[22] Tahir T., "Asteroid watch suspended and Curiosity powers down as US government closes up shop after budget battle," http://metro.co.uk/2013/10/01/asteroid-watch-suspended-and-curiosity-powers-down-as-us-government-closes-up-shop-after-budge

[23] Messier D., "ESA Faces the Limits of Expansion, Growing Power of EU," http://www.parabolicarc.com/2013/02/26/esa-faces-the-limits-of-expansion-growing-power-of-eu/, February 2013.

[24] Earth Observation resources portal, "CHAMP (Challenging Minisatellite Payload)," https://directory.eoportal.org/web/eoportal/satellite-missions/c-missions/champ.

[25] ESA, "CHAMP (Facts and Figures)," http://www.esa.int/Our_Activities/Observing_the_Earth/GOCE/Facts_and_figures.

[26] Space Flight Now, Inc., "Gravity mapping satellites launched into space)," http://www.csr.utexas.edu/grace/publications/press/02-03-17-GRACE-spaceflight.pdf.

[27] NOAA System Observation Councill, "GRACE (Gravity Recovery and Climate Experiment)," https://www.nosc.noaa.gov.

[28] Henson R., "GRACE-II GRAVITY RECOVERY AND CLIMATE EXPERIMENT II," http://www.nap.edu/openbook.php?record_id=11952&page=17.

[29] Osterwalder A., Pigneur Y. et al., *Business Model Generation*, Self published, 2009.

[30] Clyde-Space, "CubeSat Solar Panels," http://www.clyde-space.com, 2014.

[31] Montenbruck O., "Space GPS receivers. Aces and Future GNSS-Based Earth observatiob and navigation," Tech. rep., TU Munchen, 2008.

[32] Michael, "Michael's list of cubesat satellite missions," http://mtech.dk/thomsen/space/cubesat.php, 2009.

[33] NASA, "Cubesat launch initiative," http://www.nasa.gov/directorates/heo/home/CubeSats_initiative.html#.UqrHChDNk84, November 2013.

[34] van den IJssel J., Visser P., "Determination of non-gravitational accelerations from GPS satellite-to-satellite tracking of CHAMP," *Elsevier*, Vol. 36, No. 3, 2005, pp. 418–423.

[35] D. Kuang, S. Desai, A. Sibthorpe, X. Pi, "Measuring atmospheric density using GPSâĂŞLEO tracking data," *Elsevier*, Vol. 53, No. 2, January 2014.

[36] Doornbos E., "Personal communication," TU Delft, Januari 2014.

[37] Kramer H.J., "Swarm," https://directory.eoportal.org/web/eoportal/satellite-missions/s/swarm, Januari 2014.

[38] Bruninga R.E., "United States Naval Academy," http://www.nasa.gov/mission_pages/station/research/experiments/267.html, Januari 2014.

[39] ESSS, "Ethiopian space science society," http://www.ethiosss.org.et/index.php/en/home/news/95-et-sat-is-set-to-become-the-first-ethiopian-satellite, 201.

[40] European Union, "QB50, an FP7 project," https://www.qb50.eu/index.php/schedule, 2013.

[41] Wertz J.R., Larson W.J., *Space Mission Analysis and Design*, chap. Communications Architecture, Space Technology Library, Microcosm Press, Springer, third edition ed., 2010, pp. 533–575.

[42] SPACEFLIGHT, "SPACEFLIGHT schedule," http://spaceflightservices.com/manifest-schedule.

[43] D., E. C., "Sun-Synchronous Orbit Design," http://www.cdeagle.com/omnum/pdf/sunsync1.pdf.

[44] Strong K., "Satellite orbits," http://www.atmosp.physics.utoronto.ca/people/strong/phy499/section2_05.pdf, University of Toronto course:PHY 499S Earth Observations from Space.

[45] Fehringer M. et al, "A Jewen in ESA's Crown," http://www.esa.int/esapub/bulletin/bulletin133/bul133c_fehringer.pdf, february 2008, esa bulletin 133.

[46] Wagner C. et al, "Degradation of geopotential recovery from short repeat-cycle orbits: application to GRACE monthly fields," *Journal of Geodesy*, Vol. 80, No. 2, 2006, pp. 94–103.

[47] Sunehra D., "Estimation of Prominant Global Positioning system measurement errors for GAGAN applications," *European Scientific Journal*, Vol. 9, No. 15, May 2013, pp. 68 to 81.

[48] Azab B., et. al., "Precise Point Positioning Using Combined GPS/GLONASS Measurements," *Geodetic Applications in Various Situations*, 2011.

[49] Van der Marel H., De Bakker P.F., "GNSS Solutions: Single- versus Dual- Frequency Precise Point Positioning," *Inside GNSS*, 2012.

[50] Novatel Customer Service, "Personal communication," December 2013.

[51] Markgraf M., Montenbruck O., "Total Ionizing Dose Testing of the NovAtel OEM4-G2L GPS Receiver," Tech. rep., DLR, December 2004.

[52] Leyssens J.,Markgraf M., "Evaluation of a Commercial-Off-The-Shelf dual-frequency GPS receiver for use on LEO satellites," Tech. rep., Septentrio NV and DLR, september 2005.

[53] Rouquette R. E., "GPS L1 Link Budget," 2008.

[54] Bock H., et. al., "Precise orbit determination for the GOCE satellite using GPS," *Advances in Space Research*, 2007.

[55] Kahr E., Montenbruck O. , O'Keefe K. , Skone S., Urbanek J., Bradbury L., Fenton P. , "GPS TRACKING ON A NANOSATELLITE, THE CANX-2 FLIGHT EXPERIENCE," *8th International ESA conference on Guidance, Navigaion and Control Systems*, ESA, jun 2011, p. 1 to 8.

[56] Ubox, "GPS Antennas locate, communicate, accele rateRF Design Considerations for u-blox GPS Receivers Application Note," 2009.

[57] Earth Observation resources portal, "Gravity field and steady-state Ocean Circulation Explorer," https://directory.eoportal.org/web/eoportal/satellite-missions/g/goce, 2013.

[58] Christophe B., Foulen B., Lebat V., Boulanger D., "cubSTAR, an ultra-sensitive accelerometer for CubSat," june 2012.

[59] SERENUM, "Capacitive Accelerometer," http://serenum.cz/?p=229, 2013.

[60] Krishnamoorthy U., et al., "In-plane MEMS-based nano-g accelerometer with sub-wavelength optical resonant sensor," *Sensors and Actuators A: Physical*, Vol. 145–146, No. 0, 2008, pp. 283 – 290.

[61] Zandi K., et al., "VOA-Based Optical MEMS Accelerometer," Tech. rep., Department of Engineering Physics École Polytechnique de Montréal, Montréal (QC) H3C 3A7, Canada, 2011.

[62] Merritt R., "Accelerometer propels HP into sensor networks," http://www.eetimes.com/document.asp?doc_id=1172177&page_number=4, may 2009.

[63] Ditmar P., Klees R., Liu X., "Frequency-Dependent Data Weighting in Global Gravity Field Modeling from Satellite Data Contaminated by Non-Stationary Noise," *J geod*, june 2007, pp. 81–96.

[64] Ditmar P., Klees R., Liu X., "On a Feasinility of Modeling Temporal Gravity Field Variations from Orbits of Non-Dedicated Satellites," Tech. rep., Delft University of Technology, 2009.

[65] Weigelt M. , van Dam T.,et al., "Time-variable gravity signal in Greenland revealed by high-low satellite-to-satellite tracking," *JOURNAL OF GEOPHYSICAL RESEARCH: SOLID EARTH*, Vol. 118, july 2013, pp. 3848 to 3859.

[66] Weigelt M., "Email conversation," december 2013.

[67] Wertz J.R., Larson W.J., *Space Mission Analysis and Design*, chap. Chapter Spacecraft subsystems, Space Technology Library, Microcosm Press, Springer, third edition ed., 2010, pp. 395–407.

[68] NASA, "Spacecraft Aerodynamic Torques," http://www.dept.aoe.vt.edu/~cdhall/courses/aoe4065/NASADesignSPs/sp8058.pdf, 1971.

[69] Engelen S., "Personal communication," December 2013.

[70] Yin F., et. al., "Characterization of CHAMP magnetic data anomalies: magnetic contamination and measurement timing," *Measurement Science and Technology*, 2013.

[71] Bock H., et. al., "GPS-derived orbits for the GOCE satellite," *Journal of Geodesy*, 2011.

[72] Septentrio nv, *SBF Reference Guide*, 2013.

[73] Montilla E. G. B., et. al., *GPS data compression using lossless compression algorithms*, Master's thesis, Universitat Politechnica de Catalunya, 2009.

[74] Engelen S., "Personal communication," January 2014.

[75] Nils von Storch, Ground Station Engineer at Delfi-n3Xt, "personal conversation," January 2014.

[76] Gilmore D.G., et al., *Spacecraft Thermal Control Handbook*, The Aerospace Press, second edition ed., 2002.

[77] Wertz J.R. and Larson W. J., *Space Mission Analysis and Design*, chap. Appendix D, Space Technology Library, Microcosm Press, Springer, third edition ed., 2010, pp. 909,910.

[78] ESA, "Viewfactors," *ESA PSS-030108*, ESA, November 1989, pp. 39,42.

[79] Klein M., "Personal communication," Januari 2014.

[80] tsmc solar, "TSMC Solar- CIGS is now a reality," http://www.tsmc-solar.com/technology/cigs-technology, 2014.

[81] GomSpace, Inc., "GOMspace," http://gomspace.com/index.php?p=products-p110.

[82] Azur space, "28% Triple junction GaAs Solar cell," Tech. rep., Solar Power GMBH, Heilbronn, April 2012.

[83] Clyde space, "2U CubeSat EPS," http://www.clyde-space.com/cubesat_shop/eps/277_2u-eps, Jan 2014.

[84] Craig S. C., Simon E., "Evaluation of lithium polymer technology for small satellite applications," http://www.clyde-space.com/cubesat_shop/solar_panels/2u_solar_panels/79_2u-cubesat-side-solar-panel, Jan 2007.

[85] Clyde space, "2U CubeSat Structures," http://www.clyde-space.com/cubesat_shop/structures/2u_structures, Jan 2014.

[86] EUMETSAT, "Ground Segment," http://www.eumetsat.int/website/home/Satellites/GroundSegment/index.html, Januari 2014.

[87] Hartanto D., *Reliable Ground Segment Data Handling system for Delfi-n3Xt satellite Mission*, Master's thesis, Delft University of Technology, Mekelweg 4, 2628 CD Delft, 2009.

[88] von Storch N., "personal contact," email, December 2013.

[89] Kramer H.J., "CubeSat concept," https://directory.eoportal.org/web/eoportal/satellite-missions/c-missions/cubesat-concept, Januari 2014.

[90] Spaceflight, Inc., "Services: Deployed Payloads," http://spaceflightservices.com/services/deployed-payloads/, Januari 2014.

[91] Spaceflight, Inc., "Schedule," http://spaceflightservices.com/manifest-schedule, december 2013.

[92] Spaceflight , Inc., "price," http://spaceflightservices.com/pricing-plans, december 2013.

[93] Innovative Solutions In Space, "Launch Services," http://www.isispace.nl/cms/index.php/products-and-services/launches, Januari 2014.

[94] Bonnema A., Marketing Director at ISIS, "personal conversation," January 2014.

[95] ESA, "Space for educators," http://www.esa.int/Education/Students_are_you_ready_to_fly_your_satellites_in_space, Januari 2014.

[96] Sales team, Antcom, "personal conversation," January 2014.

[97] van Hees J. , Septentrino, "personal conversation," January 2014.

[98] ISIS, "ISIS UHF downlink / VHF uplink Full Duplex Transceiver," http://www.cubesatshop.com/index.php?page=shop.product_details&flypage=flypage.tpl&product_id=11&category_id=5&option=com_virtuemart&Itemid=67, Jan 2014.

[99] Sensor Systems, Inc., "GPS S67-1575-14; -76; 86; 96," 2004.

[100] Clyde Space, "CubeSat Standalone Battery," http://www.clyde-space.com/cubesat_shop/batteries/16_3u-cubesat-battery, Jan 2014.

[101] Clyde Space, "2U CubeSat EPS," http://www.clyde-space.com/cubesat_shop/eps/277_2u-eps, Jan 2014.

[102] Clyde Space, "2U Side Solar Panel w/MTQ," http://www.clyde-space.com/cubesat_shop/solar_panels/2u_solar_panels/82_2u-side-solar-panel-w-mtq, Jan 2014.

[103] Clyde Space, "1U CubeSat Side Solar Panel," http://www.clyde-space.com/cubesat_shop/eps/50_1u-cubesat-side-solar-panel, Jan 2014.

[104] Wertz J.R., Larson W.J., *Space Mission Analysis and Design*, chap. Space manufacture and test, Space Technology Library, Microcosm Press, Springer, third edition ed., 2010, pp. 519–530.

[105] Wertz J.R., Larson W.J., *Space Mission Analysis and Design*, chap. Design budgets, Space Technology Library, Microcosm Press, Springer, third edition ed., 2010, pp. 853–858.

[106] Heyman J., "CubeSats - A Costing + Pricing Challenge," http://www.satmagazine.com/story.php?number=602922274, Januari 2014.

[107] Kenny M., "personal conversation," January 2014.

[108] Wertz J.R., Larson W.J., *Space Mission Analysis and Design*, chap. Cost Modelling, Space Technology Library, Microcosm Press, Springer, third edition ed., 2010, pp. 783–811.

[109] Alvaro N., Costello K., "Guidelines for Risk Management," 2012.

[110] Curran R. , Verhagen W. , "AE3201 Systems Engineering and Aerospace Design," 2013, Lecture 8 Risk Management and Reliability.

[111] Gunter's Space Page, "Orbital Launches of 2012," http://space.skyrocket.de/doc_chr/lau2012.htm, december 2013.

[112] ISIS, "ISIPOD CubeSate Deployer," http://www.isispace.nl/brochures/ISIS_ISIPOD_Brochure_v.7.11.pdf, Januari 2014.

[113] Inter-Agency Space Debris Coordination Committee, "Stability of the future Leo environment," United Nations Committee on the Peaceful Uses of Outer Space, February 2013.

[114] Vos M., *Delfi-n3Xt's Attitude Determination and control subsystem*, Master's thesis, TU Delft, May 2013.

[115] Tafazoli M., "A study of on-orbit spacecraft failures," *Elsevier*, Vol. 64, No. 2-3, Januari-Februari 2009, pp. 195–205.

[116] Wertz J.R., Larson W.J., *Space Mission Analysis and Design*, chap. Reliability for space mission planning, Space Technology Library, Microcosm Press, Springer, third edition ed., 2010, pp. 765–782.

[117] Castet J.F, "Satellite and satellite subsystems reliability analysis and modeling," *Elsevier*, Vol. 94, No. 11, November 2009, pp. 1718–1728.

[118] SSE Group, "RAMS estimate," http://www.lr.tudelft.nl/en/organisation/departments/space-engineering/space-systems-engineering/expertise-areas/mission-concept-exploration/rams/.

[119] ESA, "Flight Safety," http://www.esa.int/Our_Activities/Space_Engineering/Flight_Safety, December 2012.

[120] World Commission on Environment and Development, "Our Common Future," *Oxford University Press*, 1987.

[121] IADC, "Support to the IADC Space Debris Mitigation Guidelines," http://www.iadc-online.org/index.cgi?item=docs_pub, October 2004.

[122] IPCC, "Climate Change 2013: The Physical Science Basis," Tech. rep., United Nations, Switzerland, October 2013.

[123] Gunter B. C., Encarnação J., Ditmar P., Klees R., "Using Satellite Constellations for Improved Determination of Earth's Time-Variable Gravity," *JOURNAL OF SPACECRAFT AND ROCKETS*, Vol. 48, No. 2, march-april 2011, pp. 368–377.

[124] Earth Observation resources, "Iridium NEXT Hosting Payloads on a Communications Constellation," https://directory.eoportal.org/web/eoportal/satellite-missions/i/iridium-next, 2013.

[125] Encarnacao J., "personal conversation," december 2013.

[126] Slater J.W., "Glossary of Verification and Validation Terms," NASA, July 2008.

[127] Analytical Graphics, Inc., "Verification and Validation of AGI Technology," http://www.agi.com/resources/user-resources/downloads/evaluation-materials/verification-and-validation-data.aspx, December 2013.

[128] Sharing Earth Observation Resources, "Delfi-n3xt Mission," https://directory.eoportal.org/web/eoportal/satellite-missions/d/delfi-n3xt, 2014.

[129] Bouwmeester J., et al, "Design Status of the Delfi-Next Nanosatellite Project," http://www.lr.tudelft.nl/fileadmin/Faculteit/LR/Organisatie/Afdelingen_en_Leerstoelen/Afdeling_SpE/Space_Systems_Eng./Publications/2010/doc/2010,_09,_27_-_J._Bouwmeester_et._al.,_Design_Status_of_the_Delfi-Next_Nanosatellite_Project,_IAC_2010,_Prague.pdf, 2010.